



UNIVERSIDAD NACIONAL AUTÓNOMA DE MÉXICO
POSGRADO EN CIENCIAS BIOLÓGICAS
INSTITUTO DE ECOLOGÍA
BIOLOGÍA EVOLUTIVA

Ratón de orejas negras (*Peromyscus melanotis*) como indicador de conectividad en el Parque Nacional La Malinche

TESIS
POR ARTÍCULO CIENTÍFICO

Highland forest's environmental complexity drives landscape genomics and connectivity of the rodent *Peromyscus melanotis*

QUE PARA OPTAR POR EL GRADO DE:
MAESTRA EN CIENCIAS BIOLÓGICAS
PRESENTA
GABRIELA ARIDAI BORJA MARTÍNEZ

TUTORA PRINCIPAL: DRA. ELLA VAZQUEZ DOMINGUEZ, INSTITUTO DE ECOLOGÍA, UNAM

COMITÉ TUTOR: DRA. ALICIA MASTRETTA YANES, CONABIO
DR. MIGUEL EMMANUEL CASTILLO RODRÍGUEZ, INSTITUTO DE GEOLOGÍA, UNAM

Cd. Mx., agosto 2021



UNAM – Dirección General de Bibliotecas

Tesis Digitales
Restricciones de uso

DERECHOS RESERVADOS ©
PROHIBIDA SU REPRODUCCIÓN TOTAL O PARCIAL

Todo el material contenido en esta tesis está protegido por la Ley Federal del Derecho de Autor (LFDA) de los Estados Unidos Mexicanos (Méjico).

El uso de imágenes, fragmentos de videos, y demás material que sea objeto de protección de los derechos de autor, será exclusivamente para fines educativos e informativos y deberá citar la fuente donde la obtuvo mencionando el autor o autores. Cualquier uso distinto como el lucro, reproducción, edición o modificación, será perseguido y sancionado por el respectivo titular de los Derechos de Autor.



UNIVERSIDAD NACIONAL AUTÓNOMA DE MÉXICO
POSGRADO EN CIENCIAS BIOLÓGICAS
INSTITUTO DE ECOLOGÍA
BIOLOGÍA EVOLUTIVA

Ratón de orejas negras (*Peromyscus melanotis*) como indicador de conectividad en el Parque Nacional La Malinche

TESIS
POR ARTÍCULO CIENTÍFICO

Highland forest's environmental complexity drives landscape genomics and connectivity of the rodent *Peromyscus melanotis*

QUE PARA OPTAR POR EL GRADO DE:
MAESTRA EN CIENCIAS BIOLÓGICAS
PRESENTA
GABRIELA ARIDAI BORJA MARTÍNEZ

TUTORA PRINCIPAL: DRA. ELLA VAZQUEZ DOMINGUEZ, INSTITUTO DE ECOLOGÍA, UNAM

COMITÉ TUTOR: DRA. ALICIA MASTRETTA YANES, CONABIO
DR. MIGUEL EMMANUEL CASTILLO RODRÍGUEZ, INSTITUTO DE GEOLOGÍA, UNAM

México, Cd. Mx., agosto 2021

COORDINACIÓN DEL POSGRADO EN CIENCIAS BIOLÓGICAS

ENTIDAD INSTITUT DE ECOLOGÍA

OFICIO CPCB/632/2021

ASUNTO: Oficio de Jurado

M. en C. Ivonne Ramírez Wence
Directora General de Administración Escolar, UNAM
P r e s e n t e

Me permito informar a usted, que el Subcomité de Biología Experimental y Biomedicina del Posgrado en Ciencias Biológicas, en su reunión ordinaria del día 21 de junio de 2021, aprobó el siguiente jurado para el examen de grado de **MAESTRA EN CIENCIAS BIOLÓGICAS** en el campo de conocimiento de **Biología Evolutiva** de la estudiante **BORJA MARTÍNEZ GABRIELA ARIDAI** con número de cuenta **307030308** con la tesis en la modalidad de artículo científico, titulada: **“Highland forest’s environmental complexity drives landscape genomics and connectivity of the rodent Peromyscus melanotis”**, que es producto del proyecto realizado en la maestría que lleva por título: **“Ratón de orejas negras (*Peromyscus melanotis*) como indicador de conectividad en el Parque Nacional La Malinche”**, , realizada bajo la dirección del **DRA. ELLA GLORIA VÁZQUEZ DOMÍNGUEZ**, quedando integrado de la siguiente manera:

Presidente: DR. LEOPOLDO GALICIA SARMIENTO
Vocal: DR. JUAN PABLO JARAMILLO CORREA
Vocal: DR. LUIS DANIEL ÁVILA CABADILLA
Vocal: DRA. ITZEL ARIAS DEL RAZO
Secretario: DRA. ALICIA MASTRETTA YANES

Sin otro particular, me es grato enviarle un cordial saludo.

A T E N T A M E N T E
“POR MI RAZA HABLARÁ EL ESPÍRITU”
Ciudad Universitaria, Cd. Mx., a 20 de julio de 2021

COORDINADOR DEL PROGRAMA

DR. ADOLFO GERARDO NAVARRO SIGÜENZA



COORDINACIÓN DEL POSGRADO EN CIENCIAS BIOLÓGICAS

Unidad de Posgrado, Edificio D, 1º Piso. Circuito de Posgrados, Ciudad Universitaria
Alcaldía Coyoacán. C. P. 04510 CDMX Tel. (+5255)5623 7002 <http://pcbiol.posgrado.unam.mx/>

Esta tesis se realizó en el Laboratorio de Genética y Ecología, Instituto de Ecología, Universidad Nacional Autónoma de México

Agradecimientos Institucionales

Al Posgrado en Ciencias Biológicas de la Universidad Nacional Autónoma de México por el apoyo proporcionado en sus aulas y fuera de ellas durante la conclusión del programa de estudios y el presente trabajo de tesis.

A la Comisión Nacional de Ciencia y Tecnología (CONACyT) por el financiamiento del proyecto (SRE CONACyT: 286794), y por la beca que me fue otorgada durante el periodo 2018-2020 (CONACyT CVU: 887756). Asimismo, al Programa de Becas Mixtas (CONACyT) y al programa de Apoyo a los Estudios de Posgrado (PAEP-UNAM) por el apoyo otorgado en 2019 para realizar una estancia de investigación.

Agradecimientos a título personal

La perspectiva a la distancia borra recuerdos y la objetividad y la experiencia les resta importancia, pero quizá, sin saberlo a ciencia cierta, esta ha sido una de las etapas más difíciles. Paradójicamente es también una de las más felices. Es por ello que esta tesis es una oda a las ciencias, a la vida y a la resiliencia; en todos los sentidos filosóficos o biológicos que la palabra vida pueda tener.

A los fascinantes ratones de orejas negras (*Peromyscus melanotis*), por permitirme realizarme académica y emocionalmente, porque no dejan de sorprenderme, de mostrarme lo limitadas que son nuestras aproximaciones y qué miles de preguntas se extienden más allá de nuestras manos. Y con ello a quienes me acompañaron en este “frío y peligroso” viaje. Por apoyarme en campo: al Dr. *Alejandro Flores Manzanero*, al M en C. *Christian Quintero Corrales* (a pesar de temerle a los ratones), al M. en C. *Óscar Romero Báez*, a la Dra. *Brenda Solórzano García* y por el apoyo en el muestreo de imágenes con drones y toda la asesoría en el proceso fotogramétrico al Ing. Geólogo *Daniel Tapia Flores* y al Dr. *Miguel Castillo Rodríguez*. Al Dr. *Aaron Shafer*, del Wildlife and Applied Genomics Lab, por asesorarme en el análisis de SNPs y permitirme conocer otro país, otra cultura y nuevos amigos. A los miembros del jurado, por enriquecer este trabajo con sus comentarios: *Dr. Leopoldo Galicia Sarmiento*, *Dr. Juan Pablo Jaramillo*, *Dr. Luis Daniel Ávila Cebadilla*, *Dra. Itzel Arias del Razo* y nuevamente a la Dra. *Alicia Mastretta Yanes*. Particularmente a mi asesora, Dra. *Ella Vázquez Domínguez*, quién me acompaña todo el camino. Gracias por impulsar las ideas de tus alumnos, por aprender a la par de nosotros otros enfoques no genéticos, por estimular nuestra mente, por el compromiso que muestras con todos tus alumnos, por tu entusiasmo, tu guía y tu amistad. Gracias por impulsarme a escribir el artículo de la tesis, fue un reto un poco aterrador pero muy estimulante. A la *UNAM*, porque me ha dado todo en sus aulas y laboratorios, y mucho más fuera de ellos.

A todos los miembros del laboratorio, por las pláticas en la terraza, los viernes de chelas y baile, pero también por todos los múltiples consejos académicos. Y una vez llegados los tiempos pandémicos por las reuniones virtuales. Al International Vázquez-team: *Alex, Brenda, Diego, Fernanda, Gerardo, Madisson, Mariana, Óscar, y Tania*. Al Pi-team: *Azalea, Christian, Heri, Idalia, Raquel*. Y al Jaramillo-team: *Gus, Jorge, Sebas y Verito*. Gracias a todos por su amistad y compañerismo.

A quienes tiñen de color el encierro de cuarentena y que lo hicieron también en los tiempos agrestes. A mis amigos de media vida o menos: *Cerezo, Clint, Crono, Gerard, Germán, Mariana, Nancy, Roy, Sebs y Yorch*.

A la familia, toda ella. A mis hermanos de vida *Pitty* (junto con *Chris* y *Leo*), *Daniel* y *Beto*. A los valientes guerreros sobrevivientes de cáncer, tía *Chave*, *La Milinga* y mi *padre*.

Mención aparte se merecen mis padres. Por esa voracidad de saber, cultura y lucha social que los caracteriza. Por ser mi impulso, mi apoyo y ejemplo constante. Por los tiempos difíciles que superamos juntos. Y porque tras un cáncer ya superado y pese a la Covid-19 nos queda vida pa rato. A *Gustavo* y *Teo*. Los amo.

El SARS-CoV-2 se llevó una potente luz, de carácter super fuerte, pero llena de amor, apoyo y ternura para todos sus sobrinos. Te extrañaré un mundo tía! A *Paula Borja Olivares* alias *Flor* (1942-2020).

“Con cada día, se me nacen los ojos del
asombro,
de la tierra parida,
el canto de los pueblos,
los brazos del obrero construyendo...
... y soy una infinita espiral que se retuerce
Entre lunas y soles,
Avanzando en los días,
Desenrollando el tiempo
Con miedo o desparpajo,
Desenvainando estrellas
Para subir más alto, más arriba,
Dándole caza al aire,
Gozándome en el ser que me sustenta,
En la eterna marea de flujos y reflujos
Que mueve el universo
Y que impulsa los giros redondos de la Tierra.

Soy mujer que piensa.

Algun día
Mis ojos
Encenderán luciérnagas “

Gioconda Belli

Índice

Resumen	1
Abstract	2
Introducción general	3
Highland forest's environmental complexity drives landscape genomics and connectivity of the rodent <i>Peromyscus melanotis</i>	12
Supporting Information Appendix 1	51
Supporting Information Appendix 2	69
Supporting Information Appendix 3	81
Discusión y conclusión	94
Referencias	107

Ratón de orejas negras (*Peromyscus melanotis*) como indicador de conectividad en el Parque Nacional La Malinche

Resumen

El objetivo de la genética del paisaje es entender cómo se relaciona el paisaje con los procesos microevolutivos, mediante la estimación de flujo genético y conectividad, y la identificación de discontinuidades genéticas y patrones ambientales asociados a estructura genética y adaptación. El objetivo de este estudio fue evaluar la estructura genética y la conectividad funcional del ratón de orejas negras (*Peromyscus melanotis*), un roedor restringido a bosque templado de tierras altas, en el Parque Nacional La Malinche, a tres escalas geográficas diferentes: global (que incluye las laderas norte (CVM) y noreste (ECLM), regional (cada ladera) y local (5 pisos altitudinales al interior de cada ladera, CVM: 3100-3500 m cada 100 m, ECLM: 2850-3450, cada 150 m). Se utilizaron datos genómicos de tipo dd-RAD (3,711 SNPs) así como datos de percepción remota (imágenes Landsat, LiDAR y fotogrametría aérea) para modelar diversos factores del paisaje (topografía, variables ambientales y estructura de la vegetación en dos y tres dimensiones). A escala global, identificamos tres clusters genéticos diferenciando dos pisos altitudinales al interior de ECLM (3,150 y 3,300m) del resto de los pisos altitudinales de ambas laderas. En concordancia con el Modelo Valle-Montaña, se observó reducida variación genética, un número bajo de migrantes, conectividad limitada y aislamiento de las poblaciones de alta montaña respecto de las poblaciones de baja montaña en CVM. En contraste, en ECLM las poblaciones de alta montaña exhiben alta diversidad genética, baja conectividad y limitado flujo genético en poblaciones de altitudes intermedias. Las variables ambientales locales también difieren entre laderas, donde el Índice de vegetación normalizado (NDVI, por sus siglas en inglés) y altura de la vegetación fueron los principales factores que promueven la conectividad, mientras que en ECLM fueron la altura de la vegetación y profundidad del mantillo. Cabe resaltar que, basado en el modelo tridimensional de la vegetación, identificamos otros factores que limitan la conectividad como los caminos secundarios, los pastizales y las áreas perturbadas. Demostramos además que las variables relacionadas con la alta conectividad se encuentran en zonas de alta montaña, donde el bosque está menos perturbado.

Abstract

Landscape genetics aims to understand how the landscape relates to microevolutionary processes, by estimating gene flow and connectivity, identifying genetic discontinuities and environmental patterns associated with genetic structure and adaptation. The black-eared mouse, *Peromyscus melanotis*, is a quasi-endemic rodent restricted to temperate forest in mexican highlands. Our aim was to evaluate the genetic structure and functional connectivity of *P. melanotis* in La Malinche National Park at three geographic scales: global (north [CVM] and northeast [ECLM] slopes), regional (each slope), and local (five elevation levels within each slope, CVM: 3100-3500m, ECLM: 2850-3450 m). We used genomic dd-RAD (3,711 SNPs), jointly with remote sensing data (Landsat images, LiDAR, aerial photogrammetry) to model landscape features (topography, environmental variables, and vegetation structure in 2 and 3-dimensions). At the global scale, we identified three genetic clusters, differentiating two ECLM levels (3150, 3300m) and all other elevation sites across the CVM and ECLM slopes. In agreement with the Valley-mountain model, we found a low genetic variation in CVM, with isolation between the populations of low and high elevations, rendering limited connectivity and few immigrants. In contrast, ECLM populations at higher elevations showed higher genetic diversity, while lowest connectivity and gene flow were observed at the intermediate levels. Notably, local environmental variables also differed per slope, normalized vegetation index (NDVI) and tree height were the main factors promoting connectivity in CVM, whilst for ECLM it was tree height and litter cover. Interestingly, based on the three-dimensional data, we identified additional factors limiting connectivity, including dirt roads, grasslands, and disturbed areas. Furthermore, we demonstrate that significant variables associated with higher connectivity are found at highest elevations of both slopes where the forest is less disturbed.

Introducción general

Introducción general

Genética del paisaje y conectividad

La genética de poblaciones permite describir y cuantificar la variación genética de las especies y los patrones de variación espacial y temporal de sus poblaciones, a partir de frecuencias alélicas. Asimismo, provee un marco teórico robusto que permite la interpretación de procesos y mecanismos asociados con cambios evolutivos (Allendorf et al., 2013). Por otro lado, la genética del paisaje integra tres campos de estudio: genética de poblaciones, ecología del paisaje y estadística espacial, con el objetivo de identificar discontinuidades genéticas entre poblaciones y/o individuos asociados con factores ambientales y antropogénicos que afectan la dispersión (flujo genético). Con base en dichos patrones de conectividad se pueden identificar factores asociados con la estructura genética, así como procesos de adaptación local (Balkenhol & Fortin, 2016; Manel & Holderegger, 2013; Row et al., 2017). La genética del paisaje provee además información sobre la preferencia de hábitat de las especies y de factores limitantes para su dispersión y distribución, la cual es útil para desarrollar e implementar estrategias de manejo y conservación de áreas naturales protegidas, diseño de corredores, reforestación informada y manejo de especies invasoras (Cleary et al., 2016; Combs et al., 2018; Mateo-Sánchez et al., 2015; Spear and Storfer, 2008; Vanhala et al., 2014)

La dispersión es un proceso determinante en la dinámica local de las poblaciones, definida como el movimiento de los individuos desde el sitio de nacimiento hasta el sitio de reproducción. La capacidad de dispersión de los organismos depende de su tamaño y sus características morfológicas y fisiológicas, entre otros. También depende de factores bióticos y abióticos como las interacciones intra e interespecíficas, la disponibilidad de recursos, la calidad del hábitat y la existencia de barreras geográficas (Matthysen, 2012; Row et al., 2017; Starrfelt & Kokko, 2012). La conectividad se define como el movimiento de los individuos a través del paisaje, que puede estimarse indirectamente con base en el flujo genético (Languth et al., 2010; Polato et al., 2017). Así, la conectividad determina los patrones de estructura genética entre y dentro de las poblaciones, que a su vez es afectada por factores geográficos, antropogénicos, ambientales y por características inherentes a las especies (Garrido-Garduño & Vázquez-Domínguez, 2013). Consta de dos componentes, la conectividad funcional y la conectividad estructural. La primera hace referencia al movimiento de individuos a través de parches de hábitat, conduciendo al movimiento de genes entre poblaciones; esto último cuantificado por la tasa de migración y el flujo genético. La conectividad estructural hace referencia a los parches de hábitat que están

espacialmente ligados y la configuración de éstos en el espacio (Manel & Holderegger, 2013; Munshi-South, 2012; Van Strien, 2017).

El ‘paisaje’ se conoce como el conjunto heterogéneo de parches de hábitat considerados desde la percepción de la especie focal o de estudio. Los parches pueden ser temporal y espacialmente dinámicos, de origen natural o antropogénico, y pueden diferir entre sí en tamaño, distribución, calidad y condiciones bióticas o abióticas. Todo ello afecta no sólo la persistencia de las poblaciones sino la reproducción diferencial, la cantidad y distribución de la variación genética y la estructura de las poblaciones o comunidades (Matthysen, 2012; Row et al., 2017; Spear et al., 2010; Waits & Storfer, 2015; Wiens, 1995). El paisaje puede representarse como superficies de conectividad, capas espaciales con valores de resistencia asignados a las diferentes variables del paisaje; estos valores dependen del grado en que impidan, limiten o faciliten la conectividad (Mastretta-Yanes et al., 2015; Peterman, 2017; Spear et al., 2016). Entre las hipótesis más comunes en genética del paisaje podemos mencionar el aislamiento por resistencia, definido como la asociación estadística de distancias genéticas con distancias de resistencia debido a la fricción del paisaje (McRae et. al., 2008; Munshi-South et al., 2016); y el aislamiento por ambiente, donde las variables del paisaje se encuentran distribuidas en gradientes asociados a presiones selectivas que pueden conducir a poblaciones estructuradas (Polato et al., 2017).

Genómica y bioinformática

Los SNPs (single nucleotide polymorphisms, por sus siglas en inglés) son mutaciones puntuales en las secuencias de ADN (Eguiarte et al., 2013). Los SNPs suelen ser bialélicos y se localizan tanto en regiones codificantes como no codificantes; tienen una tasa de mutación de moderada a alta y niveles moderados de variación. Dichas características son relevantes para evaluar diversas escalas espaciales y temporales, mientras que por el alto número de loci que se obtienen con las técnicas de secuenciación de nueva generación es posible resolver, a escala muy fina, la estructura genética aún en individuos cercanamente relacionados (Bradbury et al., 2015; McCormack et al., 2012; Zhu et al., 2016). Ello aporta alta precisión para estudiar la historia evolutiva de las especies, la variación genética dentro y entre poblaciones, la historia demográfica, los procesos de adaptación local y los efectos del paisaje (Vega et al., 2017).

Los métodos de secuenciación de nueva generación (Next-generation sequencing technologies) han permitido que pueda hacerse genómica con organismos modelo y no modelo. En particular, los métodos de representación reducida del genoma, basados en

enzimas de restricción, permiten reducir la complejidad del genoma y muestrear de forma consistente y reproducible múltiples loci (SNPs), empleando una o dos enzimas (doble digestión) (Soha et al., 2013). De igual forma, la secuenciación de fragmentos puede ser en una sola dirección (single-end) o puede ser en ambos sentidos (double-end). Los métodos de representación reducida del genoma incluyen arreglos de SNPs, RRLS (Reduced-Representation Libraries, por sus siglas en inglés), CroPs (Complexity Reduction of Polymorphic Sequences), GBS (Genotyping by Sequencing), RAD-seq (Restriction Site Association DNA Sequencing) y dd-RAD (Double Digestion Restriction Site Association DNA Sequencing) (Davey et al., 2011; Peterson et. Al., 2012; Wang et al., 2017).

La secuencia de análisis bioinformáticos requeridos para trabajar con SNPs son múltiples, que en breve incluyen: el ensamblado de lecturas y alineado con el genoma de referencia o cuando éste no está disponible, ensamblando *de novo*; el llamado de SNPs, con el cual se determina el genotipo de cada individuo por locus y se identifican los sitios variables entre individuos; y la aplicación posterior de filtros estadísticos para eliminar falsos positivos y generar un intervalo de confianza en la calidad de las variantes (Nielsen et al., 2011). Por tanto, es importante tener en mente que las inferencias genéticas realizadas son producto de una señal biológica pero también del procesamiento bioinformático (Shafer et al., 2017).

Sensores remotos en estudios del paisaje

La percepción remota permite obtener información de objetos y áreas distantes mediante sensores, los cuales detectan la energía reflejada por la Tierra. Los sensores pueden ser pasivos, cuando responden a estímulos externos de energía natural, o activos cuando utilizan un estímulo interno, emitiendo pulsos laser a la Tierra y midiendo el tiempo que estos tardan en reflejarse (NOAA, 2020). El uso de percepción remota permite obtener imágenes consistentes de la tierra a largo plazo (Balkenhol & Fortin, 2015), lo cual ha revolucionado campos como la ecología, la conservación y la genética. Se han utilizado diversas tecnologías para el estudio del paisaje y la dinámica de las especies, incluyendo sensores de moderada resolución espacial o Landsat, los cuales trabajan con 11 bandas espectrales a 30 metros de resolución; sensores de alta resolución espacial como IKONOS, QuickBird y Orb View-3, cuya resolución va de 0.5 a 10 metros; sensores hiperespectrales que generan cientos de bandas espectrales y entre los cuales encontramos sensores como Hyperion, CHRIS, y FTHSI; así como los térmicos infrarrojos (AVHRR, POES y ASTER), constelaciones de pequeños satélites (DMC) y tecnologías LiDAR (Wang et al., 2010). Las

imágenes Landsat son imágenes satelitales en dos dimensiones basadas en 10 bandas del espectro electromagnético, ubicadas entre el espectro visible y el infrarrojo cercano (443-1610 nm); se utilizan en particular las regiones rojo, azul, verde, ultravioleta, infrarrojo cercano, infrarrojo e infrarrojo de onda corta (Beaulne, 2018). Las imágenes Landsat han permitido mapear la Tierra de forma continua, así como monitorear cambios de uso de suelo, variables climáticas y funciones ecosistémicas a escala global (D'Urban et al., 2020).

Por otro lado, las imágenes espectrales en tres dimensiones tienen un enorme potencial ecológico, por ejemplo, permiten obtener una representación fina de variables paisajísticas en hábitats estructuralmente complejos, ayudando a entender las relaciones organismo-hábitat. Dichas imágenes pueden ser generadas por dos vías, tecnología LiDAR (Laser Imaging Detection and Ranging data) o por fotogrametría (D'Urban et al., 2020; Milanesi et al., 2017). La fotogrametría permite obtener medidas espaciales fiables por medio de un conjunto sobrelapante de fotografías digitales en dos dimensiones, a partir de las cuales es posible generar ortofotos, ortomosaicos, nubes de puntos y modelos digitales de superficie, estos últimos, promediando la elevación de los puntos en una celda de dos dimensiones (Wilson, 2019). El LiDAR, también llamado altimetría láser, determina la posición tridimensional de los objetos en función a la posición e intensidad de la energía emitida por un láser, la cual colisiona con la superficie de interés y es re-emitida al sensor (Guo et al., 2018; Wang et al., 2010).

El uso de imágenes tridimensionales para generar y evaluar modelos de la estructura tridimensional de la vegetación, considerando características como la cobertura del dosel, la altura de la vegetación, la complejidad vertical del dosel, la biomasa y el volumen de la vegetación (Guo et al., 2018; Jaime-González et al., 2019) es cada vez más común, particularmente en inventarios forestales, pero también para descripciones morfológicas de los organismos y la evaluación de hábitat (Tabla 1). Cabe hacer notar que el papel de la estructura tridimensional de la vegetación en la conectividad es un campo poco explorado, sobretodo en paisajes complejos como los bosques templados y bosques tropicales.

Tabla1. Uso de tecnologías LiDAR y fotogrametría en estudios ecológicos y genéticos.

Tópico de estudio	Especie focal	Método	Referencia
Inventarios forestales	Bosques	Fotogrametría	Rahlf et al., 2017
Deforestación, degradación, recolonización de bosques	Bosque de abetos	LiDAR	Pettorelli et al., 2014
Conectividad estructural de bosques	Bosque sujeto a manejo	LiDAR	Guo et al., 2018
Estructura de colonias de arrecife de coral	<i>Acropora sp.</i>	Fotogrametría	Bayley et al., 2019
Estructura del hábitat en función de abundancias	<i>Apodemus sylvaticus</i>	LiDAR	Jaime-González et al., 2017
	<i>Haematopus bachmani</i>	LiDAR	Hollenbeck et al., 2014
Idoneidad de hábitat	<i>Arborimus longicaudus</i>	Fotogrametría	Linell et al., 2018
Conectividad funcional	<i>Sylvilagus transitionalis</i>	LiDAR	Amaral et al., 2016
	<i>Tetrao urogallus</i>	LiDAR	Milanesi et al., 2017

Bosques templados de tierras altas mexicanas

México es un país con una alta diversidad de ecosistemas, incluyendo desiertos, pastizales, manglares, selva seca, bosque tropical lluvioso, bosque nublado y bosque templado. El bosque templado ocupa el 31% de la superficie terrestre y en México ocupa el segundo lugar en extensión, cubriendo cerca del 21% del territorio nacional; está restringido a zonas de montaña y sólo el 4% está bajo alguna categoría de protección dentro de un Área Natural Protegida (Velázquez et al., 2000). El bosque templado es dominado por pinos, encinos y oyameles, presenta una marcada temporada de sequía de febrero a junio y la temporada de lluvias de julio a octubre (Rzedowski, 2006). Entre sus principales amenazas se encuentran los incendios forestales, la deforestación y el cambio de uso de suelo para pastoreo y agricultura. Se estima que en México se pierde el 0.01% de bosque cada año, cifra que incluye a los bosques templados y los bosques mesófilos de montaña (Velázquez et al., 2000).

Los bosques son hábitats que presentan una estructura de la vegetación vertical y horizontal compleja, lo que aumenta la disponibilidad de nichos y permite la coexistencia de

especies con una amplia gama de especializaciones (Milanesi et al., 2017; Pelletier et al., 2014; Velázquez et al., 2000). Los bosques de montaña se distinguen además por presentar gradientes altitudinales caracterizados por cambios drásticos en la composición de las comunidades vegetales, así como cambios ambientales y climáticos marcados en distancias geográficas cortas (Féijo et al., 2019). Los gradientes altitudinales comúnmente se correlacionan con los gradientes de temperatura; mientras que estos últimos junto con la precipitación modulan la distribución y abundancia de especies arbóreas (Santibañez-Andrade & Castillo-Argüero, 2009). Su complejidad ambiental depende además de las características topográficas como pendiente, orientación y altitud (Santibañez-Andrade & Castillo-Argüero, 2009). En este contexto, la estructura de la vegetación es un componente clave en la calidad del hábitat, ya que de ella depende la persistencia de las especies y numerosos procesos ecológicos, como la retención de suelos, la disponibilidad de alimento, la dispersión de semillas, la migración, la dispersión y el flujo genético.

La respuesta de las especies a la complejidad de los bosques templados depende de la cobertura vegetal de bosque maduro y de la composición de la matriz. Por ejemplo, el efecto de la fragmentación en bosques es mayor cuando se tiene una menor cobertura vegetal y poco bosque maduro; asimismo, los bosques inmersos en matrices heterogéneas suelen tener mayor conectividad por su mayor disponibilidad de recursos tanto para especies generalistas como especialistas, como en el caso de los bosques secundarios (Carrara et al., 2014). Por otro lado, los gradientes altitudinales también moldean la respuesta de las especies, afectando la dispersión y la estructura de las poblaciones asociado con el aislamiento que existe entre las zonas de baja y alta montaña, así como por procesos de adaptación local (Polato et al., 2017). En particular en los roedores, la preferencia de hábitat en bosques se ha asociado a factores como la cobertura de materia orgánica, la edad del bosque, la estructura de las comunidades vegetales y la heterogeneidad de la matriz (Jaime-Gonzalez et al., 2017).

En el caso particular de nuestro sitio de estudio, el Parque Nacional La Malinche, la composición de la matriz depende del gradiente altitudinal que exhiben las comunidades arbóreas. La ladera noreste se caracteriza por bosque de pino-encino (a los 2850 msnm), donde el dosel es abierto, no hay arbustos y, aunque hay presencia de *Pinus leiophylla* y *Pinus montezumae*, los encinos son la especie dominante. En los 3300m predomina el bosque de pino, que se caracteriza por *P. montezumae* como especie altamente dominante, que crece en regiones donde la lava volcánica produce una topografía irregular, se caracteriza por un dosel abierto y una capa arbustiva, lo que genera una amplia variedad

de microambientes. También están presentes *Pinus pseudostrobus* y *Pinus teocote*. A los 3150m hay bosque de pino-oyamel, zona que constituye el ecotono entre bosque mixto de pino y bosque de oyamel. En la parte más alta, 3300 y 3450 m, predomina el bosque de oyamel (*Abies religiosa*) que crece en áreas de alta humedad como barrancos y pendientes pronunciadas (entre 10-30°) y los suelos son muy ricos en materia orgánica y ceniza. Los bosques más conservados de oyamel se caracterizan por la presencia de musgo como ocurre en ECLM-3300. En contraste, cuando están perturbados el sotobosque es muy abundante por la alta incidencia de luz a través del dosel abierto, paisaje que vemos en ECLM-3450 (Rzedowski, 2006; Santibañez-Andrade & Castillo-Argüero, 2009; Velázquez et al. 2000). Mientras que las comunidades vegetales de la ladera norte son comparativamente más homogéneas. Los pisos altitudinales de 3150 y 3200m están compuestas por un bosque de coníferas mixto, dominando *P. montezumae* pero donde también es posible encontrar *Quercus sp.*, *A. religiosa*, *Juniperus sp.*, y *Alnus sp.* La composición a los 3300 y 3400m es de bosque de pino-alnus (*P. montezumae*) y a 3500m es bosque mixto de pino-oyamel (*Pinus hartwii*). Los bosques pino-alnus están formados por tres capas estructurales: arboles de coníferas, arbustos y pastos densos; este tipo de bosque suele remplazar los bosques primarios cuando ocurre algún disturbio (Rzedowski, 2006).

Roedores y *Peromyscus melanotis*

Los roedores son un grupo taxonómico caracterizado por una limitada capacidad de dispersión, tamaño corporal pequeño, tiempos generacionales cortos y una amplia diversidad de historias de vida, lo que los hace ideales para estudios de evolución y genética del paisaje (Flores-Manzanero & Vázquez-Domínguez, 2019; Villanueva-Hernandez et al., 2017). El género *Peromyscus*, que incluye al menos 56 especies (Fernández et al., 2010), ha sido poco estudiado en México y América Central, a pesar de su amplia distribución y su alta diversidad (Bedford & Hoekstra, 2015). Se pueden mencionar estudios ecológicos sobre selección de hábitat en la Faja Volcánica Transmexicana, realizados con *Peromyscus difficilis*, *P. pectoralis* y *P. boylii* (Villanueva-Hernández et al., 2017); y sobre proporción de hábitat no transformado de un conjunto de 17 especies endémicas, incluyendo *P. aztecus*, *P. furvus*, *P. melanophrys* y *P. melanotis* (Sánchez-Cordero et al., 2005). Considerando estudios genéticos y genómicos, existen ejemplos con *P. leucopus* y *P. maniculatus*, especies modelo que han sido mucho más estudiadas en Norteamérica, entre los estudios resaltan los que analizan el efecto de la urbanización (Munshi-South et al., 2012; Munshi-

South et al., 2016; Richardson et al., 2020), de sistemas agroforestales (Howell et al., 2017) y bosques fragmentados (Anderson & Meikle, 2010) en la conectividad, tamaño poblacional efectivo, y tasa de migración de dichas especies; y los que han estudiado señales de adaptación local a la urbanización (Harris et al., 2013; Harris & Munshi-South, 2017) y selección natural divergente en poblaciones crípticas, en función de la coloración del suelo (Barret et al., 2019). Un ejemplo de genómica enfocada a conservación es el estudio con *P. melanophrys* que analiza los patrones de conectividad considerando factores ambientales y antrópicos en selvas secas de México (Vega et al., 2017).

El ratón de orejas negras *Peromyscus melanotis* (Rodentia: Cricetidae) es una especie casi endémica de las tierras altas mexicanas, con una distribución discontinua desde algunas montañas aisladas de Arizona hasta la Sierra Madre Oriental, la Sierra Madre Occidental, la Faja Volcánica Transmexicana y el centro del Altiplano mexicano (Álvarez-Castañeda, 2005). Habita en bosque mesófilo, bosque de coníferas y zacatal, es muy abundante en bosque de pino y encino, en un rango altitudinal entre los 2,100 a 4,300 msnm (Castro-Campillo et al., 2008; Fa et al., 1990; Flores-Peredo & Vázquez-Domínguez, 2016; García-Mendoza et al. 2018), particularmente en hábitats rocosos con pendientes pronunciadas y presencia de pastizales (Álvarez-Castañeda 2005). *Peromyscus melanotis* presenta un ámbito hogareño de 420.8 m² (Fa et al. 1996) y hábitos escansoriales, es decir, utiliza tanto el suelo como el estrato arbóreo, se alimenta de semillas y plantas herbáceas estacionales, así como de insectos con alto contenido de cardenolidos, como la mariposa monarca (Gleedining et al. 1988). Presenta dimorfismo sexual, las hembras son más grandes que los machos (Martínez-Coronel et al., 1991), alcanzando un tamaño promedio de 40g.

Entre los estudios realizados con *P. melanotis* podemos citar el uso de espacio diferencial entre hembras y machos (De la Cruz et al., 2019) y variaciones de abundancia en función de las comunidades vegetales (Flores-Peredo & Vázquez-Domínguez, 2016). Estudios morfológicos y fisiológicos incluyen evaluación de variación poblacional en la producción de testosterona (Castro-Campillo et al., 2012), variación del cráneo en función de la elevación y la productividad primaria (García-Mendoza et al., 2018), y daño tisular causado por la contaminación atmosférica en poblaciones cercanas a la Ciudad de México (Gómez-Ugalde, 2003). Se han realizado pocos estudios genéticos y estos han sido enfocados en términos taxonómicos para evaluar las relaciones filogenéticas al interior del grupo de especies de *P. maniculatus* (Bowers, 1973; Chirhart et al., 2005; Hogan et al.,

1997). Cabe resaltar que, en nuestra revisión, no encontramos ningún estudio genético con enfoque poblacional o del paisaje con esta especie.

La gran abundancia y alta afinidad de este roedor a bosques de alta montaña, así como su ciclo de vida corto, lo hacen un sistema idóneo para evaluar cómo la complejidad del paisaje afecta los patrones ecológicos y de variación genética en diferentes escalas geográficas. Es también un claro indicador de la conectividad en el bosque templado del Parque Nacional La Malinche, a lo largo de su amplio gradiente altitudinal (1000-4400 m), ambiental y climático.

Objetivos

El objetivo general de este trabajo fue evaluar la estructura y conectividad de *Peromyscus melanotis* en el Parque Nacional La Malinche (PNLM), utilizando marcadores genómicos (SNPs). Como objetivos particulares se planteó caracterizar los niveles de diversidad genética, la estructura y diferenciación genética a nivel global y al interior de dos laderas del PNLM, y evaluar la conectividad estructural y funcional con base en variables topográficas (pendiente, aspecto del terreno y posición topográfica), ambientales (elevación, temperatura, humedad y profundidad del mantillo), y de estructura de vegetación en dos y tres dimensiones (NDVI, altura de la vegetación).

Hipótesis y predicciones

Dado el gradiente altitudinal que caracteriza los ambientes de montaña, el papel fundamental de la vegetación como fuente de alimento y protección, así como la baja vagilidad de *Peromyscus melanotis*, la conectividad estará influenciada en mayor grado por la estructura vertical (altura de la vegetación) y horizontal (NDVI) de la vegetación, la pendiente, la temperatura y la humedad. También se espera encontrar diferenciación genética entre laderas y al interior de éstas asociada con diferenciación entre poblaciones de alta y baja montaña.

Estructura de la tesis

La presente tesis consta de cuatro secciones, introducción general, artículo científico “Highland forest’s environmental complexity drives landscape genomics and connectivity of the rodent *Peromyscus melanotis*” enviado a la revista *Landscape Ecology*, una discusión general, seguida de la literatura citada tanto en la introducción como en la discusión.

Artículo científico

**Highland forest's environmental complexity drives
landscape genomics and connectivity of the rodent
*Peromyscus melanotis***

Enviado a *Landscape Ecology*

Landscape Ecology
Highland forest's environmental complexity drives landscape genomics and connectivity of the rodent *Peromyscus melanotis*
--Manuscript Draft--

Manuscript Number:	LAND-D-21-00187	
Full Title:	Highland forest's environmental complexity drives landscape genomics and connectivity of the rodent <i>Peromyscus melanotis</i>	
Article Type:	Original research	
Keywords:	aerial photogrammetry; functional connectivity; genetic structure; landscape ecology; three-dimension vegetation structure models	
Corresponding Author:	Ella Vázquez-Domínguez, Ph.D. Instituto de Ecología, UNAM México, DF MEXICO	
Corresponding Author Secondary Information:		
Corresponding Author's Institution:	Instituto de Ecología, UNAM	
Corresponding Author's Secondary Institution:		
First Author:	Gabriela Borja-Martínez, Masters	
First Author Secondary Information:		
Order of Authors:	Gabriela Borja-Martínez, Masters Daniel Tapia-Flores, Masters Aaron B.A. Shafer, PhD Ella Vázquez-Domínguez, Ph.D.	
Order of Authors Secondary Information:		
Funding Information:	Consejo Nacional de Ciencia y Tecnología (CONACyT-SER grant # 286794) Consejo Nacional de Ciencia y Tecnología (CONACyT (887756))	Dr. Ella Vázquez-Domínguez MSc Gabriela Borja-Martínez
Abstract:	<p>Context Deciphering how environmental complex dynamics of highland temperate forests drive local patterns of ecological and genetic variation is key to understanding species diversity and distribution.</p> <p>Objectives Evaluate how the three-dimensional environmental complexity of La Malinche volcano influences patterns of ecological and genomic variation in <i>Peromyscus melanotis</i>, across three geographic scales, global (encompassing north (CVM) and northeast (ECLM) slopes), regional (each ECLM and CVE slope), and local (elevational gradient per slope).</p> <p>Methods Using reduced representation genomic sequencing we estimated population genetic diversity, subdivisions and migration rates. Remote sensing data and image processing were used to characterize landscape variables with their effect on connectivity using resistance surfaces, circuit theory and omnidirectional connectivity.</p> <p>Results We identified three genetic clusters at the global scale, differentiating two ECLM levels (3150, 3300m). Regionally, we found reduced genetic variation, limited connectivity, fewer immigrants and isolation in higher elevation CVM populations (valley-mountain model). ECLM populations showed higher genetic diversity and lowest connectivity at intermediate levels. Local environmental variables also differed, NDVI and tree height were the main factors promoting connectivity in CVM, whilst adding litter cover in ECLM.</p> <p>Conclusions Based on a two and 3D-landscape analyses framework, we showed how the forest environmental complexity across different geographic scales drives</p>	

Powered by Editorial Manager® and ProduXion Manager® from Aries Systems Corporation

Running head: Highland *P. melanotis* landscape genomics

Highland forest's environmental complexity drives landscape genomics and connectivity of the rodent *Peromyscus melanotis*

Gabriela Borja-Martínez^{1,4}, Daniel Tapia-Flores², Aaron B.A. Shafer³ and Ella Vázquez-Domínguez^{1,*}

¹ Departamento de Ecología de la Biodiversidad, Instituto de Ecología, Universidad Nacional Autónoma de México, Coyoacán, Ciudad de México 04510, México.

² Departamento de Dinámica Terrestre Superficial, Instituto de Geología, Universidad Nacional Autónoma de México, Coyoacán, Ciudad de México 04510, México.

³ Department of Forensics & Environmental and Life Sciences Graduate Program, Trent University, Peterborough, ON, K9L 0G2, Canada.

⁴ Posgrado en Ciencias Biológicas, Universidad Nacional Autónoma de México, Edificio D, 1er Piso, Unidad de Posgrado, Ciudad de México, 04510, México.

* Corresponding author: evazquez@ecologia.unam.mx; +5255 56229015

Gabriela Borja-Martínez: Orcid number 0000-0003-2512-7051

Aaron B.A. Shafer: Orcid number 0000-0001-7652-225X

Ella Vázquez-Domínguez: Orcid number 0000-0001-6131-2014

Abstract

Context Deciphering how environmental complex dynamics of highland temperate forests drive local patterns of ecological and genetic variation is key to understanding species diversity and distribution.

Objectives Evaluate how the three-dimensional environmental complexity of La Malinche volcano influences patterns of ecological and genomic variation in *Peromyscus melanotis*, across three geographic scales, global (encompassing north (CVM) and northeast (ECLM) slopes), regional (each ECLM and CVE slope), and local (elevational gradient per slope).

Methods Using reduced representation genomic sequencing, we estimated population genetic diversity, subdivisions and migration rates. Remote sensing data and image processing were used to characterize landscape variables with their effect on connectivity using resistance surfaces, circuit theory and omnidirectional connectivity.

Results We identified three genetic clusters at the global scale, differentiating two ECLM levels (3150, 3300m). Regionally, we found reduced genetic variation, limited connectivity, fewer immigrants and isolation in higher elevation CVM populations (valley-mountain model). ECLM populations showed higher genetic diversity and lowest connectivity at intermediate levels. Local environmental variables also differed, NDVI and tree height were the main factors promoting connectivity in CVM, whilst adding litter cover in ECLM.

Conclusions Based on a two and 3D-landscape analyses framework, we showed how the forest environmental complexity across different geographic scales drives dispersal, genomic structure and connectivity patterns in this rodent. Notably, with the three-dimensional data we identified dirt roads and disturbed areas limiting connectivity, whereas higher connectivity at the highest elevations where the forest is less disturbed. We demonstrated the utility in incorporating multidimensional variables into landscape genetic analyses.

Key words aerial photogrammetry; functional connectivity; genetic structure; landscape ecology; three-dimension vegetation structure models

Introduction

Highland temperate forests are characterized by complex dynamics associated with high environmental heterogeneity, which generates an ample array of niches that allow habitat and ecological specializations for a diverse set of taxa (Mastretta-Yanes et al. 2015; Milanesi et al. 2017). Deciphering how such environmental complexity drives patterns of ecological and genetic variation is key to understanding species diversity and distribution in these ecosystems. Environmental complexity is often related to topographic characteristics (e.g. slope, orientation, elevation), vegetation structure, soil, and elevational gradients (Pelletier et al. 2017; Féijo et al. 2019). The elevational gradients along these montane forests exhibit marked environmental and climatic changes, even at small geographic scales, enabling the development of different tree communities (Velazquez et al. 2000; Rzedowski 2006; Henry and Rusello 2013). Furthermore, the vegetation structure is a crucial component of habitat quality, tightly linked with ecological processes that support the persistence of diverse species and microhabitats (Mastretta-Yanes et al. 2015; Féijo et al. 2019). Highland temperate forests are the second largest biome in Mexico, covering 21% of the territory; they are distributed on the highest mountains and are dominated by pine, oak, alder (*Alnus*) and fir (*Abies*) species (Velázquez et al. 2000) in an elevational gradient from ca. 1000 m to > 4000 m (Rzedowski 2006).

The amount of old-growth forest cover and the matrix composition are key features that govern the species' responses to highland forest complexity; for example, the effects of fragmentation are stronger in landscapes with low or intermediate forest cover, whereas landscapes with heterogeneous habitat matrices (e.g. with both primary and secondary

forest) generally have more resources and higher species richness (Jaime-González et al. 2017). Topographic features and forest cover also influence landscape connectivity and gene flow (Garrido-Garduño et al. 2016; Adavodi et al. 2019). Moreover, elevational gradients shape the response of species, affecting dispersal and population structure as a result of isolation between low and high elevation levels, in combination with processes of local adaptation due to environmental changes (Funk et al. 2005; Polato et al. 2017; Féijo et al. 2019). Individual dispersal capacity in these landscapes can depend on characteristics like body size, physiology and morphology, while also being affected by biotic and abiotic factors including intra and interspecific interactions, resource availability, habitat quality and geographic barriers (Shafer et al 2012; Row et al. 2017).

Rodents are considered a key ecological component of forests due to their fundamental role on dynamics of these ecosystems, mainly by dispersal of seeds and soil removal. They are characterized by limited movement, small size, short generation time and diverse life histories, which make them ideal to address questions about recent evolution and landscape alterations (Bedford and Hoekstra 2015; Munshi-South et al. 2016; Howell et al. 2017). Rodents inhabiting temperate forests have habitat preferences associated with specific features, including litter cover, vegetation structure, forest age and environmental heterogeneity (Jaime-González et al. 2017). The genus *Peromyscus* has a wide distribution and high diversity across Mexico and Central America, and although it has been well studied taxonomically in this region (e.g. Castañeda-Rico et al. 2014; Pérez-Consuegra et al. 2017; Villanueva-Hernández et al. 2017; De la Cruz et al. 2019), there is considerably less information at the landscape and population level on highland temperate forests. Of note, the black-eared mouse *Peromyscus melanotis* (Rodentia: Cricetidae) is a quasi-endemic species on the Mexican highlands, encompassing a wide and discontinuous distribution from some isolated mountains in Arizona to the Sierra Madre Oriental, the Sierra Madre

Occidental, the Transmexican Volcanic Belt and the center of the Mexican Altiplano (Álvarez-Castañeda 2005).

High-throughput sequencing technologies have permitted the reproducible sampling of thousands of loci across the genome, like single nucleotide polymorphisms (SNPs), for model and non-model species. SNPs are useful to study genomic diversity and population structure, demography, environmental associations and local adaptation of species and populations (Ellegren 2014). Notably, assessments based on SNPs enable to elucidate fine-scale structure among closely related individuals, facilitating the study of genetic and landscape patterns with high precision (Bradbury et al. 2015; Vega et al. 2017). Likewise, obtaining long-term landscape data at different spatial and temporal resolutions has recently been made possible with modern remote sensing tools (Balkenhol and Fortin 2016). Different technologies can be used in remote sensing that encompass sensors with moderate (Landsat) to high spatial resolution, hyperspectral, thermal infrared, small-satellite constellation, and laser imaging detection (LIDAR) (Wang et al. 2010). Additionally, 3D vegetation structure models have recently been used to evaluate landscape features (e.g. canopy cover, tree height, above ground biomass) (Pettorelli et al. 2014; Guo et al. 2018; Jaime-González et al. 2017). The genomic and remote sensing technological revolution has significantly advanced our potential to perform landscape genetic studies from the individual to the population level and from global to rather fine geographic scales.

Our aim was to evaluate how the environmental complexity of a temperate highland forest drives patterns of ecological and genetic variation across different geographic scales in *Peromyscus melanotis*, by coupling genomic and remote sensing data with landscape analyses. We integrated novel imaging and landscape genomic approaches to evaluate the relationship between genomic parameters and landscape features (topography, vegetation structure and environment), and to describe environmental drivers of differentiation and connectivity patterns of this rodent across three geographic scales.

Considering the environmental and topographic characteristics of highland mountain systems, the fundamental role that the vegetation plays by providing resources like food and cover, and the low vagility of *P. melanotis*, we predicted that slope and aspect would significantly influence population genetic differentiation at the global scale, whereas connectivity will be associated with both the vertical and horizontal vegetation structure differently on each slope. The valley-mountain model of population structure (Funk et al. 2005) establishes that gene flow between low and high elevations is limited and that low elevation sites are characterized by higher levels of connectivity than their high-elevation counterparts. Thus, we expected *P. melanotis* to exhibit these patterns along elevation gradients.

Materials and methods

Study species and sampling

Peromyscus melanotis' main habitat is mesophilic and coniferous forests and alpine grasslands (2100-4300 m) (Álvarez-Castañeda 2005; Flores-Peredo and Vázquez-Domínguez 2016). It is a small mouse (adult average weight 40 g).

The Transmexican Volcanic Belt (TVB) in Mexico consists of a series of volcanic structures that extend from east to west (Mastretta-Yanes et al. 2015). La Malinche National Park (PNLM) is characterized by a high elevation temperate forest, where climate and vegetation are associated with the elevational gradient (2,000-4,000m).

We designed a sampling scheme that enabled to analyze the landscape matrix at three scales: a global scale encompassing the north (Centro Vacacional Malinche; CVM) and northeast (Estación Científica La Malinche; ECLM) slopes of the La Malinche volcano; the regional scale defines the connectivity between CVM and ECLM, and the local scale considers the elevation gradient within each CVM and ECLM (Fig. 1). *Peromyscus melanotis* was live-trapped along randomly set transects with Sherman traps during September 2018

on the two slopes, along five elevation levels each (CVM: 3100, 3200, 3300, 3400, 3500 m; ECLM: 2850, 3000, 3150, 3300, 3450 m) (Appendix S2: Table S1). An ear tissue sample was collected and preserved in Eppendorf tubes with 96% ethanol and all individuals were released at the sampling site.

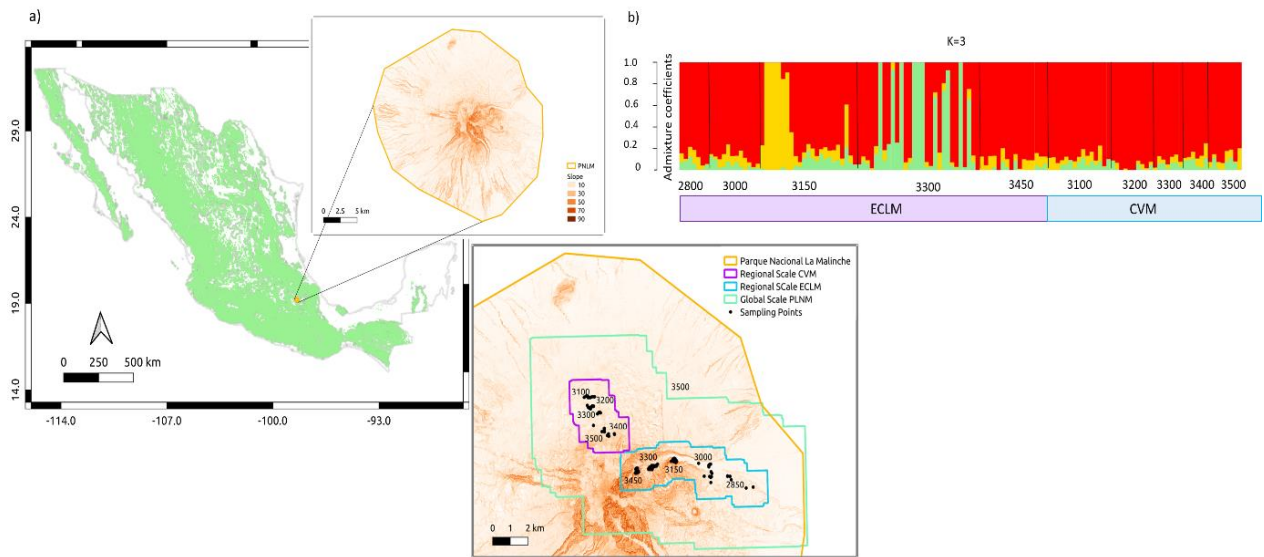


Fig. 1. (a) Map of the study site and sampling localities for *Peromyscus melanotis*. Each quadrant represents the different levels of analyses as per global, regional and local scales. Sampling at the local scale was performed at several altitudinal levels; the regional includes each the north (CVM) and northeast (ECLM) slopes, and the global encompasses all study sites on La Malinche National Park. Dots depict sampled individuals. **(b)** Bar plot of the snmf results at the global scale, indicating individual membership (each vertical line depicts one individual) to three genetic clusters ($K=3$), ECLM-3150 (green), ECLM-3300 (yellow) and all other elevation sites across slopes (red).

Landscape data and images processing

To delimit the regional study area, we calculated the maximum and median dispersion distance, based on the *Peromyscus* known home range of 420.8 m² (Fa et al. 1996), where the maximum dispersal distance=40(home range)^{1/2} was 820.53 m and the mean dispersion distance=7(home range)^{1/2} was 143.59 m (Bowman et al. 2002); accordingly, we generated a 900 m buffer for each study site. We used an additional 1000 m buffer to apply the Koen et al. (2014) method for connectivity (see below); at the global scale we used a 4 km buffer.

We generated three different datasets, for the global (resolution of 100x100 m), the regional (30x30 m) and local (5x5 m) scales. We used Landsat 8 images and environmental data collected *in situ* (temperature, humidity, litter cover) to create environmental surfaces. Values for the entire study area of these three variables were obtained by kriging interpolation using 80% of the data randomly selected, while the remaining 20% was used to calculate the mean square error of the interpolations. The normalized vegetation index (NDVI) and moisture stress index (MSI) were calculated using satellite images (Landsat 8, ID: LC80250472019086LGN00 available at <https://glovis.usgs.gov/>) in ERDAS Imagine v.13.0 and QGIS 3.8. For the topographic data, we used the 'Mexican elevational continuum surfaces' v3.0 for Tlaxcala and Puebla (available at <https://www.inegi.org.mx/app/geo2/elevacionesmex/>), based on which we generated the variables of elevation, aspect, slope in degrees, topographic position Index (TPI), and landforms, with QGIS.

We used two approaches to generate 3D vegetation layers, LiDAR (Laser Imaging Detection and Ranging data) and Digital Aerial Photogrammetry. We created a tree-height layer for regional and global scales using 20 mapping charts for Surface (SDM) and Terrain (TDM) digital models, obtained with LiDAR sensors (available at <https://www.inegi.org.mx>).

For the vegetation height we calibrated the SDM by subtracting the TDM values and reclassified the tree-height map by using zero values as absences and the rest of the values as presence, with the R package raster v.3.4-5 in R (Hijmans et al. 2020) to create the categorical vegetation cover map. The TPI and vegetation cover categorical layers were smoothed to avoid categorization subjective limits, with the *raster.gaussian.smooth* function in spatialEco v.1.3-6 (Evans 2020) in R.

For analyses at the local scale, we applied a photogrammetry approach that allows the generation of three-dimensional point clouds from digital images, from which to extract standard measurements (Rahlf et al. 2017). We used an unmanned aerial vehicle (drone) and took 3,035 georeferenced photos in ISO mode. The photo-alignment (Appendix S3: Figs. S1-S3), the point cloud reconstruction, and the Digital Elevation Model (DEM) were built with Agisoft Metashape 1.5.5. To obtain the vegetation-height, we calibrated the DEM as described for the LiDAR processing.

We evaluated correlation among predictor variables with two tests: collinearity analysis using the Variance Inflation Factor (VIF; Dormann et al. 2013) in usdm v.1.1-18 in R (Naimi 2017), using restrictive parameters (VIF >5) (Appendix S2: Table S2); and a correlation assessment with the function *vifcor* in usdm and a correlation threshold >0.8 (Appendix S2: Table S3).

Genomic sequencing and bioinformatics processing

We extracted genomic DNA from tissue samples with the DNeasy Blood and Tissue Kit (Qiagen), following the manufacturer's instructions. We performed in silico digestions with SimRAD v.0.96 in R (Lepais and Weir 2014) and identified the NsI and MsP_I restriction enzymes, using 10% of the genome of *Peromyscus maniculatus bairdii* (Ensemble: GCA_000500345.1) (Appendix S2: Table S4, Appendix S3: Fig. S4). Library preparation and

sequencing was performed in the University of Wisconsin Biotechnology Center (UWBC) following ddRAD protocol (Parchman et al. 2012).

The bioinformatic pipeline we followed was: demultiplexing of reads with *process_radtags* in Stacks v.2.55 (Catchen et al. 2013); quality filtering using Fastqc and FASTX-toolkit, discarding reads with a low-quality score (<22) and truncating the reads at 120 base pairs. We aligned the resulting reads to the *Peromyscus maniculatus bairdii* genome, using BWA v.0.7.17 under default parameters (Li and Durbin 2009); unpaired reads were removed (Appendix S3: Fig. S5). The *ref_map* pipeline in Stacks was run to call variants and the *populations* module to filter for SNPs present in at least 50% of the samples ($r=0.5$). Several filters were applied with VCFtools v.0.1.16 (Danecek et al. 2011): minimum depth of 10 samples to recognize a SNP as true; minor allele frequency >5%; 10% of samples containing the least frequent allele; only biallelic loci were retained; missing data by locus and by individual >20% were removed; monomorphic and out of Hardy-Weinberg equilibrium ($p>0.05$) loci were eliminated. To verify independent segregation of loci, we performed a linkage disequilibrium analysis within and between chromosomes and estimated identity value by descendent with a kinship analysis (Appendix S3: Fig. S6).

Genetic structure and migration

We inferred genetic structure with a Principal Components Analysis (PCA) in SNPRelate v.1.24.0 and a Discriminant Analysis of Principal Components (DAPC) with adegenet v.2.1.3 in R (Jombart et al. 2008); this approach does not assume any genetic model and uses the a-score method that determines the proportion of successful reassignment by individual in function of the number of retained PCs (15 PCs for ECLM and 21 for CVM). Coancestry levels genetic groups (K) were evaluated with Admixture v.1.3 (Alexander and Lange 2011) and snmf (LEA v.3.2.0 library in R; Fritchot et al. 2014), respectively. We tested from $K=1$ to 10 with 20 replicates for each K (global scale) and $K=1$ to 5 (regional scale). Admixture and

`snmf` use a cross-validation method in which a dataset with 10% of masked genotypes is created and a training set is used to evaluate the ability to correctly impute masked genotypes.

We analyzed migration with BA3-SNPs v.1.1 (Mussmann et al. 2019) using the BayesAss method to estimate recent bidirectional migration rates and identify recent migrants (first and second generations) and their source population. In this case, each elevation level was assumed as a population. We also estimated pairwise F_{ST} between populations with `hierfstat` v.0.5-7 in R (Goudet and Jombart 2015). We used Memgene v.1.0.1 in R (Galpern et al. 2014), which considers the spatial component of genetic variation and is adequate when gene flow patterns are expected to be cryptic and variation operates on different spatial scales. It quantifies spatial genetic autocorrelation to find and visualize spatial neighbourhoods in genetic distance data, combining Moran's eigenvectors maps with a regression framework (Priadka et al. 2018). We performed 10,000 permutations with a 0.05 alpha level for significant eigenvector.

Landscape genetic analyses

Genetic distance and structure

We estimated genetic distances based on dissimilarity of individual genotypes by calculating the Euclidean distance-based on PCA with `stats` v.3.6.2 in R. To test isolation by distance (IBD) at global and regional scales, we performed a Mantel test between the genetic and geographic distances with `vegan` v.2.5-6 in R (Oksanen et al. 2011), using 10,000 Spearman permutations. Euclidean geographic distances were estimated in `gstudio` v.1.5.2 in R (Dyer 2014). To evaluate autocorrelation we used `EcoGenetics` v.1.21-5 in R (Roser et al. 2017), by considering all the distances and taking only the first 1000 m of the distribution, with 10,000 Monte-Carlo simulations and Spearman permutations.

Resistance hypotheses and connectivity analyses

We followed the optimization framework developed by Peterman et al. (2014) to determine the resistance values of our surfaces; the fitness of each surface was evaluated based on Maximum-likelihood population effects mixed models (MLPE), to maximize the relationship between the pairwise genetic distance and the pairwise landscape distances, while also accounting for the non-independence of genetic data. We optimized each resistance surface for global and regional scales with the *commuteDistance* function in gstudio, with three independent runs to verify convergence of parameters. Support of the optimized resistance surfaces was assessed with AICc (Akaike's information criterion corrected for small/finite sample size; Akaike 1974) and robustness with the function *Resist.boot* (Peterman et al. 2019). We selected the best-supported features to construct composite hypotheses that potentially affect connectivity in a multi-optimization approach. Specific hypotheses were built considering characteristics of the environment that are biologically relevant for *P. melanotis* (Table 1). Due to uncertainty of environmental variable interpolations, we only tested topography and vegetation structure hypotheses for the global scale.

Table 1. Composite hypotheses of features that potentially affect connectivity for *Peromyscus melanotis* populations in La Malinche National Park, built as a multi-optimization approach and evaluated at the global and regional scales (CVM and ECLM slopes).

Hypothesis	Parameters
Environment	Aspect + Moisture + Slope + temperature + TPI
Hydroperiod	Moisture + NDVI + Temperature + Tree height
Microclimate	Moisture + Temperature
Productivity 1	Litter cover + NDVI + Tree height
Productivity 2	Litter cover + NDVI
Productivity 3	Litter cover + Tree Height
Topography	Aspect + Slope + TPI
Vegetation orientation	Aspect + NDVI + Tree height
Vegetation structure	NDVI + Tree height

We modeled omnidirectional connectivity surfaces using circuit theory to explore current flow, an approach that enables to identify restricted corridors and barriers to movement (Pelletier et al. 2014). We created a buffer with 20% of the regional areas (CVM=1000 m, ECLM=1200 m) and 50 random points (nodes) were selected on those buffers to avoid saturation of current flow within the study area (Koen et al. 2014). To build the global model, all the optimized resistance surfaces obtained in ResistanceGA v.4.1 for each landscape feature were summarized and standardized, dividing by the minimum resistance value to obtain one final resistance layer. In addition, the resistance surface corresponding to the best hypothesis from the multivariate framework was used to create a current density map. We ran Circuitscape 4.0.5 (McRae et al. 2008) to connect each node to all the others, and each connection between nodes generated a current map that was multiplied to create the final map.

An extended description of all the methods and analyses performed is presented in Appendix S1.

Results

A total of 169 *Peromyscus melanotis* individuals were captured over the study area, 58 in the CVM and 111 in ECLM. Genomic data were successfully generated for 152 samples, 73.6% of reads were mapped to the *P. maniculatus bardii* genome and properly paired (Appendix S3: Fig. S5), resulting in an average of 3,973,160 reads per individual (min=1,745,168; max=5,236,054), with a minimum 10X coverage required to call a SNP. We obtained 36% polymorphic loci (166,729 polymorphic sites) prior to filtering. As a result of linkage-disequilibrium pruning (correlation coefficient >0.4), 243 loci in 278 significative interactions were eliminated. Likewise, 15 paired comparisons were detected with a signal

of IBD >0.25 in 8 individuals, which were eliminated. The final dataset based on the applied filters consisted of 135 individuals for the global analyses, 46 and 89 individuals for CVM and ECLM respectively (regional scale), and a total of 3,711 SNPs were called with 1.9% of missing data.

Genetic structure, diversity and migration

Principal component analysis showed minimal differentiation between mountain slopes (CVM and ECLM), except when examining PC4 (Appendix S3: Fig. S7). At the regional scale, two elevation levels in ECLM (3150m and 3300m) showed moderate differentiation. DAPC results showed that the different elevation levels function as separate units in CVM, except for the intermediate levels 3300-3400m that overlapped (Appendix S3: Fig. S8a, b). In ECLM, although four groups were identified (2800-3000m, 3150m, 3300m and 3400m), their separation was less clear (Appendix S3: Fig. S8c, d). Both ancestry population genetic structure analyses (Admixture and snmf) showed $K=3$ as the most likely number of genetic clusters globally (cross validation error=0.532; cross-entropy=0.747), two clusters corresponding to ECLM-3150 and ECLM-3300, while the third cluster included all other elevation sites across the CVM and ECLM slopes (Fig. 1b).

When considering the regional scale, two genetic clusters were obtained with Admixture (cross validation error=0.5407) for ECLM, while three clusters were supported with snmf (cross-entropy=0.7659) (Appendix S3: Fig. S9). In contrast, Admixture detected two clusters (0.6077) and snmf only one (0.8915) for CVM. Genetic diversity results were similar for the CVM and ECLM slopes, with an observed heterozygosity of 0.305 and 0.308, respectively. Within slopes, ECLM showed a pattern where genetic diversity increased along the elevation gradient, where the three highest levels (3300m to 3450m) exhibited the lowest F_{IS} values ($F_{IS}=-0.016$ and -0.007) (Appendix S2: Table S5). The opposite occurred in CVM, where higher elevation levels had lower diversity (3400m, $F_{IS}=0.042$). The F_{ST} pairwise

comparisons between elevation levels per slope showed that the highest elevation levels 3300-3400 ($F_{ST}=0.045$) and 3400-3500 ($F_{ST}=0.042$) were more differentiated in CVM, while the greatest differentiation in ECLM was mostly between the lower levels 2850-3000 ($F_{ST}=0.039$), 2850-3150 ($F_{ST}=0.027$) (Appendix S2: Table S5).

Spatial genetic patterns and migration

Results of the spatial neighborhoods identified three significant Moran's eigenvectors for CVM and, although in total only a small portion of genetic variation can be explained by spatial patterns (mean adjusted $R^2=-0.0017$), it was sufficient to identify neighborhoods that correspond to a landscape pattern: two distinct spatial genetic neighborhoods were identified, a split between the 3400-3500m elevation levels and the rest; the second and third axes separated the 3100m level (Fig. 2; Appendix S3: Fig. S10). A similar pattern was observed for ECLM, but with six significant Moran's eigenvectors (mean adjusted $R^2=0.019$), where the first and fourth axes separated the higher (3450., 3300m) from the lower elevation levels. Furthermore, two splits were also identified for the 3150m and the 3300m levels, each coinciding with a narrow dirt road (Fig. 2; Appendix S3: Fig. S11).

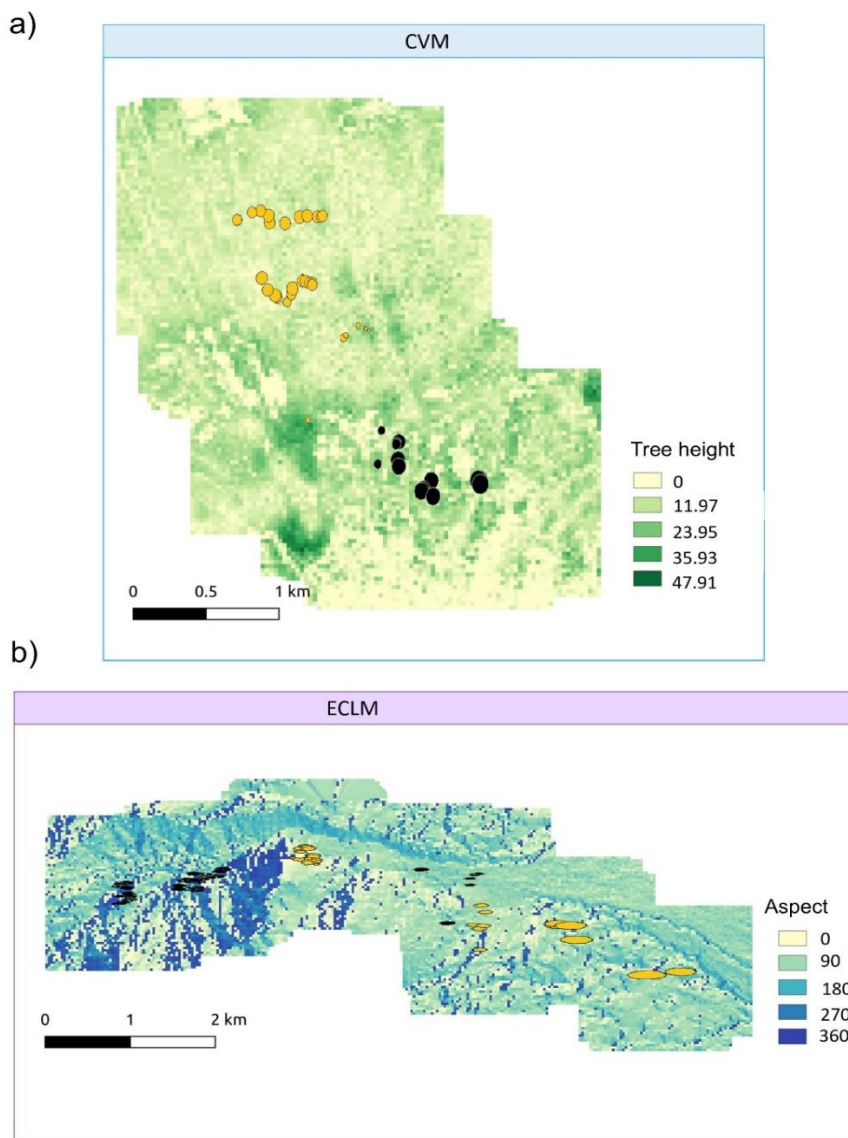


Fig. 2. Genetic neighborhoods estimated with Memgene for *Peromyscus melanotis* from La Malinche National Park. **a)** Results for CVM identified three significant Moran's eigenvectors, explaining 30% of the spatial genetic variation (proportional variances: 0.355, 0.345, and 0.299), **b)** six eigenvectors and 18% variation for ECLM (proportional variances: 0.180, 0.179, 0.178, 0.175, 0.150, and 0.136). The size of the circles is proportional to the autocorrelation value, where circles of similar size and color depict individuals with similar score; color of circles depicts positive and negative autocorrelation in black and orange, respectively. The surface plotted corresponds to the best-supported variable based on AICc (tree height for CVM, aspect for ECLM).

Contemporary bidirectional migration rates indicated a high proportion of resident individuals (0.899) at the 3300m level for the ECLM slope (Fig. 3a), which also contributed the largest number of migrants to the other elevation levels, except to 3150m. Although geographically closest, the 3150m and 3300m levels showed the lowest migration rates between them. For the CVM slope we combined the highest (3400m and 3500m) levels to redefine the populations based on the spatial neighborhoods. This 3400-3500m elevation is formed almost entirely by residents (0.921), receiving few migrants but contributing with the highest migrant rates to all the other levels (Fig. 3b).

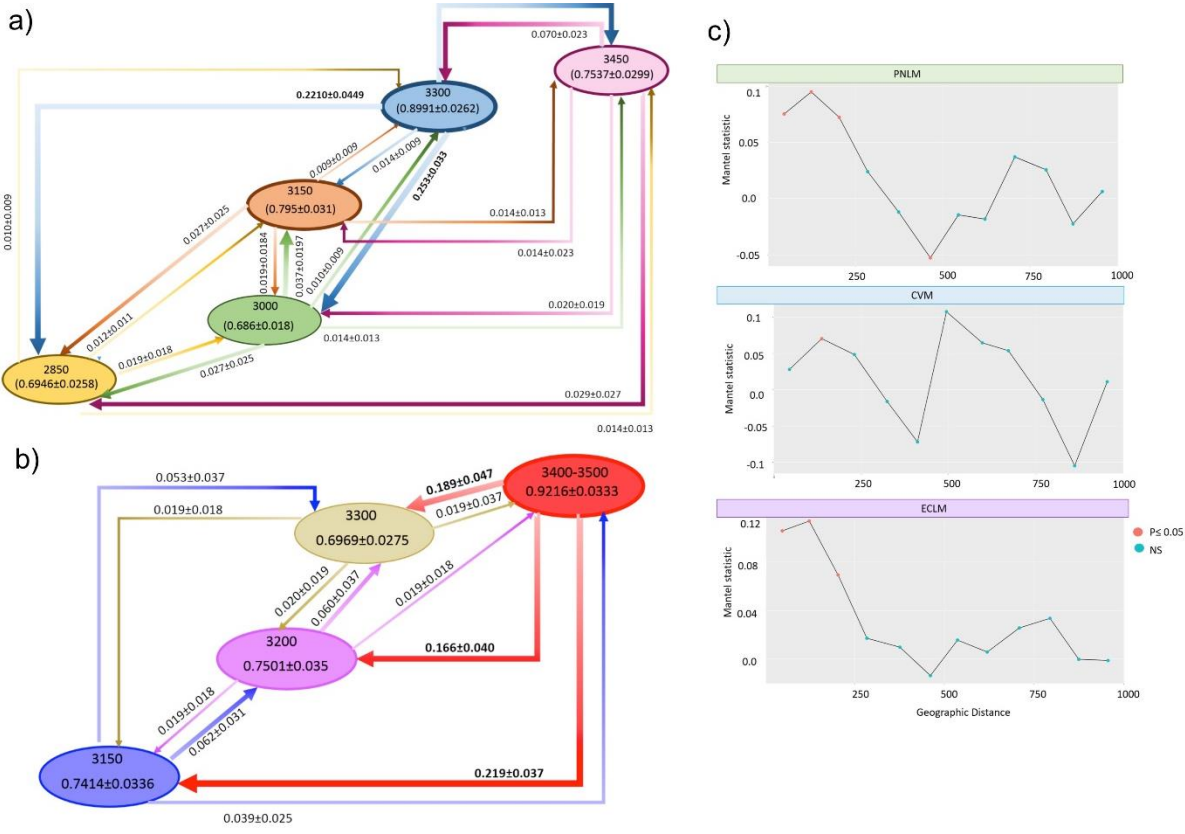


Fig. 3. Bidirectional contemporary migration rates for *Peromyscus melanotis* from La Malinche National Park between elevation levels within (a) the ECLM and (b) the CVM slopes, where the proportion of no migrant individuals by generation per elevation (within the ovals) and the direction of migrant individuals by generation between levels (next to each arrow) are shown. The thickness of the arrows varies depending on the intensity of migration between sites. (c) Mantel correlograms between Euclidean geographic distance (in meters) and genetic distance based on PCA, built considering the first 1000 m of the distribution and divided into 83 m classes. The global and the regional scales (ECLM and CVM slopes) are shown. Significant values are indicated with red circles ($p < 0.05$).

Landscape genomics

The Mantel test showed low and positive significant ($p<0.001$) correlations between geographic and genetic distances for the global (Mantel $r=0.1854$) and regional (CVM Mantel $r=0.1556$; ECLM Mantel $r=0.2925$) scales, showing local genetic structure, in agreement with the Mantel correlograms (Appendix S3: Fig. S12). When only the first 1000m of the distribution were evaluated, both the global and regional scales showed significant positive autocorrelation at the lowest elevations <250m (CVM 181m and ECLM 203m) (Fig. 3c). Results of model selection from the optimization models showed that different landscape variables influenced connectivity patterns in the two slopes, and that the environmental variables evaluated showed better performance than geographic distance in all cases. While the best-supported model in CVM was tree height (explaining almost 50% of the variation), in ECLM it was aspect, explaining 47% of the variation. Another variable related to vegetation, NDVI, was the second most selected model in CVM (38% of variation), while litter cover (36%) was the second for ECLM. Slope (45%) and aspect (30%) were the main factors modelling connectivity between slopes at the global scale (Appendix S2: Tables S6-S9).

Topographic position and NDVI resistance surfaces had a similar trend on both slopes (Appendix S3: Fig. S13). The optimized tree height surface assigned high resistance in ECML to areas without vegetation (<5m), as well as from medium height vegetation (>15m). In contrast, resistance in CVM had a less narrow range (<10m and >30m). High resistance was found for slope values >40 degrees in ECLM, while below 20 degrees in CVM, while the lowest resistance for moisture occurred at 60% in CVM and between 70-80% in ECLM. Aspect, temperature and elevation exhibited contrasting patterns between slopes.

The linear mixed-effects models tests of the composite resistance hypotheses (Table 1) showed that vegetation structure best explained connectivity in CVM ($AIC_c=-1366.12$), followed by Productivity3 (Table 2), where tree height contributed the most to the models (>90%). The three Productivity hypotheses were the best-ranked models in ECLM, litter cover contributing more than 85% to the model. For the global scale, topography and vegetation structure explained 85.6% and 14.4% of the variation, respectively (Appendix S2: Tables S5 and S10). The results of the main connectivity areas depicting high current density regions with high gene flow for CVM showed a surface with resistance values distributed in a heterogeneous spatial configuration (Fig. 4b) and little variation in current density (5.4-10.1). Considering all the variables we evaluated, high elevation levels and the east slope were identified as important connectivity areas. Using vegetation structure as the connectivity indicator, we found a clearly defined pattern, where the current density drops as elevation decreases; thus, the 3400m and 3500m elevation levels reached the highest current density (41.0; i.e. lowest connectivity and highest differentiation). Results for ECLM showed a clearer pattern of optimal and suboptimal zones with high connectivity while, similarly to CVM, the resistance values had a heterogeneous spatial configuration (Fig. 4a). Based on the Productivity3 resistance model, two levels (3150m and 2800m) stand out for being isolated. This pattern is in agreement with the snmf result that differentiated the 3150m level as one genetic cluster.

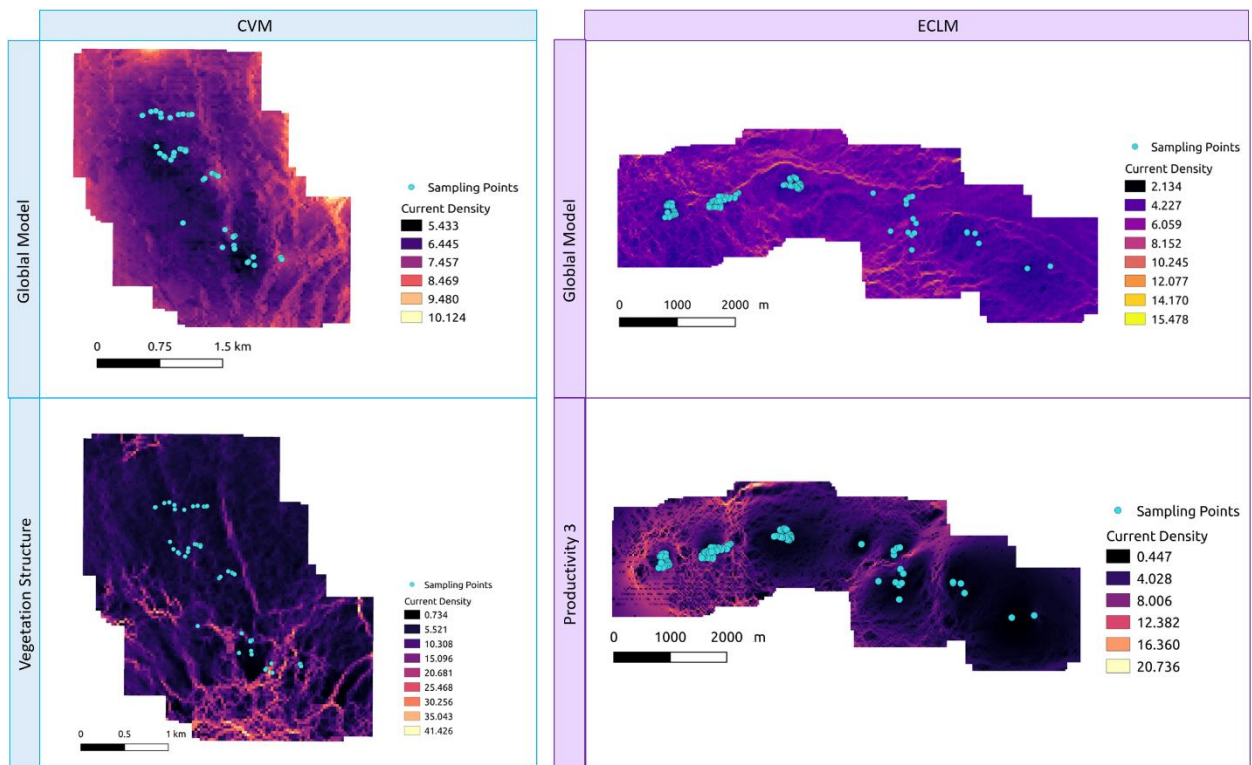


Fig. 4. Current density maps derived from Circuitscape for *Peromyscus melanotis* from (a) the CVM slope and (b) the ECLM slope at La Malinche National Park. The global model was built using all the standardized simple optimization resistance surfaces. The vegetation structure was constructed by a multivariate approach using the best model for CVM (NDVI+tree height, AICc=-1366.12) and for ECLM (litter cover+tree height, AICc=-6001.93) (Table 2).

Table 2. Model selection results for multivariate surfaces optimized showing the contribution percentage (CModel) of each variable to the hypothesis, contrasting the two regional scales (CVM and ECLM slopes). *K = number of parameters used for the transformation of continuous surface plus the intercept; AICc = Akaike's information criterion corrected for sample size. The numbers in parentheses rank the AICc from least to greatest; Top M: Top model.*

Hypothesis	K	Surface	CVM		ECLM			
			AICc	CModel (%)	Top model (%)	AICc	CModel (%)	Top model (%)
Environment	16	aspect	-1329.03 ⁽⁹⁾	23.45	0	-5897.12 ⁽⁹⁾	73.30	0
		moisture		42.39			7.60	
		slope		0.25			0.20	
		temperature		33.65			17.20	
		TPI		0.25			1.40	
Hydroperiod	13	Moisture	-1352.02 ⁽⁷⁾	2.03	0	-5928.60 ⁽⁸⁾	4.40	0
		NDVI		5.47			4.40	
		temperature		2.03			86.79	
		tree height		90.46			4.40	
Microclimate	7	moisture	-1354.45 ⁽⁶⁾	83.45	8.16	-5939.50 ⁽⁷⁾	15.30	0.40
		temperature		16.54			84.60	
Productivity1	10	litter cover	-1360.82 ⁽⁵⁾	2.76	0	-5986.08 ⁽³⁾	88.90	0.59
		NDVI		2.76			5.50	
		tree height		94.76			5.50	
Productivity2	7	litter cover	-1365.13 ⁽³⁾	5.94	38.91	-5998.98 ⁽²⁾	93.10	37.36
		NDVI		94.05			6.80	
Productivity3	7	litter cover	-1366.07 ⁽²⁾	2.73	12.52	-6001.93 ⁽¹⁾	85.00	42.85
		tree height		97.26			14.90	
Topography	10	aspect	-1350.21 ⁽⁸⁾	25.51	0	-5939.95 ⁽⁶⁾	97.20	0.98
		slope		73.81			1.30	
		TPI		0.67			1.30	
		NDVI		2.84		-5943.15 ⁽⁵⁾	78.66	5.66
Vegetation orientation	10	aspect	-1360.86 ⁽⁴⁾	2.84			10.66	
		NDVI		2.84			10.66	
		tree height		94.30			10.66	
Vegetation structure	7	NDVI	-1366.12 ⁽¹⁾	2.77	40.41	-5968.05 ⁽⁴⁾	2.40	12.16
		tree height		97.22			97.50	

Discussion

Using a two- and three-dimension landscape analyses framework, we showed how the forest environmental complexity across different geographic scales, in conjunction with elevational gradients, drive dispersal, genomic structure and connectivity patterns in *Peromyscus melanotis*. This study shows clear promise and value from including 3D vegetation variables to evaluate genetic connectivity in complex environments, like these temperate highlands, as we demonstrated how they were disproportionately important variables in our model. Fine-scale topography and 3D vegetation structure control key variables that can be modeled at finer scales, like microclimate, soil pH, and hydrodynamic forces (D'Urban et al. 2020), and thus influence ecosystem dynamics. *Peromyscus melanotis* is escansorial (i.e. uses both ground and tree spaces), and thus is particularly well suited for a 3D landscape genomic analysis. Moreover, many *Peromyscus* species remain understudied, particularly in Mexico and Central America (Bedford and Hoekstra 2015), but are key players in regional ecosystems. We present the first landscape genome assessment of the black-eared mouse in a Mexican temperate highland forest and the approach applied we hope motivates studies of similar nature.

Geology, vegetation structure and the valley-mountain model

La Malinche or 'Matlalcueyetl' (in nahuatl, *The lady or goddess of the blue skirts*) is an active, yet quiescent stratovolcano, characterized by steep slopes and deep ravines shaped by glacial fluctuations and hydrogeomorphic processes during the late Pleistocene and Holocene (Castillo-Rodriguez et al. 2010; Franco-Ramos et al. 2016). The most recent eruption of La Malinche happened 3,100 years ago, generating a complex topography associated mainly with the northeast and northwest slopes (Castro-Govea and Siebe 2007). Interestingly, the ECLM slope that is located on the Axaltzintle valley has dendrochronological evidence of 17 contemporary lahar events that occurred between 1970

and 2005, distinguished by volcanic debris, rocks, wood, and water tumbling down at high velocities (Franco-Ramos et al. 2016). Such events significantly and recently modified the habitat and, as a result, the ECLM and CVM slopes have markedly different topography and vegetation structure.

Our results at the global scale depict three genetic groups, differentiating two ECLM sites, 3150m and 3300m, and all the other studied sites across both slopes. The highland forest community on ECLM changes drastically along the slope, dominated by pine-oak forest at the lowest elevation (2850m), where oaks are most abundant plus *Pinus leiophylla* and *P. montezumae*, with an open canopy and absence of shrubs, bordering with crop areas. Followed by mixed-pine (3000m; *P. montezumae*, *P. pseudostrobus* and *P. teocote*) and pine-Abies (3150m), the former with an open canopy and shrubby layers found where volcanic lava produced an irregular topography. Fir forests (*Abies religiosa*) dominate on the highest levels (3300-3450m), growing in ravines with steep slopes (10-30°) and high humidity, rich in organic matter and ash; moss is present in the more undisturbed forest at 3300m, but absent at 3450m due to a more open canopy and understory vegetation (Velázquez et al. 2000; Rzedowski 2006). These communities promote different microenvironments and ecological dynamics that can restrict gene flow and lead to genetic differentiation (Bradburd et al. 2013; Henry and Rusello 2013). ECLM-3150 and ECLM-3300, the most divergent environments within this slope, have the highest genetic diversity values, receive the fewest migrants and, despite their geographic proximity, show the lowest migration rates between them. They also supply more migrants to the other elevation sites supporting a pattern of genetic divergence with gene flow and potential local adaptation processes (Henry and Rusello 2013; Barrat et al. 2018), although we did not directly evaluate the latter.

In contrast, the vegetation structure on the CVM slope is characterized by a mixed of coniferous species, dominated by *P. montezumae* but also *Quercus* sp., *A. religiosa*,

Juniperus sp. and abundant *Alnus* sp., present at the lowest 3100m and 3200m levels. The gradient follows with predominantly alder-pine forest (*P. montezumae*) at 3300-3400m, including three structural layers: conifers, shrubs, and dense grass, where primary forest is replaced by mixed forest with alder species as more disturbed forest is found. At the highest 3500m level is mostly pine-fire forest (*Pinus hartewii*) (Rzedowski 2006). Importantly, extractive and touristic activities are more common in CVM, contributing to a higher perturbation than in ECLM. High gene flow limits detecting environmental associated differentiation because it homogenizes neutral genomic regions under weak selection (Adavodi et al. 2019), which is likely the case for *P. melanotis* on CVM. The lack of genetic structuring in this slope could be associated with the more homogenous habitats, allowing for more long-distance dispersal. The maximum dispersal distance estimated based on *Peromyscus*' home range is 820.5 m, males and females show overlapping distributions throughout the year while, during the raining season, mean distance dispersal increases in males and is reduced in females (De la Cruz et al. 2019). Hence, the different genetic structuring across and between ECLM and CVM slopes can reflect historical demographic differences in effective population size and gene flow, due to their distinct ancient and contemporary geomorphologic activity, anthropogenic impact, and the environmental changes along the elevation gradient (Polato et al. 2017).

Indeed, the ECLM and CVM slopes showed different patterns along the elevational gradient. In agreement with the valley-mountain model (Funk et al. 2005), we found reduced genetic variation in higher CVM populations compared with the lower ones. Furthermore, our findings showed that limited gene flow between low and high mountain sites promotes spatial isolation of high altitudes (Polato et al. 2017; Féijo et al. 2019), where the 3400-3500m levels function as a genetic neighborhood (Memegene analysis) with limited connectivity, fewest immigrants and isolation. The pattern observed in ECLM is somewhat different; although contrastingly higher populations have higher genetic diversity, the lowest

connectivity and gene flow occurs at the 3150m and 3300m intermediate levels. The weakest migration occurs between these levels regardless of their geographic proximity, in accord with their observed structure. It is noteworthy the detail detected by the spatial neighborhoods, identifying a split at each 3150m and 3300m levels that coincides with a narrow dirt road. Despite these dirt roads have limited traffic, microclimate can be affected by forest removal, while the increase of forest edges leads to higher evaporation and lower soil moisture (Haugen et al. 2020). Some examples of dirt roads affecting rodent dispersal and genetic structure include *Liomys pictus* inhabiting dry forests (Garrido-Garduño et al. 2016), *Calomys venustus* in agrosystems (Chiappero et al. 2016) and *P. leucopus* in a boreal forest (Howell et al. 2017). The valley-mountain model also postulates high connectivity in lowlands compared with high elevation sites (Polato et al. 2017), a pattern not found in any slope. The latter could be a consequence of the fact that the lowlands on both slopes neighbor highly transformed areas, with disturbed landscapes and potential higher predation risk, which *Peromyscus* species commonly avoid (Léon-Tapia et al. 2020).

Environmental drivers of connectivity

Connectivity studies help to elucidate the ecological and evolutionary role that genetic diversity and adaptation play in wildlife persistence, key to rescue natural populations and maintain genetic diversity in a changing world (Samarasin et al. 2017; Barrat et al. 2018). Genetic structure in forests mammals is often explained by vegetation cover, precipitation, geographic distance and presence of natural barriers (Montgelard et al. 2014; Féijo et al. 2019). Specifically for some *Peromyscus* species, it is known that landscape fragmentation is not enough to explain genetic structure (Howell et al. 2017). Accordingly, we would expect that a variety of environmental and landscape variables influence connectivity patterns in these highland forests.

As we predicted, topography and vegetation structure are the most significant environmental features influencing connectivity on this highland forest rodent in La Malinche. Local topography shapes biophysical attributes like soil distribution, hydrology, and erosion processes (Castillo-Rodríguez et al. 2010). Additionally, aspect influences the intensity and duration of solar energy and radiation, respectively, modulating climate and vegetation communities (Burnett et al., 2008; Meliyo et al. 2014). Topography also affects dispersal, since it can function as a barrier by influencing the choice of routes with lower energy cost (Polato et al. 2017). Indeed, *Peromyscus melanotis* gene flow was best explained by aspect and slope, exhibiting the highest resistance only for values above 40° in the topographically more complex ECLM. Comparatively, CVM showed high resistance for values below 20°. Avoiding gentle slopes as a strategy to evade predators has been documented in *Capreolus capreolus* (Norum et al. 2015); in agreement, cougar movement is associated with slopes below 6° (Dickson et al. 2005). In contrast, *P. difficilis* has been found in habitats with gentle slopes in Sierra de Coneto, Durango (Villanueva-Hernández et al. 2017). Furthermore, as a result of orographic effects, ECLM exhibits higher precipitation and moisture values, which explains the optimum of 70-80% and 60% moisture in ECLM and CVM, respectively. Thermal and moisture tolerance impose ecological and physiological limits to dispersal in different species, specifically affecting demographic processes in small rodents by altering food supply, parasitism and predation. For example, habitat selection in *P. difficilis* depends on high humidity (Villanueva-Hernández et al. 2017), whereas autumn precipitation, winter cold and summer heatwaves affect abundance in *P. leucopus* (Dhawan et al. 2018) and, in *P. melanotis*, abundance is related to higher temperature that increases the opening of *Alnus* cones and favors seed presence on the ground (Flores-Peredo and Vázquez-Domínguez 2016). Hence, one should always keep in mind which are the crucial environmental and biological variables of the focal species.

Both the normalized vegetation index (NDVI) and the tree height optimized surface results indicated low resistance (higher connectivity) along medium height vegetation for both slopes (ECML 5m-15m; CVM 10m-30m). Vegetation cover is a good predictor of gene flow in different environments and species, for example in the rodent *Dipodomys merriami* (Flores-Manzanero et al. 2019) in desert ecosystems, *P. leucopus* (Munshi-South 2012) and the lizard *Podarcis muralis* (Beninde et al. 2016) in cities, and the marten *Martes americana* in boreal forests (Aylward et al. 2020). Importantly, Milanesi et al. (2017) recommend the inclusion of tridimensional vegetation data into models to evaluate functional connectivity, especially in complex environments. In fact, the authors found that 3D variables explain functional connectivity and habitat preference better than two-dimensional data in the western capercaillie *Tetrao urogallus*. In agreement, the interaction between NDVI and tree height constituted the best-ranked model in CVM, while in ECLM it was Productivity (litter cover, tree height and NDVI), results that highlight the different microenvironments and ecological dynamics of the two slopes. Rodents commonly prefer areas with greater resources availability, like the wood mouse (*Apodemus sylvaticus*) that has preference for pine forest with a complex vertical structure (Jaime-González et al. 2017) and *P. difficilis* that prefers high vegetation cover (Villanueva-Hernández et al. 2017). Accordingly, *P. melanotis* in CVM favored areas with complex vegetation cover, where food availability (seed density) and shelter are higher under the canopy (Flores-Peredo and Vázquez-Domínguez 2016). In ECLM it was litter cover, in addition to vegetation structure, the key feature explaining variability. Litter cover contributes to reduce temperature variation and maintain moisture, influences foraging efficiency by affecting seed odor detection, and also affects predation risk (Nicolai 2020). The distribution of *Peromyscus hooperi* also is associated with the amount of litter on the ground (Villanueva-Hernández et al. 2017). It should be noted that despite the advantage of photogrammetry for evaluating three-dimensional landscapes, it is

limited to assess below canopies (Rahlf et al. 2017). Thus, using other approaches like LiDAR or short-range photogrammetry at ground level is strategic.

Closing considerations

Landscape genetics is still underrepresented in conservation practices (Keller et al. 2015; Bowman et al. 2016), despite providing the necessary information to understand ecological processes affecting wild animal population dynamics at several scales. One reason is the uncertainty about the generalization of connectivity patterns to other species or geographies (Mims et al. 2018). Our findings provide useful information to propose specific conservation recommendations in our study system. Based on the genetic structure patterns, prioritization should be given to the unique ECLM-3150 and ECLM-3300 populations given their high diversity and significant differentiation. Furthermore, we show how the processes that shape structure, connectivity and diversity differ between slopes within a mountain, but also that a shared key feature is the three-dimensional vegetation structure. Hence, we recommend strengthening the control of extractive activities within the PNLM to avoid the loss of mature forest. This is especially important because subsistence extraction activities are allowed in these natural parks for local communities, and illegal logging is frequent. Reforestation and restoration campaigns also should be intensified, using native pines to promote connectivity.

Environmental clines have been associated with local adaptation in rodent species. For example, seven candidate loci were identified in the pika *Ochotona princeps* associated with an elevational gradient (Henry and Rusello 2013), while selected loci are linked with latitudinal thermic gradients, involved in protection against iron-dependent oxidative-stress during torpor, cell cycle arrest, glucose metabolism, and inhibition of muscle atrophy in *P. leucopus* (Garcia-Elfring et al. 2019). Our future perspectives include evaluating candidate loci subject to selection along *P. melanotis* elevational gradients, regarding physiological and behavioral traits potentially related with elevation, moisture and thermal adaptation.

Acknowledgments

We are grateful with all those that helped during fieldwork, A. Flores-Manzanero, C. Quintero-Corrales, O. Romero-Baéz and B. Solórzano. We deeply thank Miguel Salinas Hernández, Director of Parque Nacional La Malinche, for his support at the National Park, and Comisión Nacional de Áreas Naturales Protegidas that kindly granted permission for fieldwork and sample collection. Special thanks to A. Mastretta-Yanes and Miguel Castillo-Rodríguez for their valuable advice. Our gratitude to T. Garrido-Garduño and M. T. Solano-De la Cruz, and J. M. Baltazar-Gálvez and A. R. González-Ponce for molecular laboratory and computational assistance, respectively. GBM acknowledges that this paper was a part of her Master's thesis in the Posgrado en Ciencias Biológicas de la Universidad Nacional Autónoma de México.

Declarations

Funding

This project was partly funded by Consejo Nacional de Ciencia y Tecnología (CONACyT-SER grant # 286794). GBM was supported by a postgraduate scholarship from CONACyT (887756) and with a PAEP-UNAM grant for a research visit to Trent University.

Conflict of interest/Competing interests

Authors declare no conflict of or competing interests

Ethics approval

Field sampling and animal handling procedures were conducted in strict accordance with the American Society of Mammalogists guidelines for use of wild mammal species (Sikes et al. 2016) and with the corresponding collecting permits provided to EVD by Secretaría de Medio Ambiente y Recursos Naturales (Semarnat-FAUT-0168).

Consent to participate Not applicable

Consent for publication Not applicable

Availability of data and material

Data used in the study and bioinformatic analyses are explained in the Methods section and included in the Supplementary information; genotypes are available as a vcf file from the digital repository XXXX.

Code availability Not applicable

Authors' contributions

GBM and EVD conceptualized and designed the research. GBM, DTF and EVD performed fieldwork. GBM performed laboratory work. GBM, DTF and ABAS conducted and advised on data analyses. GBM and EVD wrote the paper and all authors reviewed the manuscript and agreed on the submission.

References

- Adavodi R, Khosravi R, Cushman SA, Kaboli M (2019) Topographical features and forest cover influence landscape connectivity and gene flow of the Caucasian pit viper, *Gloydius caucasicus* (Nikolsky, 1916), in Iran. Landsc Ecol 34:2615-2630
- Akaike H (1974) A new look at the statistical model identification. IEEE Trans Autom Control 19:716-723.
- Alexander DH, Lange K (2011) Enhancements to the ADMIXTURE algorithm for individual ancestry estimation. BMC Bioinformatics 12:246
- Álvarez-Castañeda T (2005) *Peromyscus melanotis*. Mamm Species 764:1-4
- Aylward CM, Murdoch JD, Kilpatrick CW (2020) Multiscale landscape genetics of American marten at their southern range periphery. Heredity 124:550-561
- Balkenhol N, Fortin MJ (2016) Basics of study design: sampling landscape heterogeneity and genetic variation for landscape genetic studies. In: Balkenhol N, Cushman SA, Storfer AT, Waits LP (eds) Landscape genetics: concepts, methods and applications. John Wiley & Sons, Oxford, pp 35-57
- Barrat CD, et al (2018) Vanishing refuge? Testing the forest refuge hypothesis in Coastal East Africa using genome-wide sequence data for seven amphibians. Mol Ecol 27:4289-4308
- Bedford N, Hoekstra H (2015) *Peromyscus* mice as a model for studying natural variation. Elife 4:e06813
- Beninde J, Feldmeier S, Werner M, Peroverde D, Schulte U, Hochkirch A, Veith M (2016) Cityscape genetics: structural vs. functional connectivity of an urban lizard population. Mol Ecol 25:4984-5000
- Bowman J, Jaeger AG, Fahrig L (2002) Dispersal distance of mammals is proportional to home range size. Ecology 83:2049-2055
- Bowman J, Greenhorn JE, Marotte RR, McKay MM, Morris KY, Prentice MB, Wehtje M (2016) On applications of landscape genetics. Conserv Genetics 17:753-760
- Bradburd G, Ralph P, Coop G (2013) Disentangling the effects of geographic and ecological isolation on genetic differentiation. Evolution 67:3258-3273
- Bradbury I, Hamilton L, Dempson B, Robertson M, Bourret V, Bernatchez L, Verspoor E (2015) Transatlantic secondary contact in Atlantic salmon, comparing microsatellites, a single nucleotide polymorphism array and restriction-site associated DNA sequencing for the resolution of complex spatial structure. Mol Ecol 24:5130-5144
- Burnett BN, Meyer GA, McFadden LD (2008) Aspect-realted microclimatic influences on slope forms and processes, northeastern Arizona. J Geophys Res Earth Surf 113(F3). DOI: 10.1029/2007JF000789
- Castañeda-Rico S, León-Paniagua L, Vázquez-Domínguez E, Navarro-Sigüenza AG (2014) Evolutionary diversification and speciation in rodents of the Mexican lowlands: the *Peromyscus melanophrys* species group. Mol Phylogenet Evol 70:454-463
- Castillo-Rodríguez M, López-Blanco J, Muñoz-Salinas E (2010) A geomorphologic GIS-multivariate analysis approach to delineate environmental units, a case study of La Maliche volcano (Central México). Appl Geogr 30:629-638
- Castro-Govea R, Siebe C (2007) Late Pleistocene-Holocene stratigraphy and radiocarbon dating of La Malinche Volcano, Central Mexico. J Volcanol Geotherm Res 162:20-42
- Catchen J, Hohenlohe P, Bassham S, Amores A, Cresko W (2013) Stacks: an analysis tool set for population genomics. Mol Ecol 22:3124-3140
- Chiappero MB, Sommaro LV, Priotto JW, Wiernes MP, Steinmann AR, Gardenal CN (2016) Spatio temporal genetic structure of the rodent *Calomys venustus* in linear, fragmented habitats. J Mamm 97:424-435

- D'Urban J, Williams GJ, Walker-Springett G, Davies AJ (2020) Three-dimensional digital mapping of ecosystems: a new era in spatial ecology. *Proc Royal Soc B* 287:20192383
- Danecek PA, et al (2011) The variant call and VCFtools. *Bioinformatics* 27:2156-2158
- De la Cruz IM, Castro-Campillo A, Zavala-Hurtado A, Salame-Méndez A, Ramírez-Pulido J (2019) Differentiation pattern in the use of space by males and females of two species of small mammals (*Peromyscus difficilis* and *P. melanotis*) in a temperate forest. *Therya* 10:3-10
- Dhawan R, Fischhoff IR, Ostfeld RS (2018) Effects of weather variability on population dynamics of white-footed mice (*Peromyscus leucopus*) and eastern chipmunks (*Tamias striatus*). *J Mamm* 99:1436-1443
- Dickson BG, Jennes JS, Beier P (2005) Influence of vegetation, topography, and roads on cougar movement in Southern California. *J Wildl Manage* 69:264-276
- Dyer RJ (2014) An R package for the spatial analysis of population genetic data. R package version 1.5.2. <https://dyerlab.github.io/gstudio/>
- Ellegren H (2014) Genome sequencing and population genomics in non-model organism. *Trends Ecol Evol* 29:51-63
- Evans J (2020) spatialEco: Spatial Analysis and Modelling Utilities. R package version 1.3-1. <https://github.com/jeffreyevans/spatialEco>
- Fa JE, Sánchez-Cordero V, Méndez A (1996) Interspecific agonistic behavior in small mammals in a Mexican high-elevational grassland. *J Zool* 239:396-401
- Féijo A, Wen Z, Cheng J, Ge D, Xia L, Yang Q (2019) Divergent selection gradient along elevational gradients promotes genetic and phenotypic disparities among small mammal populations. *Ecol Evol* 9:7080-7095
- Flores-Manzanero A, Luna-Bárcenas MA, Dyer RJ, Vázquez-Domínguez E (2019) Functional connectivity and home range inferred at a microgeographic landscape genetics scale in a desert-dwelling rodent. *Ecol Evol* 9:437-453
- Flores-Perezo R, Vázquez-Domínguez G (2016) Influence of vegetation type and season on rodent assemblage in a Mexican temperate forest mosaic. *Therya* 7:357-369.
- Franco-Ramos O, Stoffel M, Vázquez-Selem L (2016) Tree-ring based record of intra-eruptive lahar activity: Axaltzintle Valley, Malinche Volcano, Mexico. *Geochronometria* 43(1). DOI: 10.1515/geochr-2015-0033
- Fritchot E, Mathieu F, Trouillon T, Bouchard G, François O (2014) Fast and efficient estimation of individual ancestry coefficients. *Genetics* 196:973-983
- Funk WC, Blouin MS, Corn PS, Maxell BA, Pilliod DS, Amish S, Allendorf FW (2005) Population structure of Columbia spotted frogs (*Rana luteiventris*) is strongly affected by the landscape. *Mol Ecol* 14:483-496
- Galpern P, Peres-Neto P, Polfus J, Manseau M (2014) MEMGENE: Spatial pattern detection in genetic distance data. *Methods Ecol Evol* 5:1116-1120
- García-Elfring A, Barret RDH, Millien V (2019) Genomic signatures of selection along a climatic gradient in the northern range margin of the white-footed mouse (*Peromyscus leucopus*). *J Hered* 110:684-695
- Garrido-Garduño T, Téllez-Valdés O, Manel S, Vázquez-Domínguez E (2016) Role of habitat heterogeneity and landscape connectivity in shaping gene flow and spatial population structure of a dominant rodent species in a tropical dry forest. *J Zool* 298:293-302
- Goudet J, Jombart T (2015) Hierfstat: Estimation and test of hierarchical F-statistics. <https://github.com/jgx65/hierfstatBugR>
- Guo X, Coops NC, Gergel SE, Bater CW, Nielsen SE, Stadt JJ, Drever M (2018) Integrating airborne lidar and satellite imagery to model habitat connectivity dynamics for spatial conservation prioritization. *Landsc Ecol* 33:491-511.

- Haugen H, Linlokken A, Ostbye K, Heggenes J (2020) Landscape genetics of northern crested newt *Triturus cristatus* populations in a contrastating natural and human-impacted boreal forest. *Conserv Genetics* 21:515-530.
- Henry P, Rusello MA (2013) Adaptative divergence along environmental gradients in a climate-change-sensitive mammal. *Ecol Evol* 3:3906-3917
- Hijmans RJ, et al (2020) raster: Geographic Data Analysis and Modeling. <https://rdrr.io/cran/raster/>
- Howell P, Delgado L, Scribner K (2017) Landscape genetic analysis of co-distributed white-footed mice (*Peromyscus leucopus*) and prairie deer mice (*Peromyscus maniculatus bairdii*) in an agroecosystem. *J Mamm* 98:793-803
- Jaime-González C, Aceves P, Mateos A, Mezquida ET (2017) Bringing GAPs: On the performance of airbone Lidar to model wood mouse-habitat structure relationship in pine forest. *PLoS One* 12:e0182451
- Jombart T, Devillard S, Balloux F (2008) Discriminant analysis of principal components: a new method for the analysis of genetically structured populations. *BMC Genetics* 11:94
- Keller D, Holderegger R, Van Strien MJ, Bolliger J (2015) How to make landscape genetics beneficial for conservation management? *Conserv Genetics* 16:503-512
- Koen EL, Bowman J, Sadowski C, Walpole AA (2014) Landscape connectivity for wildlife: development and validation of multispecies linkage maps. *Methods Ecol Evol* 5:626-623
- León-Tapia MA, Fernández JA, Rico Y, Cervantes FA, Espinosa de los Monteros A (2020) A new mouse of the *Peromyscus maniculatus* group species complex (Cricetidae) from the highlands of central Mexico. *J Mamm* 101:1117-11132
- Lepais O, Weir JT (2014) SimRAD an R package for simulation-based prediction of the number of loci expected in RADseq and similar genotyping by sequencing approaches. *Mol Ecol Res* 14:1314-1321
- Li H, Durbin R (2009) Fast and accurate short read alignment with Burrows-Wheeler Transform. *Bioinformatics* 24:1754-1760
- McRae BH, Dickson BG, Keitt TH, Shah VB (2008) Using circuit theory to model connectivity in ecology and conservation. *Ecology* 89:2712-2724
- Mastretta-Yanes A, Moreno-Letier A, Piñeiro D, Jorgensen T, Emerson B (2015) Biodiversity in Mexican highlands and the interaction of geology, geography and climate within the Trans-Mexican Belt. *J Biogeog* 42:1586-1600
- Meliyo JL, et al (2014) Landform and surface attributes for prediction of rodent burrows in the Western Usambara Mountains, Tanzania *J Health Res* 16:182-193
- Milanesi P, Holderegger R, Bollmann K, Gugerli F, Zellweger F (2017) Three-dimensional habitat structure and landscape genetics: a step forward in estimating functional connectivity. *Ecology* 98:393-402
- Mims MC, Hartfield Kirk EE, Lytle DA, Olden JD (2018) Traits-based approaches support the conservation relevance of landscape genetics. *Conserv Genetics* 19:17-26
- Montgelard C, Zenboudji S, Ferchaud AL, Arnal V, Van Vuuren BJ (2014) Landscape genetics in mammals. *Mammalia* 78:139-157
- Munshi-South J (2012) Urban landscape genetics: canopy predicts gene flow between white-footed mouse (*Peromyscus leucopus*) populations in New York City. *Mol Ecol* 21:1360-1378
- Munshi-South J, Zolnik C, Harris S (2016) Population genomics of the Anthropocene: urbanization is negatively associated with genome-wide variation in white-footed mouse populations. *Evol Appl* 9:546-564.
- Mussmann SM, Douglas MR, Chafin TK, Douglas ME (2019) BA3-SNPs: Contemporary migration reconfigured in BayesAss for next-generation sequence data. *Methods Ecol Evol* 10:1808-1813

- Naimi B (2017) usmd: Uncertainty analysis for species distribution model. <https://CRAN.R-project.org/package=usdm>
- Nicolai N (2020) Rodents' responses to manipulated plant litter and seed densities: implications for restoration. PeerJ 8:e9465
- Norum JK, Lone K, Linell JDC, Odden J, Loe LE, Mysterud A (2015) Landscape of risk to roe deer imposed by lynx and different human hunting tactics. Eur J Wildl Res 61:831-840
- Oksanen J, et al (2011) Vegan: Community Ecology Package. <https://github.com/vegandevelopers/vegan>
- Parchman TL, Gompert Z, Mudge J, Schilkey FD, Benkman CW, Buerkle CA (2012) Genome-wide association genetics of an adaptive trait in lodgepole pine. Mol Ecol 21:2991-3005
- Pelletier D, Lapointe M-E, Wulder M, White J, Cardille J (2017) Forest connectivity regions of Canada using circuit theory and image analysis. PLoS One 12:e0169428
- Pelletier D, Clark M, Anderson MG, Rayfield B, Wulder MA, Cardille JA (2014) Applying circuit theory for corridor expansion and management at regional scales: Tiling, pinch points, and omnidirectional connectivity. PLoS One 9:e84135
- Pérez-Consuegra SG, Vázquez-Domínguez E (2017) Intricate evolutionary histories in montane species: a phylogenetic window into craniodental discrimination in the *Peromyscus mexicanus* species group (Mammalia: Rodentia: Cricetidae). J Zool Syst Evol Res 55:57-72
- Peterman WE, Connette GM, Semlitsch RD, LS Eggert (2014) Ecological resistance surfaces predict fine-scale genetic differentiation in a terrestrial woodland salamander. Mol Ecol 23:2402-2413
- Peterman WE, Winiarski KJ, Moore CE, Da Silva Carvalho E, Gilbert AL, Spear SF (2019) A comparison of popular approaches to optimize landscape resistance surfaces. Landsc Ecol 34:2197-2208
- Pettorelli N, Laurance WF, O'Brien TG, Wegmann M, Nagendra H, Turner W (2014) Satellite remote sensing for applied ecologists: opportunities and challenges. J Appl Ecol 51:839-848
- Polato NR, et al (2017) Genetic diversity and gene flow decline with elevation in mayflies. Heredity 119:107-116
- Priadka P, Manseau M, Trottier T, Hervieux D, Galpern P, McLoughlin P, Wilson P (2018) Partitioning drivers of spatial genetic variation for a continuously distributed population of boreal caribou: Implications for management unit delineation. Ecol Evol 9:141-143
- QGIS, Development Team (2020) QGIS Geographic Information System. Open Source Geospatial Foundation Project. <http://qgis.osgeo.org>
- Rahlf J, Breidenbach J, Solberg S, Naesset E, Astrup R (2017) Digital aerial photogrammetry can efficiently support large-area forest inventories in Norway. Forestry 90:710-718
- Roser LG, Ferreyra LI, Saidman BO, Vilardi JC (2017) EcoGenetics an R package for the management and exploratory analysis of spatial data in landscape genetics. Mol Ecol Res 17:e241-e250
- Row JR, Knick ST, Oyler-McCance SJ, Lougheed S, Fedy BC (2017) Developing approaches for linear mixed modeling in landscape genetics through landscape direct dispersal simulations. Ecol Evol 7:3751-3761
- Rzedowski J (2006) Vegetación de México. 1a edición digital. Comisión Nacional para el Conocimiento y Uso de la Biodiversidad, México
- Samarasin P, Shuter B, Wright S, Rodd H (2017) The problem of estimating recent genetic connectivity in a changing world. Conserv Biol 31:126-135

- Shafer ABA, Northrup JM, White KS, Boyce MS, Coté SD, Coltman DW (2012) Habitat selection predicts genetic relatedness in an alpine ungulate. *Ecology* 93:1317-1329
- Sikes RS, Animal Care and Use Committee of the American Society of Mammalogists (2016) 2016 Guidelines of the American Society of Mammalogists for the use of wild mammals in research and education. *J Mamm* 97:663-688
- Vega R, Vázquez-Domínguez E, White TA, Valenzuela-Galván D, Searle J (2017) Population genomics applications for conservation: the case of the tropical dry forest dweller *Peromyscus melanophris*. *Conserv Genetics* 18:313-326
- Velázquez A, Toledo V, Luna-Vega I (2000) Mexican temperate vegetation. In: Barbour MG, Billings WD (eds) North American Terrestrial Vegetation. Cambridge University Press, Cambridge, pp 573-592
- Villanueva-Hernández A, Delgado-Zamora D, Heynes-Silerio, Ruacho-González L, López-González C (2017) Habitat selection by rodents at the transition between the Sierra Madre Occidental and the Mexican Plateau, México. *J Mamm* 98:293-301
- Wang K, Franklin SE, Guo X, Cattet M (2010) Remote sensing of ecology, biodiversity and conservation: a review from the perspective of remote sensing specialists. *Sensors* 10:9647-9667

Supporting information

Additional supporting information may be found in the online version of this article at <https://XXXX>

Appendix S1: Extended description of materials and methods;

Appendix S2: Tables S1-S10;

Appendix S3: Figures S1-S13.

Highland forest's environmental complexity drives landscape genomics and connectivity of the rodent *Peromyscus melanotis*

Gabriela Borja-Martínez, Daniel Tapia-Flores, Aaron B.A. Shafer and Ella Vázquez-Domínguez

Supporting information

Appendix 1. Extended description of all materials and methods used in the study.

Study species, study region and sampling

Peromyscus melanotis' main habitat is mesophilic and coniferous forests and zacatalonal (high moorland), along a 2100-4300 m elevational range, predominantly on rocky habitats with steep slopes and grasslands (Álvarez-Castañeda 2005; Flores-Peredo and Vázquez-Domínguez 2016). It is a small mouse (adult average weight 40 g) with escansorial habits (i.e. that use both ground and tree spaces); main food sources are seeds of seasonal herbaceous plants and grasses, as well as insects containing cardenolides (Gleedining et al. 1988).

The Transmexican Volcanic Belt (TVB) in Mexico consists of a series of volcanic structures that extend from east to west (Mastretta-Yanes et al. 2015). The TVB receives moisture from the Pacific Ocean and the Gulf of Mexico, which renders a marked seasonality along the lowlands. Additionally, drastic climatic changes occur on the TVB across short geographic distances associated with the elevational gradient, topographic complexity and orographic history (Rzedowski 2006; García-Mendoza et al. 2018). Given the complex geology, particularly the intense volcanic activity that has historically modified the landscape, the TVB is considered a biodiversity hotspot (Mastretta-Yanes et al. 2015). Due to its high biodiversity, 39 natural protected areas have been established that protect 7.9% of this region, including the La Malinche National Park (PNLM) (Fuller et al. 2006).

The PNLM is located on the Balsas basin between the states of Puebla and Tlaxcala, covering 42,112 ha (Fig. 1). It is considered a conservation priority region (CONANP 2013) due to the numerous ecosystem services it provides, including water storage and regulation of climate and carbon cycles. The park is characterized by a high elevation temperate forest, where climate and vegetation are associated with the elevational gradient: temperate sub-humid with rains in summer (at heights of 2,000-3,000 m), semi-cold (3,000-3,500) and cold (3,500-4,400) sub-humid with rains in summer (Castillo-Rodríguez 2010). Likewise, predominant vegetation includes oak (2,200-2,800 m), pine (2,800-4,200) and oyamel forests (2,700-3,800), chaparral (3,300-4,000) and high moorland (4,000-4,400); some areas have also *Alnus* forest and grasslands (CONANP 2013). The diverse vegetation supports the presence of 37 species of mammals, 18 of which are rodents, five belonging to the *Peromyscus* genus (Ruíz-Soberanes 2009).

We designed a sampling scheme that allowed us to analyze the landscape matrix at three scales: global, regional and local (Fig. 1). The global scale encompasses the north (Centro Vacacional Malinche; CVM) and northeast (Estación Científica La Malinche; ECLM) slopes of the La Malinche volcano; the regional scale defines the connectivity between the CVM and ECLM, and the local scale considers the elevation gradient within each CVM and ECLM. *Peromyscus melanotis* was live-trapped during September 2018 on the two slopes, along five elevation levels each (CVM: 3100, 3200, 3300, 3400, 3500 m; ECLM: 2850, 3000, 3150, 3300, 3450 m). Trapping was done along randomly set transects consisting of 80 Sherman traps separated 10 m, baited with a mixture of oat, vanilla extract and peanut butter. On each sampling locality where individuals were trapped, we recorded coordinates and different climatic and environmental variables (see below). Individuals were sexed and weighted and conventional morphological measures were taken (Table S1). An ear tissue sample was collected and preserved in Eppendorf tubes with 96% ethanol. All individuals were released at the sampling site. Field sampling and animal handling procedures were

conducted in strict accordance with the American Society of Mammalogists on (Sikes et al. 2016) and with the local collection permits.

Landscape data and images processing

To delimit the regional study area, we calculated the maximum and median dispersion distance, based on the *Peromyscus* known home range of 420.8 m² (Fa et al. 1996), where the maximum dispersal distance = $40(\text{home range})^{1/2}$ was 820.53 m and the mean dispersion distance= $7(\text{home range})^{1/2}$ was 143.59 m (Bowman et al. 2002); accordingly, we generated a 900 m buffer for each study site. We used an additional 1000 m buffer to apply the Koen et al. (2014) method for connectivity (see below); at the global scale we used a 4 km buffer.

We generated three different datasets depending on the working scale: the global scale at a resolution of 100 x 100 m, the regional (30 x 30 m) and local (5 x 5 m). We used Landsat 8 images and environmental data collected in situ to create environmental surfaces. We measured three environmental variables at each individual trapping locality: temperature and humidity with HOBO data loggers (UX100-003, ONSET Computer Corporation) and litter cover using a ruler. Values for the entire studied area of these three variables were obtained by kriging interpolation using 80% of the data randomly selected, while the remaining 20% was used to calculate the mean square error of the interpolations (litter cover: CVM ± 3.08 cm, ECLM ± 1.56 cm; moisture: CVM ± 2.53%, ECLM ± 3.20%; temperature: CVM ± 0.295°C, ECLM ± 0.561°C). Litter cover, moisture and temperature were not used for the global scale due to lack of adequate data for interpolation. The normalized vegetation index (NDVI) and moisture stress index (MSI) were calculated using satellite images (Landsat 8, ID: LC80250472019086LGN00 available at <https://glovis.usgs.gov/>) in ERDAS Imagine V.13.0 and QGIS 3.8. The MSI is sensitive to the amount of water accumulated by the leaves and has values from 0 to 3; it can be used

as an indirect approach to classify plant communities. NDVI is based on red and infrared spectral bands, where the highest value (-1 to 1) is an indicator of extent plant cover, biomass and vegetation health, but has the limitation that it does not allow to differentiate vegetation types (Kinyanjui 2010; Measho et al. 2019).

For the topographic data, we used the ‘Mexican elevational continuum surfaces’ v3.0 for Tlaxcala and Puebla (available at <https://www.inegi.org.mx/app/geo2/elevacionesmex/>), based on which we generated the variables of elevation, aspect, slope in degrees, topographic position Index (TPI), and landforms, with QGIS. Aspect is a measure of slope orientation, in which values indicate 60-180 (south-southeast), 180-300 (south-southwest), 300-360 (north-northwest) and 0-60 (north-northeast) (Iniguez et al. 2008). The TPI is the difference between a central point elevation and the surrounding neighborhood, thus positive values represent higher areas than the mean and negative values lower areas. Landform is a categorical layer that represents the TPI classified as low, plain and high terrain (De Reu 2013).

3D vegetation layers were generated with two approaches: LiDAR (Laser Imaging Detection and Ranging data) and Digital Aerial Photogrammetry. We created a tree-height layer for regional and global scales using 20 mapping charts (E13B33D3, E13B33D4, E13B33E4, E13B33F3, E13B33F4, E13B34D1, E13B34D3, E13B34D4, E13B43B2, E13B43B4, E13B43C1, E13B43C2, E13B43C3, E13B43C4, E13B43F2, E13B44A1, E13B44A2, E13B44A3, E13B44A4, E13B44D1) for Surface (SDM) and Terrain (TDM) digital models, obtained with LiDAR sensors (available at <https://www.inegi.org.mx>). To obtain the vegetation height, we calibrated the SDM by subtracting the TDM values. To create the categorical vegetation cover map, we reclassified the tree-height map by using zero values as absences and the rest of the values as presence, with the R package raster (Hijmans et al. 2020). Because the landscape representation by categorical classes depicts discontinuities as discrete limits but which do not represent reality (McGarigal and Cushman

2005), the TPI and vegetation cover categorical layers were smoothed to avoid categorization subjective limits. We performed the latter with the *raster.gaussian.smooth* function in spatialEco (Evans 2020) in R, which applies a Gaussian Smoothing kernel in a focal matrix window of 3x3. In the Gaussian Smoothing Kernel, the smoothing degree depends on the standard deviation of the Gaussian function, producing a weighted average of each pixel neighborhood, and preserving the edges better than other filters (Fisher et al. 2003).

The local configuration of the landscape affects the correlation of predictors (Prunier et al. 2015). We evaluated correlation among predictor variables with two tests: collinearity analysis using the Variance Inflation Factor (VIF; Dormann et al. 2013) in usdm (Naimi 2017). Although VIF >10 is considered a sign of collinearity, we took more restrictive parameters using a VIF >5. The variable MSI showed high collinearity and was not used for further analysis (Table S2). A correlation assessment was done with the function *vifcor* in usdm to eliminate variables with a correlation >0.8 (Table S3). We also discarded the variable vegetation cover because it was uninformative; that is, vegetation in our study sites behaved as a continuum, thus the variable tree height allowed us to identify those sites with no vegetation.

Photogrammetric process

Specifically for analyses at the local scale, we applied a photogrammetry approach that allows the generation of three-dimensional point clouds from digital images, from which to extract standard measurements (Rahlf et al. 2017). To that end, we used an unmanned aerial vehicle (drone) and took 3,035 georeferenced photos in ISO mode. The photo-alignment (Figs. S1, S2, S3), the point cloud reconstruction, and the Digital Elevation Model (DEM) were built with Agisoft Metashape 1.5.5. To obtain the vegetation-height, we calibrated the DEM as described for the LiDAR processing.

Photogrammetry allows to obtain reliable measurements from digital images. For our study, we took 3,035 georeferenced photos with an unmanned aerial vehicle (drones DJI/phantom4 and DJI/Mavic pro). To improve white balance, both contrast (-23) and highlight (-83) parameters were modified in 1,752 photos corresponding to the CVM slope (ECLM photos did not require it), using the GNU Image Manipulation Program 2.0. The Agisoft Metashape v.1.5.5 software detects image features using computational vision algorithms and similarity indices between the overlapping images, allowing to correct the deformation generated by the focal point, as well as the radial and tangential errors, to align the photos and assemble a 3-dimensional point cloud (Probst, 2018). The quality of point cloud depends on the amount of photographic overlap, the physical characteristics of the target object, and the contrast between the images due to light effects (Dandois et al., 2017). We tested different quality combinations (high, medium) between alignment and reconstruction, excluding significantly low parameters to keep adequate precision. Performance of each model was evaluated comparing the total error, the number of points generated, and the resolution of the digital elevation model (DEM) obtained; the latter was done for four elevations from ECLM (2800m, 3000m, 3150m, 3450m) due to extreme computation time limits. In addition, we prioritized the number of photos assembled and the points obtained from the point cloud and the DEM. Results showed that the HighHigh combination had a high error associated, despite better density of points, and where the occupied area is reduced compared to the other combinations. Based on the performance of all combinations evaluated, we chose the parameters of medium quality for the alignment and high quality for the reconstruction of all the remaining altitudinal levels.

The point cloud was filtered by removing points that lose color and spectral characteristics. For the mesh reconstruction, each point is connected with the three closest points (Cloudcompare), however, because our point recovery was not enough to generate

a continuous mesh, we had to remove isolated points. As a result, we generated the digital elevation model directly from the point cloud. The generated model captures the elevation above the sea level of all the objects on the landscape, therefore it had to be recalibrated in QGIS by an algebraic subtraction with the Digital Terrain Model obtained from INEGI.

Working photogrammetry with vegetation is a true challenge. The scattered position of the leaves and tree branches produce a not homogenous distribution of colors, with a changing position due to the wind, affecting the performance of the vision algorithms (Probst 2018). Also, dense plant coverage reduces point cloud quality, since complex structures tend to affect the assemblies (Wilson, 2019) as was the case of the Parque Nacional La Malinche. Notwithstanding, we reconstructed 8,464 m² and 16,161 m² for the ECLM (Fig. S2) and CVM (Fig. S3) slopes respectively, with a resolution of centimeters. The local areas were transformed into a 5 x 5 m resolution.

DNA extraction and genomic sequencing

We extracted genomic DNA from tissue samples with the DNeasy Blood and Tissue Kit (Qiagen), following the manufacturer's instructions. DNA quality and quantity were verified using nanodrop and Qubit. We corroborated DNA integrity and absence of inhibitors to the enzymatic reaction by digesting 10% of the samples with the enzyme Hind III (O'Leary et al. 2018). The genome sequencing protocol used was a double-digest restriction site-associated (ddRADseq; Parchman et al. 2012; Peterson et al. 2012), for which we performed in silico digestions with SimRAD v0.96 in R (Lepais and Weir 2014) to identify the appropriate set of restriction enzymes, using 10% of the genome of *Peromyscus maniculatus bairdii* (Ensemble: GCA_000500345.1), and testing methylation-sensitive and no-sensitive enzymes. We chose the Nsil and Mspl enzymes based on the in silico digestions results (Table S4 and Fig. S4). Library preparation and sequencing was performed in the University of Wisconsin Biotechnology Center (UWBC).

In silico digestions

Reduced-representation sequencing methods rely on the use of restriction enzymes to reduce the genome complexity using one or two enzymes (Heriten et al., 2015; Zhu et al., 2016). One way to identify the best set of enzymes is applying in silico digestions to complete genomes to identify the number and the distribution of restriction sites, as well as the size of reads (Sohan et al., 2013). We tested both methylation-sensitive (Apkl, EcoRI, Hindl) and no-sensitive (Msel, Mspl, Nsil, Pstl, Sphl, Sbfl) enzymes with SimRAD v0.96 (Lepais & Weir, 2014) in R. We also evaluated some sets of paired enzymes (Nsil/Mspl, Pstl/Mspl) that have been used in previous studies (Barbosa et al., 2018; García-Elfring et al., 2017; White et al., 2013). We randomly selected 10% of the *Peromyscus maniculatus bairdii* genome (Ensemble: GCA_000500345.1), which encompasses 2,473,536,444 bp. Additionally, we implemented a size selection filter to account for the number of reads with a distribution between 100 and 500 bp long.

The enzymes that have a common restriction site and produce fragments of short length are ideal for RAD-methods (Table S3). We discarded Apkl despite its good performance and all the methylation-sensitive enzymes because they can decrease the number of sites available, potentially leading to consistency and reproducibility errors during the variant calling process between individuals (Wang et al., 2017). Thus, we aimed to have a double digestion protocol that increased the number of restriction sites available and decreased the size of the reads (Fig. S2). Prioritizing short sequences is necessary because, during enrichment, short fragments have preferential amplification (O’Leary et al., 2018). As a result, we chose the double-digest restriction site-associated DNA sequencing protocol (ddRADseq) with the Nsil and Mspl enzymes.

Bioinformatics processing

We performed demultiplexing of reads with *process_radtags* in Stacks (Catchen et al. 2013); quality filtering using Fastqc and FASTX-toolkit, discarding reads with a low-quality score (<22) and truncating the reads at 120 base pairs. We aligned the resulting reads to the *Peromyscus maniculatus bairdii* genome, using BWA under default parameters (Li and Durbin 2009); unpaired reads were removed (Fig. S5). Next, we ran the *ref_map* pipeline in Stacks to call variants and the *populations* module to filter for SNPs present in at least 50% of the samples ($r=0.5$). Several filters were applied with VCFtools (Danecek et al. 2011): minimum depth of 10 samples to recognize a SNP as true; minor allele frequency >5%; 10% of samples containing the least frequent allele. Final filtering parameters performed were: only biallelic loci were retained; missing data by locus and by individual >20% were removed; monomorphic and out of Hardy-Weinberg equilibrium loci were eliminated.

Kinship and disequilibrium linkage filters

To verify independent segregation of loci, we performed a linkage disequilibrium analysis within and between chromosomes and estimated kinship (Fig. S6). Linkage disequilibrium is the statistic association between alleles of different loci, which can occur due to genetic drift (the selection force generating a drag of close alleles or physical proximity in the chromosome) in small populations (Waits & Storfer, 2015). We performed a linkage disequilibrium analysis with Plink (Purcell et al. 2007) that allowed to identify and remove one of the locus from each significant paired comparison (correlation coefficient >0.4). As a result, 243 loci in 278 significative interactions were randomly eliminated. Likewise, the identity value by descent (IBD) is the probability that two alleles are identical by descent (Goudet et al., 2018), which we evaluated by a kinship analysis performed with SNPRelate in R (Zheng et al. 2012). Paired comparisons between individuals with an IBD >0.25 (a

parent-childhood or full-siblings relationship) were randomly eliminated; 15 paired comparisons were detected with a signal of IBD in 8 individuals.

Genetic structure and migration analyses

In order to evaluate genetic differentiation of populations and individuals, we inferred structure using four approaches and software programs: (i) to identify trends in the genetic variation without assuming a genetic model we used Principal Components Analysis (PCA) in SNPRelate, (ii) to describe variation within elevational levels we performed a Discriminant Analysis of Principal Components (DAPC) with adegenet in R (Jombart et al. 2008). The appropriate number of principal components and discriminant functions was evaluated with the a-score method, which determines the proportion of successful reassignment by individual in function of the number of retained PCs (15 PCs for ECLM and 21 for CVM). Next, to evaluate coancestry levels and identify genetic groups (K) we applied two tests iii) Admixture, which uses maximum likelihood to estimate ancestry coefficients (Alexander and Lange 2011), and (iv) snmf, with the LEA library in R (Frichot et al. 2014), that utilizes a sparse Non-Negative Matrix Factorization algorithm and K is based on the regulation parameter (alpha=100). We tested from $K=1$ to 10 with 20 replicates for each K (global scale) and $K=1$ to 5 (regional scale). Admixture and snmf use a cross-validation method in which a dataset with 10% of masked genotypes is created and a training set is used to evaluate the ability to correctly impute masked genotypes.

To discern differentiation patterns at the local scale, we analyzed migration with BA3-SNPs (Mussmann et al. 2019). We applied the BayesAss method in order to estimate recent bidirectional migration rates, which implements the Metropolis-Hastings algorithm for Markov chain Monte Carlo (MCMC) sampling to identify recent migrants (first and second generations) and their source population (Wilson and Rannala 2003). In this case, each elevation level was assumed as a population. For the ECLM we performed five runs with

1×10^7 interactions and 2×10^6 burnin; mixing parameters were $a=0.7$, $f=0.5$ and $m=0.5$, values that fall within the acceptance rate (0.42, 0.38 and 0.44). For CVM we could not calibrate the model using the elevation level as population, thus we determined which levels would function as spatial neighborhoods (see below); mixing parameters were $a=0.9$, $f=0.1$ and $m=0.5$, and acceptance values of 0.42, 0.35 and 0.39. Chain convergence was evaluated with Tracer v1.7.1 (Rambaut et al. 2018). We also estimated pairwise F_{ST} between populations with hierfstat in R (Goudet and Jombart 2015).

Spatial genetic patterns can be elucidated using analysis based on spatial genetic autocorrelation, which enables to estimate the distance at which gene flow occurs and to define spatial neighborhoods (Leempoel et al. 2017; Priadka et al. 2018). We used Memgene in R (Galpern et al. 2014), at the regional scale, with 10,000 permutations and an alpha level for significant eigenvector of 0.05. Memgene is useful to detect cryptic structure when genetic flow is high and variation operates on different spatial scales. It uses Moran's Eigenvector Maps to create orthogonal eigenvectors describing whether there is positive or negative spatial autocorrelation, and applies a regression model to identify significant spatial genetic patterns by quantifying the genetic variation explained by each eigenvector, enabling the assessment of the amount of genetic variation that is associated with spatial pattern (i.e. adjusted R²).

Landscape genetic analyses

Genetic distance and structure

We estimated genetic distances based on dissimilarity of individual genotypes by calculating the Euclidean distance-based on PCA with stats in R, based on the number of components that capture at least 80% of the variation in each scale (87 components for the global scale; regionally, 57 for ECLM and 33 for CVM). This metric is thought to improve landscape genetic inferences given that no unexplained axes are used, hence no biological

assumptions as endogamy, population structure or ploidy are considered (Shrink et al. 2017). To test isolation by distance (IBD) at global and regional scales, we performed a Mantel test between the genetic and geographic distances with vegan in R (Oksanen et al. 2011), using 10,000 Spearman permutations. Euclidean geographic distances were estimated in gstudio in R (Dyer 2014). To evaluate autocorrelation we used EcoGenetics in R (Roser et al. 2017), by considering all the distances and taking only the first 1000 m of the distribution, with 10,000 Monte-Carlo simulations and Spearman permutations.

Resistance hypotheses and connectivity analyses

Resistance surfaces represent hypotheses of the relationship between gene flow and a set of predictor variables (Mastretta-Yanes et al. 2015; Peterman 2018), providing values in function of the degree to which a feature of the landscape limits or promotes connectivity across the landscape. Based on an optimization process, several resistance surfaces are statistically compared without priors assumption, and the one with the best fit to the genetic data is selected (Spear et al. 2016; Wittische et al. 2019). We followed the optimization framework developed by Peterman et al. (2014) to determine the resistance values of our surfaces; the fitness of each surface was evaluated based on Maximum-likelihood population effects mixed models (MLPE), to maximize the relationship between the pairwise genetic distance and the pairwise landscape distances, while also accounting for the no independence of genetic data (Bolker et al. 2009). We independently optimized each resistance surface for global and regional scales with the *commuteDistance* function in gstudio, with three independent runs to verify convergence of parameters; support of the optimized resistance surfaces was assessed using the AICc (Akaike's information criterion corrected for small/finite sample size; Akaike 1974).

The *commuteDistance* function is based in circuit theory, which randomly generates several possible resistance routes with different costs. It constitutes an appropriate approach for generalist species since it assumes that organisms use the entire landscape (Spear et al. 2016). In addition, we estimated robustness with the function *Resist.boot* that performs a bootstrap resampling, with 10,000 interactions and 75% of the samples without replacement, and readjusts the surfaces with MLPE (Peterman et al. 2019). We selected the best-supported features to construct composite hypothesis of features that potentially affect connectivity in a multi-optimization approach. Specific hypotheses were built considering characteristics of the environment that are biologically relevant for *P. melanotis* (i.e. environment, productivity, topography, vegetation; Table 1). Specifically for the global scale, due to uncertainty of environmental variables interpolations, we only tested topography and vegetation structure hypotheses.

Finally, we modeled omnidirectional connectivity surfaces using circuit theory to explore current flow, an approach that allows to identify restricted corridors and barriers to movement, based on the arrangement of the resistance values without assumptions of directional conductance between nodes (Pelletier et al. 2014). Nodes function as resistors in which current flow is applied and the voltage reached depends on the resistance surface (McRae et al. 2008). We created a buffer with 20% of the regional areas (CVM=1000 m, ECLM=1200 m) and 50 random points (nodes) were selected on those buffers to avoid saturation of current flow within the study area (Koen et al. 2014). We summarized and standardized all the optimized resistance surfaces obtained in ResistanceGA for each landscape feature to build the global model, by dividing by the minimum resistance value to obtain one final resistance layer. In addition, the resistance surface corresponding to the best hypothesis from the multivariate framework was used to create a current density map. We ran Circuitscape 4.0.5 (McRae et al. 2008) to connect each node to all the others, and

each connection between nodes generated a current map that was multiplied to create the final map, in which the buffer zone containing the nodes was removed.

References

- Akaike, H. 1974. A new look at the statistical model identification. *IEEE Transactions on automatic control* 19(6): 716-723. Alexander, D.H. and K. Lange. 2011. Enhancements to the ADMIXTURE algorithm for individual ancestry estimation. *BMC Bioinformatics* 12, 246.
- Alvarez-Castañeda, T. 2005. *Peromyscus melanotis*. Mammalian Species 764:1-4.
- Barbosa, S., F. Mestre, T. A. White, J. Paupério, P. C. Alves and J. B. Searle. 2018. Using genomics to define conservation units and functional corridors. *Molecular Ecology* 27(17):3452-3465.
- Bolker, B. M., M. E. Brooks, C. J. Clark, S. W. Geange, J. R. Poulsen, H. H. Stevens and J. S. White. 2009. Generalized linear mixed models: a practical guide for ecology and evolution. *Trends in Ecology and Evolution* 24(3):127-135.
- Bowman, J., A. G. Jaeger and L. Fahrig. 2002. Dispersal distance of mammals is proportional to home range size. *Ecology* 83(7): 2049-2055.
- Castillo-Rodríguez, M., J. López-Blanco and E. Muñoz-Salinas. 2010. A geomorphologic GIS-multivariate analysis approach to delineate environmental units, a case study of La Maliche volcano (Central México). *Applied Geography* 30: 629-638.
- Catchen, J., P. Hohenlohe, S. Bassham, A. Amores and W. Cresko. 2013. Stacks: an analysis tool set for population genomics. *Molecular Ecology* 22(11): 3124-3140.
- CONANP, Comisión Nacional de Áreas Naturales Protegidas. 2013. Programa de manejo Parque Nacional La Malinche o Matlalcuéyatl. Comisión Nacional de Áreas Naturales Protegidas. Ciudad de México, México.
- Danecek, P., A. Auton, G. Abecasis, C. Albers, E. Banks, M. De Pristo, R. E. Handsaker, G. Lunter, G. T. Marth, S. T. Sherry, G. McVean and R. Durbin. 2011. The variant call and VCFtools. *Bioinformatics* 27(15): 2156-2158. doi: 10.1093/bioinformatics/btr330
- Dandois, J. P., M. Baker, M. Olano, G. G. Parker and C. C. Ellis. 2017. What is the point? Evaluating the structure, color and semantic traits of computer vision point clouds of vegetation. *Remote sensing* 9(4): 355
- De Reu, J., J. Burgeois, M. Bats, A. Zweertvaegher, V. Gelormini, P. Smedt, M. Antrop, P. De Maeyer, P. Finke, M. Van Meirvenne, J. Verniers and P. Crombé. 2012. Application of the topographic position index to heterogeneous landscapes. *Geomorphology* 186: 39-49.
- Doormann, C. F., J. Elith, S. Bacher, C. Buchmann, G. Carl, G. Carré, J. R. García-Marquéz, B. Gruber, B. Lafourcade, P. J. Leitao, T. Münkemüller, C. McClean, P. E. Osborne, B. Reineking, B. Schroder, A. K. Skidmore, D. Zurell and S. Lautenbach. 2012. Collinearity: a review of methods to deal with it and a simulation study evaluating their performance. *Ecography* 36(1):27-46.
- Dyer, R. J. 2014. An R Package for the Spatial Analysis of Population Genetic Data. R package version 1.5.2.
- Evans, J., 2020. spatialEco: Spatial Analysis and Modelling Utilities. R package version 1.3-1
- Fa, J. E., V. Sánchez-Cordero and A. Méndez, 1996. Interspecific agonistic behavior in small mammals in a Mexican high-elevational grassland. *Journal of Zoology* 239(2):396-401.
- Fisher, R., S. Perkins, A. Walker and E. Wolfart. 2003. Gaussian smoothing. Available in <https://homepages.inf.ed.ac.uk/rbf/HIPR2/gsmooth.htm>.
- Flores-Peredo, R. and G. Vázquez-Domínguez. 2016. Influence of vegetation type and season on rodent assemblage in a Mexican temperate forest mosaic. *Therya* 7(3):357-369.

- Frichot, E., F. Mathieu, T. Trouillon, G. Bouchard and O. François. 2014. Fast and efficient estimation of individual ancestry coefficients. *Genetics*, 196(4), 973–983.
- Fuller, T., M. Munguía, M. Mayfield, V. Sánchez-Cordero and S. Sarkar. 2006. Incorporating connectivity into conservation planning: A multi-criteria case study from central Mexico. *Biological Conservation* 133(2): 131-142.
- Galpern, P., P. Peres-Neto, J. Polfus and M. Manseau. 2014. MEMGENE: Spatial pattern detection in genetic distance data. *Methods in Ecology and Evolution* 5(10): 1116-1120. R package version 1.0.1.
- García-Elfring, A., R. D. H. Barrett, M. Combs, T. J. Davies, J. Munshi-South and V. Millien. 2017. Admixture on the northern front: population genomics of range expansion in the white-footed mouse (*Peromyscus leucopus*) and secondary contact with the deer mouse (*Peromyscus maniculatus*). *Heredity* 119: 447-458.
- García-Mendoza, D. F., C. López-González, Y. Hortelano-Moncada, R. López-Wilchis, and J. Ortega. 2018. Geographic cranial variation in *Peromyscus melanotis* is related to primary productivity. *Journal of Mammalogy* 9(4):898-905.
- Glendinning, J. I., A. A. Mejia and L. P. Brower. 1988. Behavioral and ecological interactions of foraging mice (*Peromyscus melanotis*) with overwintering monarch butterflies (*Danaus plexippus*) in Mexico. *Oecologia* 75: 222-227.
- Goudet, J. and T. Jombart. 2015. Hierfstat: Estimation and test of hierarchical F-statistics. R package
- Goudet, J., T. Kay and B. Weir. 2018. How estimate kinship. *Molecular Ecology* 27: 4121-4135.
- Herten, K., M. S. Hestand, J. R. Vermeesch and J. K. J. Van Houdt. 2015. GBSX: a toolkit for experimental design and demultiplexing genotyping by sequencing experiments. *BMC Bioinformatics* 16:73
- Hijmans, R. J., J. Van Etten, M. Summer, J. Cheng, A. Bevan, R. Bivand, L. Busetto, M. Canty, D. Forrest, A. Ghosh, D. Golisher, J. Gray, J. A. Greenberg, P. Hiemstra, K. Hingee, C. Karney, M. Mattiuzzi, S. Mosher, J. Nowosad, E. Pebesma, O. Perpinam-Lamigueiro, E. B. Racine, B. Rowlingson, A. Shortridge, B. Venables and Wueest. 2020. raster: Geographic Data Analysis and Modeling. R package version 3.0-12.
- Jombart, T., S. Devillard, F. Balloux. 2008. Discriminant analysis of principal components: a new method for the analysis of genetically structured populations. *BMC Genetics* 11(94)
- Kinyanjui, M. 2010. NDVI based vegetation monitoring in Mau Forest complex, Kenya. *African Journal of Ecology* 49(2):165-174.
- Koen, E. L., J. Bowman, C. Sadowski and A. A. Walpole. 2014. Landscape connectivity for wildlife: development and validation of multispecies linkage maps. *Methods in Ecology and Evolution* 5(7):626-623.
- Lampoel, K., S. Duruz, E. Rochat, I. Widmer, P. Orozco-terWengel and S. Joost, 2017. Simple rules for an efficient use of geographic information system in molecular ecology. *Frontiers in Ecology and Evolution. Evolutionary and Population Genetics* 5(33).
- Lepais, O. and J. T. Weir. 2014. Simulations to predict the number of RAD and GBS loci. R package version 0.96.
- Li, H., R. Durbin. 2009. Fast and accurate short read alignment with Burrows-Wheeler Transform. *Bioinformatics* 24(14): 1754-1760.
- Mastretta-Yanes, A., A. Moreno-Letier, D. Piñeiro, T. Jorgensen and B. Emerson; 2015. Biodiversity in mexican highlands and the interaction of geology, geography and climate within the Trans-Mexican Belt. *Journal of Biogeography* 42(9): 1586-1600.

- McGarigal, K. U. and S. Cushman, 2005. The Gradient Concept of Landscape Structure. In: Wiens, John A.; Moss, Michael R., eds. *Issues and Perspectives in Landscape Ecology*. Cambridge University Press. p. 112-119.
- McRae, B.H., B. G. Dickson, T. H. Keitt, and V. B. Shah. 2008. Using circuit theory to model connectivity in ecology and conservation. *Ecology* 89(10): 2712-2724.
- Measho, S., B. Chen, Y. Trisurat, P. Pellikka, L. Guo, S. Arunyawat, V. Tuankrue, W. Ogbazghi and T. Yemane. 2019. Spatio temporal analysis of vegetation dynamics as a response to climate variability and drought patterns in the semiarid region, Eritrea. *Remote Sensing* 11(6): 724.
- Mussmann, S. M., M. R. Douglas, T. K. Chafin and M. E. Douglas. 2019. BA3-SNPs: Contemporary migration reconfigured in BayesAss for next-generation sequence data. *Methods in Ecology and Evolution* 10(10):1808-1813.
- Naimi, B. 2017. usmd: Uncertainty Analysis for Species Distribution Model. R package version 1.1-18
- O'Leary, S. J., J. B. Puritz, S. C. Willis, C. M. Hollenbeck and D. S. Portnoy. 2018. These aren't the loci you're looking for: Principles of effective SNPs filtering for molecular ecologists. *Molecular Ecology* 27(16):3193-3206.
- Oksanen, J., F. G. Blanchet, R. Kindt, P. Legendre, R. B. O'hara, G. L. Simpson, P. Solymos, M. H. Stevens and H. Wagner. 2011. Vegan: Community Ecology Package. R package version 2.5-6
- Parchman, T. L., Z. Gompert, J. Mudge, F. D. Schilkey, C. W. Benkman and C. A. Buerkle. 2012. Genome-wide association genetics of an adaptive trait in lodgepole pine. *Molecular Ecology* 21(12): 2991-3005.
- Pelletier, D., M. Clark, M. G. Anderson, B. Rayfield, M. A. Wulder and J. A. Cardille. 2014. Applying Circuit Theory for Corridor Expansion and Management at Regional Scales: Tiling, Pinch Points, and Omnidirectional connectivity. *PLoS ONE* 9(1): e84135.
- Peterman, W. E., G. M. Connette, R. D. Semlitsch and L. S. Eggert. 2014. Ecological resistance surfaces predict fine-scale genetic differentiation in a terrestrial woodland salamander. *Molecular Ecology* 23(10): 2402-2413.
- Peterman, W. E. 2018. Resistance GA: An R package for the optimization of resistance surfaces using genetic algorithms. *Methods in Ecology and Evolution* 9:1630-1647.
- Peterman, W. E., K. J. Winiarski, C. E. Moore, E. Da Silva Carvalho, A. L. Gilbert and S. F. Spear. 2019. A comparison of popular approaches to optimize landscape resistance surfaces. *Landscape Ecology* 34(9): 2197-2208.
- Priadka, P., M. Manseau, T. Trottier, D. Hervieux, P. Galpern, P. McLoughlin and P. Wilson. 2018. Partitioning drivers of spatial genetic variation for a continuously distributed population of boreal caribou: Implications for management unit delineation. *Ecology and Evolution* 9(1):141-143.
- Probst, A., D. Gatziolis and N. Strigul. 2018. Intercomparison of photogrammetry software for three-dimensional vegetation modelling. *Royal Society Open Science* 5(7):72192.
- Prunier, J. G., M. Colyn, X. Legendre,N. F. Nimon and M. C. Flamand. 2015. Multicollinearity in spatial genetics: separating the wheat from the chaff using communality analyses. *Molecular Ecology* 24(2): 263-283.
- Purcell, S., B. Neale, K. Tood-Brown, L. Thomas, M. Gerreira, D. Brender, J. Maller, P. Sklar, P De Bakker, M. J. Daly and P. C. Sham. 2009. PLINK: a tool set for whole-genome association and population-based linkage analysis. *American Journal of Human Genetics* 81.
- QGIS Development Team, 2020. QGIS Geographic Information System. Open Source Geospatial Foundation Project. <http://qgis.osgeo.org>

- Rahlf, J., J. Breidenbach, S. Solberg, E. Naesset and R. Astrup. 2017. Digital aerial photogrammetry can efficiently support large-area forest inventories in Norway. *Forestry* 90(5):710-718.
- Rambaut, A., A. J. Drummond and M. Suchard. 2018. Tracer v1.6.
- Roser, L. G., L. I. Ferreyra, B. O. Saidman and J. C. Vilardi. 2017. EcoGenetics an R package for the management and exploratory analysis of spatial data in landscape genetics. *Molecular Ecology Resources* 17(6): e241-e250.
- Ruiz-Soberanes, J. 2009. Estudio mastofaunístico del Parque Nacional La Malinche, Tlaxcala, México. Dissertation Facultad de Ciencias, UNAM
- Rzedowski, J. 2006. Capítulo 17 Bosque de Coníferas. Vegetación de México. Comisión Nacional para el Conocimiento y Uso de la Biodiversidad, CONABIO. 1° edición.
- Shrink, A. J., E. L. Landguth and S. A. Cushman. 2017. A comparison of individual based genetic distance metrics for landscape genetics. *Molecular Ecology* 17(6):1308-1317.
- Sikes, R. S., Animal Care and Use Committee of the American Society of Mammalogists, 2016. 2016 Guidelines of the American Society of Mammalogists for the use of wild mammals in research and education. *Journal of Mammalogy* 97(3): 663-688.
- Spear, S. F., S. Cushman and B. H. McRae. 2016. Resistance surface modelling in landscape genetics. *Landscape genetics: concepts, methods and applications*, 1st edition. Wiley and Sons.
- Sohan, M., M. Bastien and E. Inquia. 2013. An improved genotyping by sequencing GBS approach offering increased versatility and efficiency of SNPs discovery and genotyping. *Plos One* 8(1): e54603.
- Waits, L. and A. Storfer. 2015. Basics of population Genetics: Quantifying Neutral and Adaptive Genetic Variation for Landscape Genetic Studies. *Landscape genetics: Concepts, Methods, Applications*. Pp 35-57.
- Wang, Y., X. Cao, Y. Zhao, J. Fei, X. Hu and N. Li. 2017. Optimized double digest genotyping by sequencing (dd-GBS) method with high density SNP markers and high genotyping accuracy for chickens. *Plos One* 12(6): e0179073.
- White, T. A., S. E. Perkins, G. Heckel and J. B. Searle. 2013. Adaptive evolution during an ongoing range expansion: the invasive bank vole (*Myodes glareolus*) in Ireland. *Molecular Ecology* 22(11):2971-2985.
- Wilson, G. and B. Rannala. 2003. Bayesian inference of recent migration rates using multilocus genotypes. *Genetics* 163(3): 1177-1191.
- Wilson, I. 2019. Using unnamed aerial systems to classify land cover and assess productivity in forested wetlands in Nova Scotia. Dissertation from Saint Mary's University, Halifax, Nova Scotia, Canada.
- Wittische, J., J. Janes and P. James. 2019. Modelling landscape genetic connectivity of the mountain pine beetle in western Canada. *Canadian Journal of Forest Research* 49(11): 1339-1348.
- Zheng, X., D. Lavine, S. Gogarten, C. Laurie and B. Weir. 2012. A high-performance Computing Toolset for relatedness and Principal Component Analysis of SNP Data. *Bioinformatics* 28(24): 3326-3328. R package version 1.16
- Zhu, F., Q. Cui and Z. Hou. 2016. SNP discovery and genotyping using genotyping by sequencing in Pekin ducks. *Scientific reports* 6(36223).

**Highland forest's environmental complexity drives landscape genomics and connectivity
of the rodent *Peromyscus melanotis***

Gabriela Borja-Martínez, Daniel Tapia-Flores, Aaron B.A. Shafer and Ella Vázquez-Domínguez

Supporting information

Appendix 2: Tables S1-S10

Table S1. Data for *Peromyscus melanotis* individuals sampled on La Malinche National Park, México used in this study. ID per individual, sampling locality coordinates (X, Y), slope (ECLM=Estación Científica La Malinche; CVM=Centro Vacacional Malinche), Sex (F=female, M=male) and reproductive status (ST =scrothed testicles, UT= unscrothed testicles, CV= closed vagina, OV= open vagina, BP= breast present, BA= breast absent) are included. Morphological measurements include weight (in grams) and length of the body, tail, left foot and left ear (in mm).

ID	Coordinates					Sex	Reproductive status	Morphological measurements			
	X	Y	Slope	Elevation level				Weight (g)	Tail length (cm)	Body length (mm)	Foot length (mm)
01_01	606953	2127951	ECLM	3,000	M	UT	26	5.0	7.5	19.81	16.3
01_02	607644	2127510	ECLM	2,987	F	CV, BP	30	6.0	9.0	18.82	19.38
01_05	607621	2127226	ECLM	3,006	M	UT	27	6	7.3	18.75	15.94
01_07	607557	2127275	ECLM	2,997	M	UT	25	5.3	7.5	17.93	16.9
01_10	607695	2127429	ECLM	2,999	M	ST	29	6.5	7.5	20.36	20
01_11	607667	2127262	ECLM	3,000	F	CV, BP	32	6.3	8	17.53	19.12
01_12	607623	2126072	ECLM	3,009	M	ST	29	6.0	7.5	13.5	19.6
02_01	604630	2127955	ECLM	3,245	M	UT	28	6.0	8.5	20	16.53
02_02	604605	2127935	ECLM	3,275	M	UT	28	6.0	7.0	19.67	15.74
02_03	604583	2127922	ECLM	3,278	F	CV, BA	27	6.0	7.5	17.72	19.6
02_04	604567	2127864	ECLM	3,298	M	UT	28	6.5	8.5	18.95	16.45
02_06	604493	2127880	ECLM	3,310	M	UT	24	5.0	6.5	18.06	13.0
02_07	604469	2127853	ECLM	3,322	F	OV	25	7.0	7.5	19.14	15.73
02_08	604416	2127888	ECLM	3,311	----	-----	22	5.5	7.0	19.78	17.28
02_09	604372	2127881	ECLM	3,316	M	UT	23	6.0	7.0	19.45	17.34
02_10	604341	2127894	ECLM	3,311	M	UT	23	6.0	7.5	19.0	15.92
02_11	604325	2127895	ECLM	3,324	F	CV, BP	32	6.0	8.5	20.03	20.23
02_12	604285	2127895	ECLM	3,329	M	UT	27	6.0	7.5	18.86	16.08
03_01	604389	2127831	ECLM	3,331	M	UT	27	6.5	7.0	16.65	19.9
03_03	604319	2127802	ECLM	3,311	F	CV, BA	25	5.0	7.0	16.94	17.63
03_06	604324	2127723	ECLM	3,319	F	CV, BA	24	6.5	8.5	16.54	16.04
03_07	604317	2127695	ECLM	3,298	F	CV, BP	26	5.9	7.0	18.14	19.24
03_08	604253	2127705	ECLM	3,311	M	UT	24	6.0	8.0	19.04	17.55
03_10	604217	2127709	ECLM	3,331	F	CV, BP	22	6.3	9.0	19.64	20.00
03_12	604153	2127704	ECLM	3,326	M	UT	23	5.5	7.0	18.19	17.10
03_13	604130	2127712	ECLM	3,335	F	CV, BA	24	6.0	7.0	18.30	17.86
03_14_1	604117	2127714	ECLM	3,330	F	CV, BA	24	5.0	8.0	17.87	19.07
03_14_2	604117	2127714	ECLM	3,330	M	UT	23	6.5	8.5	19.64	18.08
03_15	604120	2127747	ECLM	3,341	M	UT	28	7.0	8.5	19.53	17.70
03_16	604121	2127706	ECLM	3,340	M	UT	28	5.5	7.5	19.0	17.43
03_17	604173	2127813	ECLM	3,343	M	UT	28	7.0	8.3	20.0	18.82
03_18	604184	2127807	ECLM	3,344	F	CV, BA	24	5.5	6.5	19.13	16.89
03_20	604217	2127826	ECLM	3,351	--	-----	23	5.5	7.5	19.99	16.91
03_21	604253	2127805	ECLM	3,345	M	UT	26	6.5	7.5	19.60	17.84
03_22	604260	2127805	ECLM	3,342	M	UT	27	6.0	8.0	19.54	18.15
03_24	604300	2127817	ECLM	3,318	--	-----	23	4.5	7.5	18.42	18.37
04_01	605525	2128168	ECLM	3,190	M	UT	23	5.8	8.5	19.57	14.05
04_02	605518	2128197	ECLM	3,186	F	CV, BA	19	5.0	7.0	19.1	17.61
04_03	605515	2128206	ECLM	3,190	F	CV, BA	25	6	7.5	13.5	19.33
04_05	605583	2128230	ECLM	3,208	M	UT	31	7	7.5	19.2	19.47

04_07	605606	2128221	ECLM	3,197	M	UT	27	6.5	8.0	18.57	15.56
04_08	605627	2128204	ECLM	3,181	M	UT	29	6.5	8.5	19.84	18.07
04_10	605671	2128127	ECLM	3,181	F	CV, BA	27	6	8.5	18.68	15.16
04_11	605681	2128111	ECLM	3,168	M	UT	28.5	6.0	8.5	18.27	18.58
04_12	605695	2128113	ECLM	3,179	M	UT	23.5	5.0	7.5	17.89	15.99
04_13	605695	2128113	ECLM	3,169	M	UT	24	6.3	7.5	20.60	17.38
05_01	605706	2128072	ECLM	3,177	M	UT	26	7.0	8.5	19.8	16.66
05_02	605705	2128051	ECLM	3,181	F	CV, BA	29	5.5	8.5	19.55	16.67
05_03	605672	2128024	ECLM	3,168	F	CV, BP	34	7.0	9.5	20.45	18.78
05_04	605669	2128020	ECLM	3,170	M	UT	27.5	6.2	8.0	19.62	17.43
05_05	605655	2128031	ECLM	3,171	M	UT	27	6.0	8.5	18.79	16.43
05_06	605645	2128031	ECLM	3,172	M	UT	23	5.5	8.0	18.98	15.48
05_08_1	605604	2128076	ECLM	3,190	M	UT	23	7.0	8.5	18.7	16.12
05_08_2	605604	2128076	ECLM	3,190	M	UT	23	6.0	7.5	19.55	15.57
05_09	605554	2128067	ECLM	3,194	M	UT	27	5.4	7.5	17.15	16.27
05_10	605547	2128068	ECLM	3,205	M	UT	26	6.5	8.5	19.81	17.04
05_14	605437	2128095	ECLM	3,200	M	UT	27	6.3	8.0	17.37	15.97
05_15	605404	2128088	ECLM	3,199	F	CV, BA	25	5.5	8.5	17.69	16.33
06_01	609617	2126651	ECLM	2,844	M	UT	25.5	6.0	8.0	17.84	16.01
06_04	610015	2126689	ECLM	2,803	M	UT	26.5	6.0	8.0	18.89	16.64
07_01	603445	2127784	ECLM	3,438	F	CV, BA	29	6.0	8.0	18.63	17.57
07_02	603481	2127781	ECLM	3,436	M	UT	29.5	7.0	9.0	20.09	18.92
07_04	603406	2127767	ECLM	3,444	F	OV, BA	26	6.0	7.5	18.96	18.01
07_06	603386	2127733	ECLM	3,451	M	UT	29	6.0	8.5	19.05	18.16
07_07	603414	2127734	ECLM	3,452	F	OV, BP	29	6.2	7.5	18.29	16.44
07_08	603487	2127719	ECLM	3,440	F	OV, BP	27.5	6.5	8.0	19.26	17.75
08_01	603514	2127650	ECLM	3,438	M	UT	28	7.5	8	19.42	17.53
08_02	603521	2127628	ECLM	3,437	F	CV, BP	31	6.5	8.5	19.61	17.13
08_03	603526	2127634	ECLM	3,426	---	-----	22	4.9	6.5	17.68	17.49
08_04	603533	2127613	ECLM	3,433	F	CV, BP	22	6.0	7.0	17.81	18.18
08_05	603545	2127582	ECLM	3,423	F	CV, BP	31	7.0	7.5	19.34	16.06
08_06	603517	2127573	ECLM	3,430	M	UT	27.5	7.0	7.5	19.19	16.57
08_07	603489	2127568	ECLM	3,419	F	CV, BP	27	6.0	8.0	19.73	17.75
08_09	603458	2127556	ECLM	3,433	M	UT	25.5	6.5	7.5	19.29	17.31
08_10	603459	2127554	ECLM	3,423	M	UT	31	6.5	8.5	19.42	17.59
08_11	603433	2127534	ECLM	3,424	F	CV, BP	25	5.0	7.5	18.65	15.05
08_13	603359	2127531	ECLM	3,436	M	UT	24	5.5	8.0	18.07	16.92
08_14	603402	2127619	ECLM	3,407	F	CV, BP	28.5	7.0	8.5	17.86	16.47
09_02	608780	2127085	ECLM	2,912	M	UT	20.5	6.0	7.0	17.64	15.72
09_04	608576	2127263	ECLM	2,932	F	CV, BP	29	6.5	9.0	19.66	17.92
09_05	608575	2127280	ECLM	2,928	M	UT	24.5	6.3	8.5	18.07	15.53
09_06	608715	2127256	ECLM	2,910	M	UT	25.5	7.0	7.5	20.0	16.43
10_01	607527	2127761	ECLM	3,029	H	CV, BA	21	5.8	7.0	19.61	15.64
10_02	607525	2127836	ECLM	3,013	H	CV, BP	30	6.8	9.0	20.7	18.75
10_03	607583	2127881	ECLM	3,017	M	UT	23	6.0	7.5	18.57	16.61
10_04	607633	2127893	ECLM	3,013	M	UT	23	6.5	7.5	18.81	17.43
11_01	601886	2129537	CVM	3,459	M	UT	26.5	5.8	9.0	20.18	19.94
11_02	601827	2129475	CVM	3,488	M	UT	22	4.0	6.5	19.71	13.94
11_03	601817	2129463	CVM	3,493	M	UT	30	5.0	8.0	19.76	18.67
11_04	601898	2129426	CVM	3,508	M	UT	24	4.5	7.0	18.59	16.84
12_01	602217	2129536	CVM	3,470	F	CV, BA	34	5.0	7.0	18.96	17.04

12_02	602211	2129532	CVM	3,478	M	UT	29	5.0	8.0	18.26	16.81
12_03	602226	2129506	CVM	3,466	M	UT	30	4.5	8.0	18.61	16.09
13_02_1	601663	2129816	CVM	3,418	M	UT	24	6.0	7.0	18.41	14.11
13_02_2	601663	2129816	CVM	3,418	F	CV, BA	19	5.7	6.5	19.07	15.43
13_03	601645	2129812	CVM	3,413	M	UT	27	5.5	8.0	18.62	16.2
13_04	601644	2129800	CVM	3,419	F	CV, BA	27	6.0	7.5	17.85	14.8
13_05	601653	2129688	CVM	3,443	F	CV, PB	28	6.5	8.0	18.50	16.67
13_06	601659	2129645	CVM	3,459	F	CV, BA	20.5	5.5	6.8	17.53	17.10
14_01	601515	2129662	CVM	3,465	F	CV, BA	27	5.5	7.5	18.28	15.02
15_01	601041	2129662	CVM	3,374	M	UT	24	6.3	7.6	18.67	16.04
16_02	601283	2130559	CVM	3,304	F	CV, PB	30	6.8	7.5	18.09	18.9
16_03	601299	2130575	CVM	3,313	M	UT	24	5.6	7.5	18.47	18.8
16_04	601386	2130642	CVM	3,292	F	CV, BA	23	6.0	7.2	19.72	19.05
16_05	601431	2130625	CVM	3,292	F	OV, BA	25	5.8	7.4	18.84	16.98
16_06	601441	2130617	CVM	3,300	M	UT	28	6.5	7.4	19.54	16.35
16_07	601459	2130606	CVM	3,300	M	UT	31	6.9	8.1	19.65	18.42
17_02	600822	2130854	CVM	3,239	F	CV, PB	33.5	6.9	8.0	18.4	19.36
17_03	600811	2130867	CVM	3,237	M	UT	27	6.6	7.3	17.96	17.62
17_05	600759	2130904	CVM	3,238	F	CV, PB	34	6.4	7.2	18.13	19.38
17_06	600719	2130993	CVM	3,229	F	CV, PB	28	5.5	7.5	17.04	18.6
18_02	600893	2130818	CVM	3,254	F	CV, BA	21	5.8	6.4	18.5	15.57
18_05	600924	2130873	CVM	3,252	F	CV, BA	24	6.6	7.4	18.34	16.87
18_08	600930	2130915	CVM	3,230	F	CV, BP	29	7.0	8.5	18.47	17.58
18_09	601002	2130966	CVM	3,230	F	OV, BP	30	5.7	8.2	19.33	16.53
18_10	601022	2130962	CVM	3,227	M	UT	25	6.0	7.2	18.44	17.68
18_11	601050	2130953	CVM	3,235	F	OV, BP	26	6.5	7.6	18.40	16.42
18_12	601070	2130952	CVM	3,246	M	UT	28.5	7.0	7.8	18.61	16.36
18_13	601067	2130935	CVM	3,246	F	CV, BP	26	6.0	7.6	18.24	15.83
19_01	600772	2131382	CVM	3,157	M	UT	26	6.5	7.6	19.15	16.72
19_03	600767	2131435	CVM	3,163	M	UT	27	5.6	8.0	19.16	17.77
19_05_1	600709	2131467	CVM	3,160	M	UT	25.5	6.5	7.8	18.66	19.02
19_05_2	600709	2131467	CVM	3,160	M	UT	20	5.0	6.9	17.95	14.99
19_06	600651	2131457	CVM	3,156	M	UT	24.5	6.5	8.0	18.32	18.33
19_07	600553	2131408	CVM	3,155	F	CV, BA	28	6.5	8.2	18.94	16.96
19_08	600546	2131405	CVM	3,152	M	UT	28	5.8	7.6	19.05	18.5
20_02	600880	2131378	CVM	3,176	F	CV, BA	28	6.5	7.5	18.77	15.72
20_03	600980	2131419	CVM	3,185	M	UT	22	7.3	7.8	19.29	16.60
20_04	601032	2131427	CVM	3,172	M	UT	25	5.8	7.6	19.13	18.06
20_05	601105	2131418	CVM	3,174	F	CV, BA	20.5	7.0	7.1	19.19	17.13
20_06	601131	2131418	CVM	3,177	M	ST	29	7.0	8.6	19.78	18.89
20_07	601140	2131423	CVM	3,178	M	UT	23.5	6.4	7.2	18.47	16.83
M4CLM	607254	2127295	ECLM	-----	----	-----	-----	-----	-----	-----	-----

Table S2. Collinearity analysis based on the variance inflation factor (VIF) for the two slopes, CVM and ECLM on La Malinche National Park. VIF_a comprises all the variables, VIF_b is the adjusted VIF when variables with a VIF >5 are removed.

		CVM		ECLM		Global	
Variables		VIF _a	VIF _b	VIF _a	VIF _b	VIF _a	VIF _b
Aspect		1.2110	1.1548	1.1378	1.0950	1.0657	1.05832
Elevation		3.6361	3.4060	2.9756	2.4749	1.8617	1.7820
Landforms		3.1087	2.6459	2.2545	2.1533	2.5925	2.0085
Litter cover		2.6075	2.2115	1.2358	1.2065	--	--
Moisture		1.4601	1.3377	3.7762	3.9092	--	--
MSI		249.3475	-----	81.9881	-----	122.8146	--
NDVI		247.8878	1.8432	81.5375	1.5491	121.9666	1.6029
Slope		1.7012	1.8922	2.1660	1.8151	1.7548	1.6219
Temperature		1.6287	1.4001	4.6763	4.7263	--	--
Topographic position		3.1132	2.6658	2.2598	2.1500	2.5988	2.0234
Tree height		1.2339	1.2107	1.3812	1.3932	1.4803	1.5453
Vegetation cover		1.2825	1.1899	1.4823	1.4495	1.5652	1.4586

Table S3. Correlation matrix of landscape variables between the elevation levels within ECLM (blue) and CVM (purple) slopes. Name of columns indicate the layer evaluated (1=aspect, 2=elevation, 3=landforms, 4=litter cover, 5=moisture, 6=MSI, 7=NDVI, 8=slope, 9=temperature, 10=topographic position, 11=tree height, 12=vegetation cover).

	(1)	(2)	(3)	(4)	(5)	(6)	(7)	(8)	(9)	(10)	(11)	(12)
(1)	1.0	-0.137	0.020	0.201	0.200	- 0.035	- 0.032	-0.08	-0.166	0.034	0.053	0.047
(2)	0.233	1.0	0.042	-0.716	-0.140	- 0.629	- 0.619	0.612	0.215	0.028	0.028	-0.234
(3)	-0.019	0.037	1.0	-0.014	-0.031	- 0.004	- 0.004	0.005	0.022	0.789	0.058	0.011
(4)	0.056	0.290	0.003	1.0	0.077	0.415	0.402	-0.398	-0.220	-0.004	-0.164	0.135
(5)	-0.083	-0.368	-0.010	-0.261	1.0	- 0.010	- 0.004	-0.135	-0.443	-0.013	-0.019	-0.021
(6)	-0.048	0.240	0.023	0.072	-0.389	1.0	0.997	-0.474	-0.082	0.014	0.127	0.321
(7)	-0.035	0.251	0.023	0.074	-0.382	0.994	1.0	-0.474	-0.092	0.014	0.136	0.328
(8)	0.218	0.690	0.014	0.133	-0.227	0.162	0.169	1.0	0.252	-0.014	0.005	-0.108
(9)	0.080	0.564	0.006	0.155	-0.831	0.419	0.411	0.402	1.0	0.008	-0.087	-0.115
(10)	-0.023	0.030	0.720	-0.006	-0.014	0.020	0.019	0.014	0.005	1.0	0.079	0.009
(11)	-0.020	-0.041	0.048	-0.038	-0.164	0.370	0.372	-0.036	0.126	0.046	1.0	0.309
(12)	-0.041	-0.186	0.002	-0.076	-0.142	0.321	0.330	-0.167	-0.039	0.002	0.448	1.0

Table S4. Results of the In silico digestions assessment performed with SimRAD v0.96 (Lepais & Weir, 2014), showing the number of cutting sites produced with the different restriction enzymes and the number of reads between 100 and 500 bp length.

Restriction enzymes	Number of restriction sites	Number of loci bw 100 and 500 bp
Apk I	380,777	145,678
EcoR I	58,093	6,258
EcoT22 I	73,539	9,863
Hind I	98,133	18,653
Mse I	1,260,811	511,355
Msp I	146,235	39,652
Nsi I	58,934	6,636
Pst I	86,385	14,373
Sbf	6,482	167
Sph I	52,679	5,174
Nsi I + Msp I	204,169	60,835
Pst I + Msp I	232,620	74,443

Table S5. Pairwise F_{ST} between the elevation levels within ECLM (blue) and CVM (purple), and between slopes (green). First left column and top of each following column include the different elevation levels (m), and bold numbers depict the F_{IS} for each elevation level.

	2850	3000	3150	3300	3450	3150	3200	3300	3400	3500
2850	0.005	0.039	0.001	0.027	0.021	0.028	0.025	0.041	0.045	0.047
3000			3150	3300	3450					
3150		0.023	-0.024							
3300		0.019	0.017	-0.016						
3450		0.024	0.019	0.020	-0.007	3150				
3150		0.023	0.022	0.019	0.023	-0.010	3200			
3200		0.037	0.026	0.024	0.030	0.026	-0.011	3300		
3300		0.045	0.039	0.024	0.019	0.026	0.024	0.036	0.016	3400
3400		0.041	0.025	0.021	0.027	0.025	0.040	0.045	0.018	3500
3500		0.038	0.022	0.019	0.025	0.023	0.037	0.041	0.042	0.042

Table S6. Univariate optimized model selection results for the global and regional (CVM and ECLM slopes) scales, based on maximum-likelihood population effects mixed models, for *Peromyscus melanotis* populations from La Malinche National Park. K= number of parameters used for the transformation of continuous surface plus the intercept; AICc= Akaike's information criterion corrected for sample size.

Surface	K	Equation	AICc	Average weight	Average rank	Top model (%)
Regional scale: CVM						
Tree height	4	Inverse Ricker	-1,369.031	0.366	1.890	49.05
NDVI	4	Inverse-Reverse Ricker	-1,367.273	0.385	4.844	38.77
Elevation	4	Inverse Monomolecular	-1,361.658	0.015	5.609	0.19
Litter cover	4	Inverse Ricker	-1,359.984	0.024	4.693	0.61
Aspect	4	Inverse Ricker	-1,358.372	0.051	4.295	3.04
Temperature	4	Ricker	-1,357.230	0.023	6.170	0.62
Distance	2	NA	-1,356.821	0.046	5.868	6.87
TPI	4	Inverse-Reverse Ricker	-1,356.797	0.036	6.099	0.42
Slope	4	Inverse-Reverse Ricker	-1,356.645	0.022	6.812	0.0
Moisture	4	Reverse Ricker	-1,356.532	0.038	6.524	0.51
Regional scale: ECLM						
Aspect	4	Inverse Monomolecular	-5,951.349	0.468	2.121	46.96
Litter Cover	4	Inverse Ricker	-5,948.893	0.356	1.856	35.69
Temperature	4	Inverse-Reverse Ricker	-5,926.462	0.233	3.725	23.39
Slope	4	Reverse Ricker	-5,898.844	0.045	5.405	4.52
Moisture	4	Inverse-Reverse Ricker	-5,899.468	0.058	5.439	5.80
Tree height	4	Inverse Ricker	-5,896.020	0.0004	5.601	0.02
NDVI	4	Inverse-Reverse Ricker	-5,891.231	0.001	6.341	0.17
TPI	4	Inverse-Reverse Ricker	-5,886.733	<0.001	7.112	0.001
Elevation	4	Inverse-Reverse Ricker	-5,873.774	<0.001	9.075	0.0
Distance	2	NA	-5,873.491	<0.001	9.154	0.0
Global Scale: PNLM						

Slope	4	Inverse Ricker	-16,871.31	0.456	1.734	45.66
Aspect	4	Inverse Monomolecular	-16,846.16	0.301	2.864	30.16
TPI	4	Inverse Ricker	-16,826.26	0.185	3.423	18.57
Tree Height	4	Inverse Ricker	-16,809.85	0.033	3.781	3.35
Elevation	4	Inverse-Reverse Ricker	-16,793.86	0.019	4.571	1.94
NDVI	4	Inverse-Reverse Monomolecular	-16,792.63	0.003	4.745	0.31
Distance	2	NA	-16,746.06	<0.001	6.879	0.0

Table S7. Model selection results for multivariate surfaces optimized for the global scale, showing the percentage contribution of each variable to the hypothesis.

Hypotheses	K	Surface	AICc	Contribution to model (%)	Top model (%)
Topography	10	Slope	-16,852.63	72.2199	85.6166
		TPI		6.1570	
		Aspect		21.6230	
Vegetation structure	7	Tree height	16,811.14	98.9537	14.3833
		NDVI		1.0462	

Table S8. Parameters estimates for the regional scales (CVM and ECLM) from the mixed effects model fit to optimized resistances surfaces. Beta, standard error and t-value are estimated by restricted maximum likelihood.

Resistance surface	Parameter	β	SE	t-value
Regional scale: CVM				
Tree height	Intercept	1.1887	0.0282	42.0472
	Tree height	0.0348	0.0046	7.5624
NDVI	Intercept	1.1887	0.0286	41.4601
	NDVI	0.0397	0.0055	7.2135
Elevation	Intercept	1.8887	0.0269	44.1731
	Elevation	0.0322	0.0050	6.4001
Litter cover	Intercept	1.1887	0.0274	43.3332
	Litter cover	0.0189	0.0031	5.9363
Aspect	Intercept	1.1887	0.0271	43.7657
	Aspect	0.0157	0.0025	6.0919
Temperature	Intercept	1.1887	0.0274	43.3781
	Temperature	0.0216	0.0035	6.2559
Distance	Intercept	1.1887	0.0270	43.9953
	Distance	0.0127	0.0022	5.6641
Topographic position	Intercept	1.1887	0.0272	43.6888
	TPI	0.0158	0.0027	5.8737
Slope	Intercept	1.1887	0.0274	43.3394
	Slope	0.0129	0.0022	5.8546
Moisture	Intercept	1.1887	0.0274	43.2389
	Moisture	0.0139	0.0024	5.8149
Regional scale: ECLM				
Aspect	Intercept	1.1251	0.0268	41.9579
	Aspect	0.0521	0.0030	17.1346
Litter cover	Intercept	1.1251	0.0250	44.8717
	Litter cover	0.0723	0.0043	16.5825
Temperature	Intercept	1.1251	0.0256	43.8597
	Temperature	0.0361	0.0025	14.2756
Slope	Intercept	1.1251	0.0266	42.1608
	Slope	0.0475	0.0031	15.2796
Moisture	Intercept	1.1251	0.0242	46.4633
	Moisture	0.0536	0.0038	13.7578
Tree height	Intercept	1.1251	0.0240	46.7288
	Tree height	0.0196	0.0014	13.3808
NDVI	Intercept	1.1251	0.0231	48.5528
	NDVI	0.0392	0.0030	12.9784
Topographic position	Intercept	1.1251	0.0243	46.1300
	TPI	0.0276	0.0021	12.7363
Elevation	Intercept	1.1251	0.0238	47.1411
	Elevation	0.0157	0.0013	11.7667

Distance	Intercept	1.1251	0.0239	48.9263
	Distance	0.0138	0.0011	11.6106

Table S9. Parameters estimates for the regional scales (CVM and ECLM) from the mixed effects model fit to multivariate optimized resistances surfaces. Beta, standard error and t-value are estimated by restricted maximum likelihood.

Resistance surface	Parameter	β	SE	t-value
Regional scale: CVM				
Environment	Intercept	1.1887	0.0283	41.9903
	Environment	0.0225	0.0037	6.0917
Hydroperiod	Intercept	1.1887	0.0282	42.0954
	Hydroperiod	0.0316	0.0042	7.4453
Microclimate	Intercept	1.1887	0.0273	43.4073
	Environment	0.0137	0.0023	5.9331
Productivity1	Intercept	1.1887	0.0280	42.3786
	Productivity1	0.0322	0.0043	7.3555
Productivity2	Intercept	1.1887	0.0267	44.3706
	Productivity2	0.0406	0.0058	6.9346
Productivity3	Intercept	1.1887	0.0280	42.3542
	Productivity3	0.0323	0.0043	7.3607
Topography	Intercept	1.1887	0.0289	41.0481
	Topography	0.0291	0.0047	6.1482
Vegetation orientation	Intercept	1.1887	0.0281	42.1698
	Vegetation orientation	0.0337	0.0044	7.5167
Vegetation structure	Intercept	1.1887	0.0282	42.1070
	Vegetation structure	0.0345	0.0045	7.5480

Regional Scale: ECLM				
Environment	Intercept	1.1251	0.0244	45.9512
	Environment	0.0173	0.0012	14.3355
Hydroperiod	Intercept	1.1251	0.0253	44.4645
	Hydroperiod	0.0529	0.0032	16.0866
Microclimate	Intercept	1.1251	0.0255	43.9651
	Microclimate	0.0589	0.0035	16.4378
Productivity1	Intercept	1.1251	0.0256	43.8987
	Productivity1	0.0574	0.0029	19.2357
Productivity2	Intercept	1.1251	0.0250	44.8870
	Productivity2	0.0853	0.0049	17.0775
Productivity3	Intercept	1.1251	0.0250	44.9174
	Productivity3	0.0852	0.0049	17.0720
Topography	Intercept	1.1251	0.0248	45.2059
	Topography	0.0258	0.0015	16.6229
Vegetation orientation	Intercept	1.1251	0.0265	42.3637
	Vegetation orientation	0.0485	0.0028	16.9607
Vegetation structure	Intercept	1.1251	0.0246	45.6429
	Vegetation structure	0.0569	0.0032	17.4433

Table S10. Parameters estimates for the global scale from the mixed effects model fit to univariate and multivariate optimized resistances surfaces. Beta, standard error and t-value are estimated by restricted maximum likelihood.

Resistance surface	Parameter	β	SE	t-value
Univariate hypotheses				
Slope	Intercept	1.1305	0.0175	65.5200
	Slope	0.0220	0.0008	24.8240
Aspect	Intercept	1.1305	0.0178	63.3406
	Aspect	0.0342	0.0014	23.8999
Topographic position	Intercept	1.3505	0.0172	65.4670
	TPI	0.0300	0.0013	23.0685
Tree height	Intercept	1.1305	0.0168	67.2541
	Tree height	0.0162	0.0007	22.4606
Elevation	Intercept	1.1305	0.0162	69.5837
	Elevation	0.0193	0.0008	21.6648
NDVI	Intercept	1.1305	0.0166	67.8391
	NDVI	0.0154	0.0007	21.6794
Distance	Intercept	1.1305	0.0163	68.9965
	Distance	0.0101	0.0005	19.5253
Multivariate hypotheses				
Topography	Intercept	1.1305	0.0175	64.4568
	Topography	0.0251	0.0010	23.9761
Vegetation structure	Intercept	1.1305	0.0168	67.2647
	Vegetation structure	0.0162	0.0007	22.4516

**Highland forest's environmental complexity drives landscape genomics and connectivity
of the rodent *Peromyscus melanotis***

Gabriela Borja-Martínez, Daniel Tapia-Flores, Aaron B.A. Shafer and Ella Vázquez-Domínguez

Supporting information

Appendix 3: Figures S1-S13

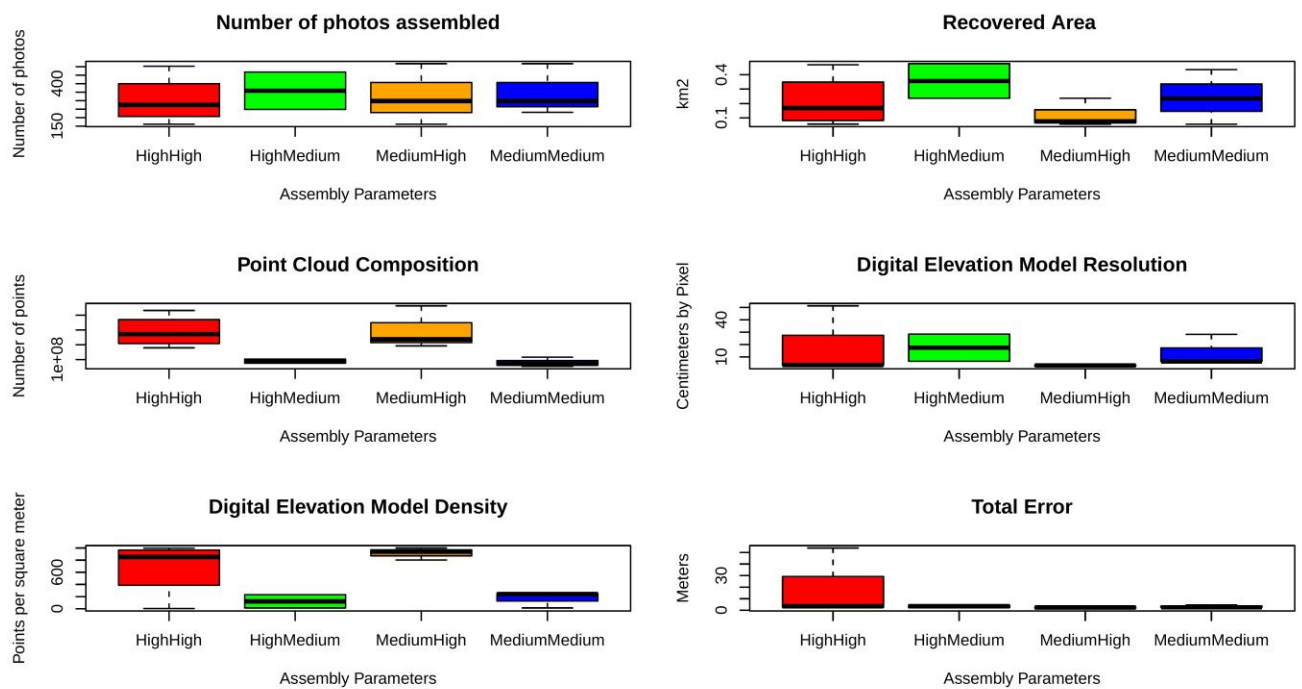


Figure S1. Results for the combinations of parameters evaluated for quality assessment to generate a digital elevation model. The first parameter on the pair HighHigh, HighMedium, MediumHigh and MediumMedium corresponds to the alignment quality and the second to the reconstruction quality.

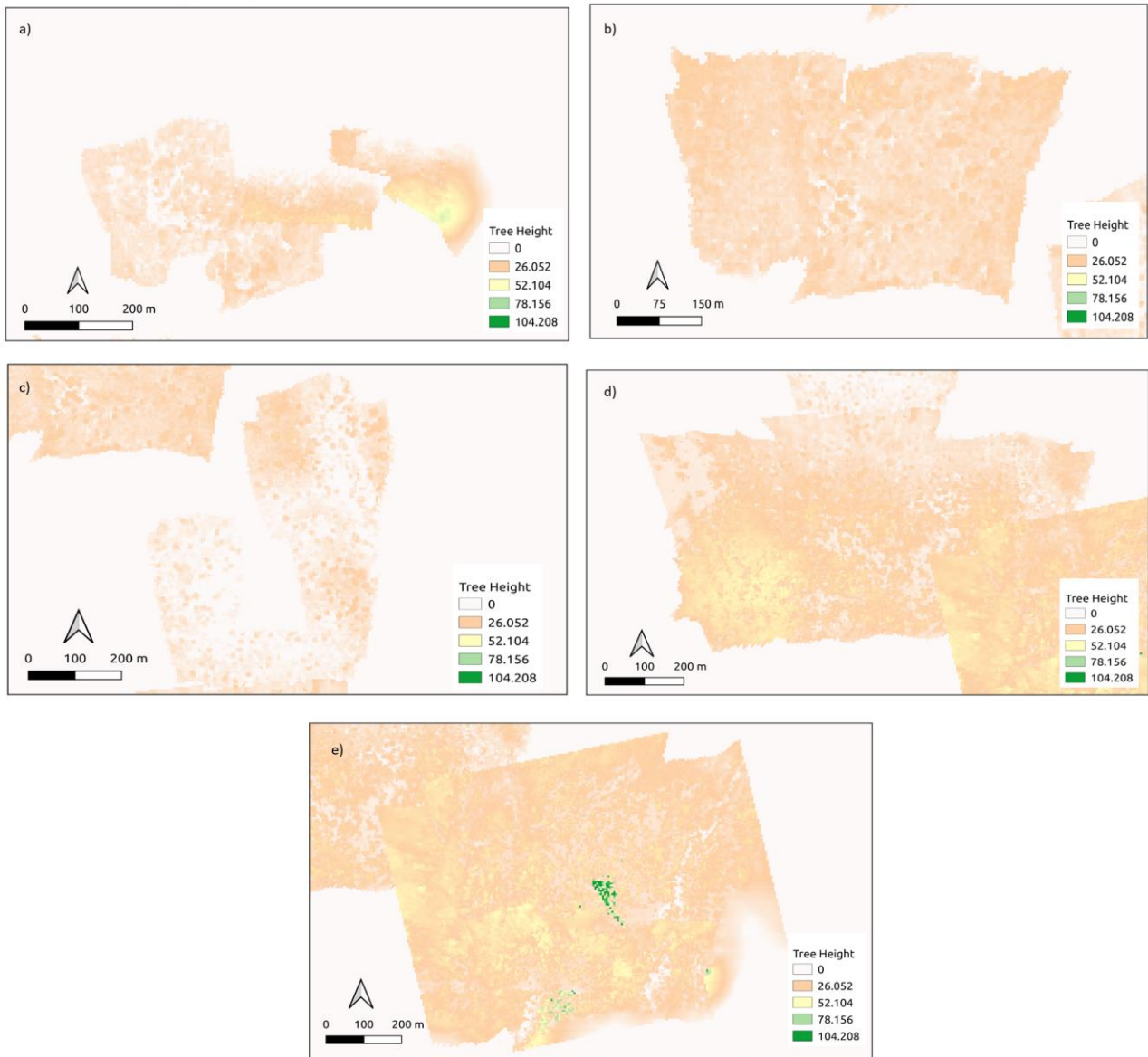


Figure S2. Photogrammetric reconstruction of tree height at the regional level on CVM **a)** 3100m, **b)** 3200m, **c)** 3300 m, **d)** 3400m, **e)** 3500m.

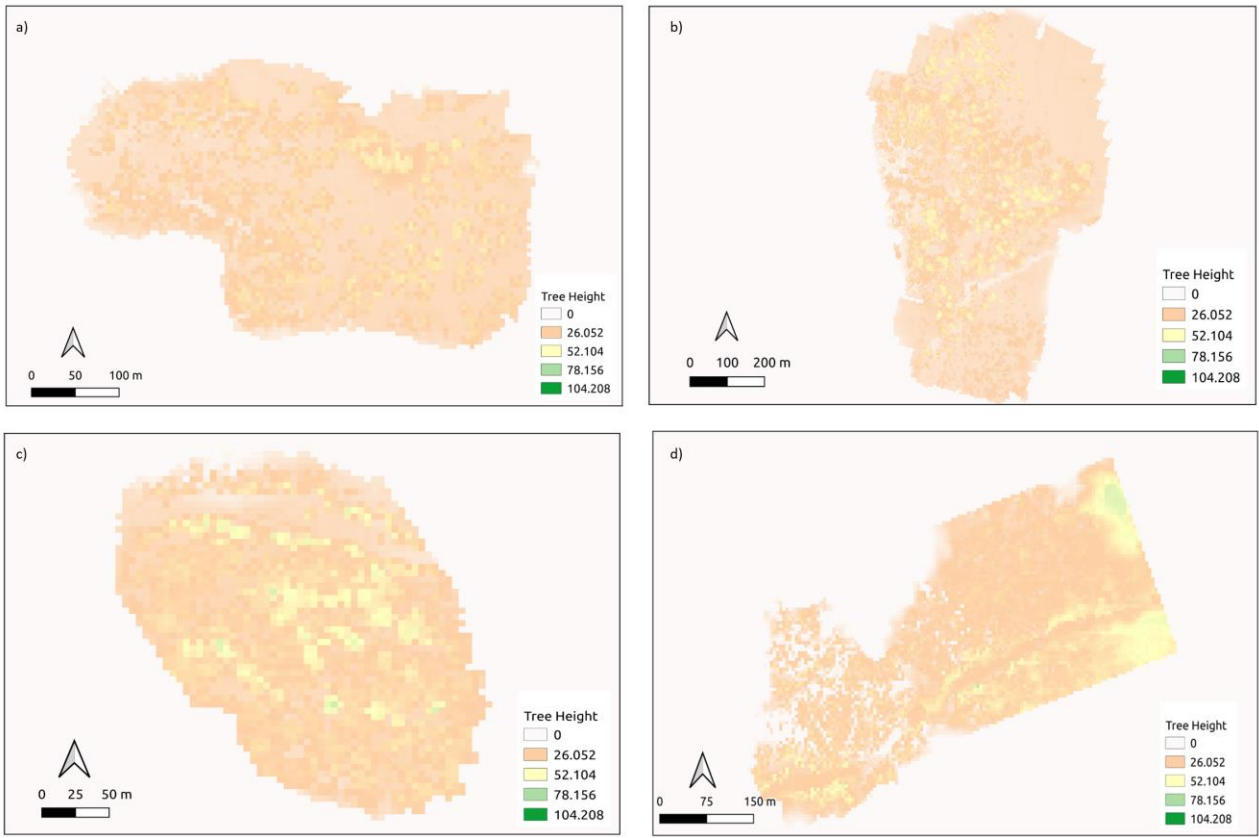


Figure S3. Photogrammetric reconstruction of tree height at the regional level on ECLM **a)** 2800m, **b)** 3000m, **c)** 3300m, **d)** 3450m.

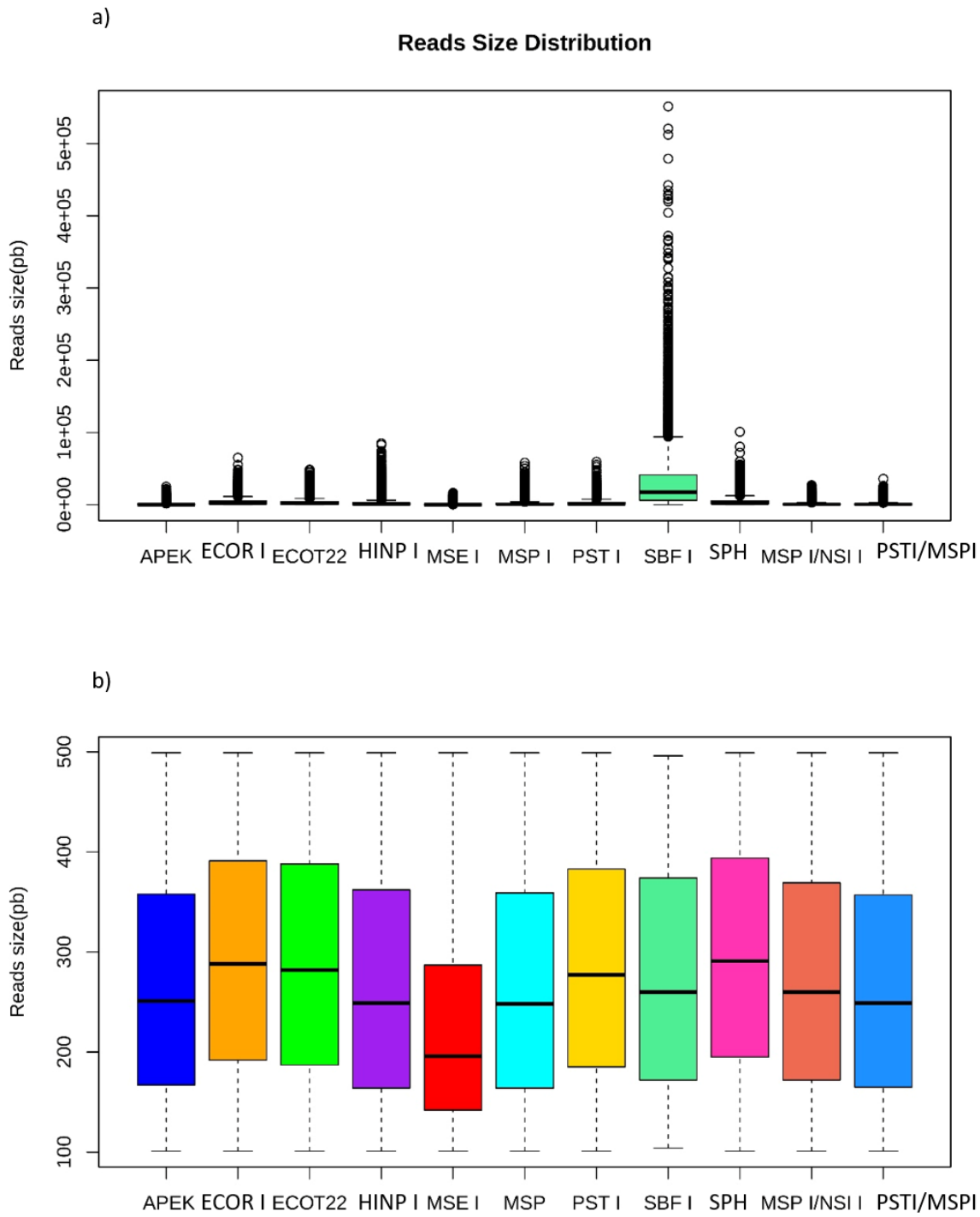


Figure S4. Fragments size distribution. **a)** Distribution size of all the fragments generated with the different combinations of enzymes; **b)** Distribution size of fragments between 100 and 500 bp length.

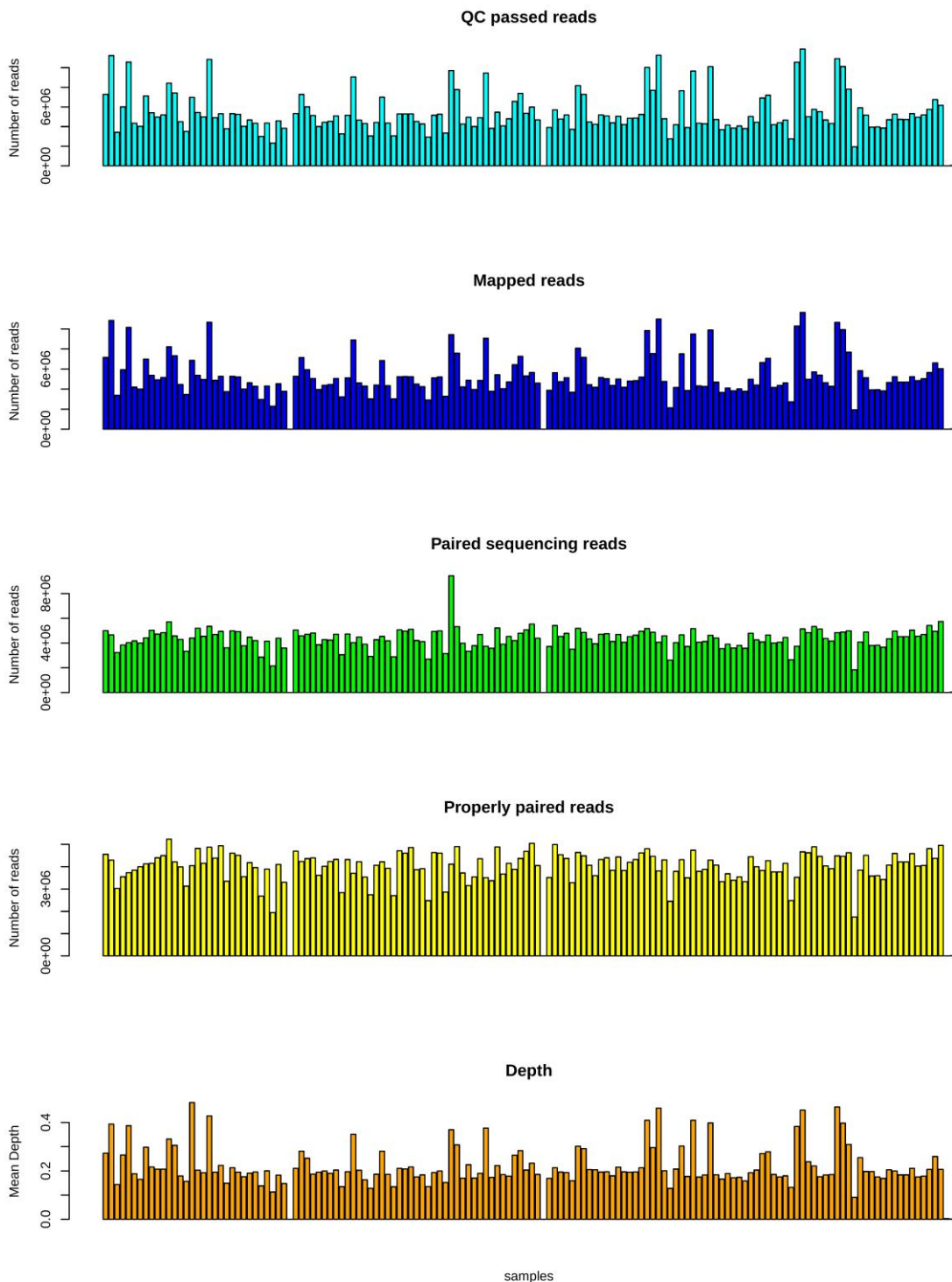


Figure S5. Distribution of reads by sample. Number of reads by sample that passed the QC filter score >22. Most reads were aligned and mapped with the reference genome *Peromyscus maniculatus bairdii* (Ensemble: GCA_000500345.1); reads that did not pair properly were discarded.

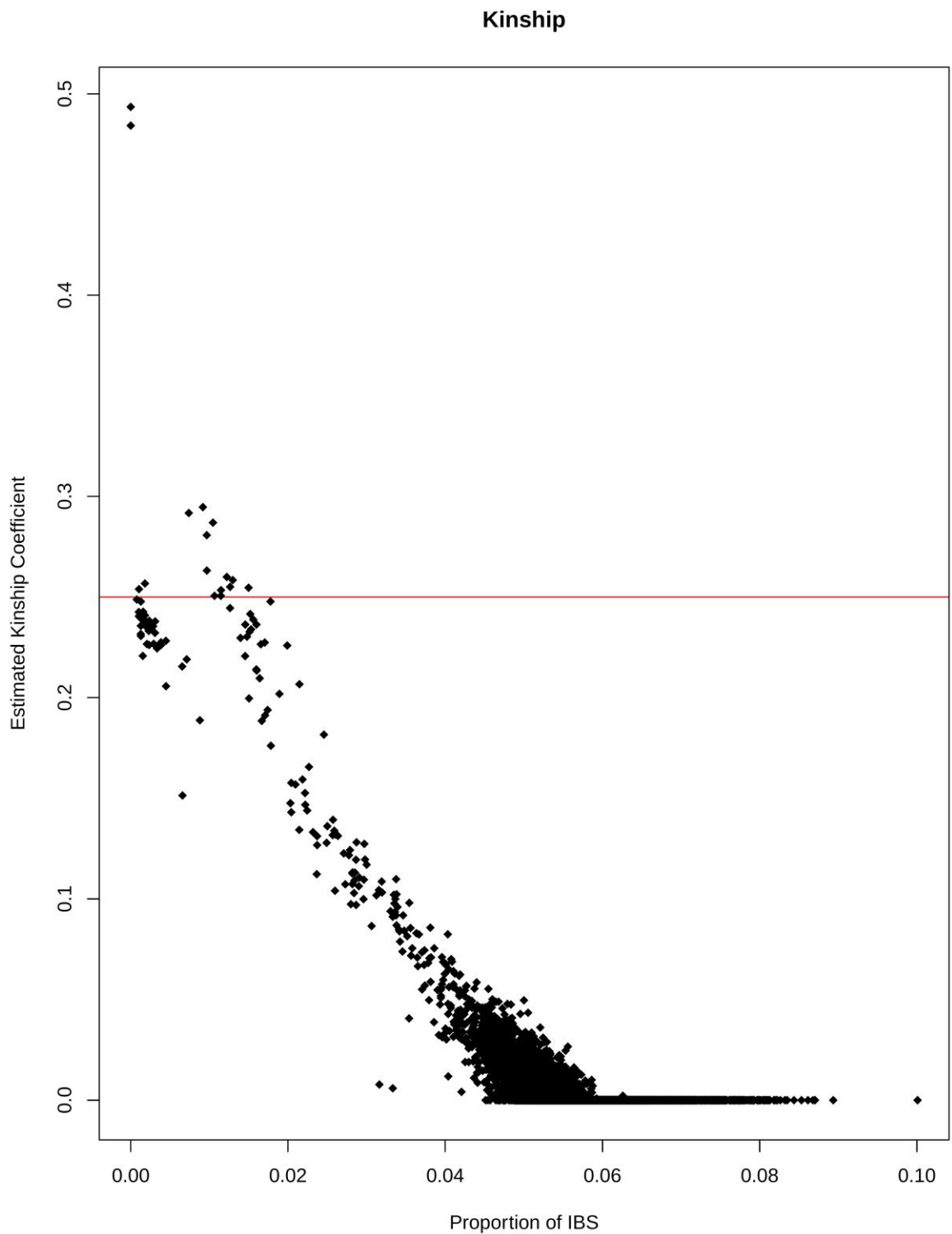


Figure S6. Proportion of paired comparisons of individuals who were identical by descent (Kinship Coefficient) and those identical by state (IBS).

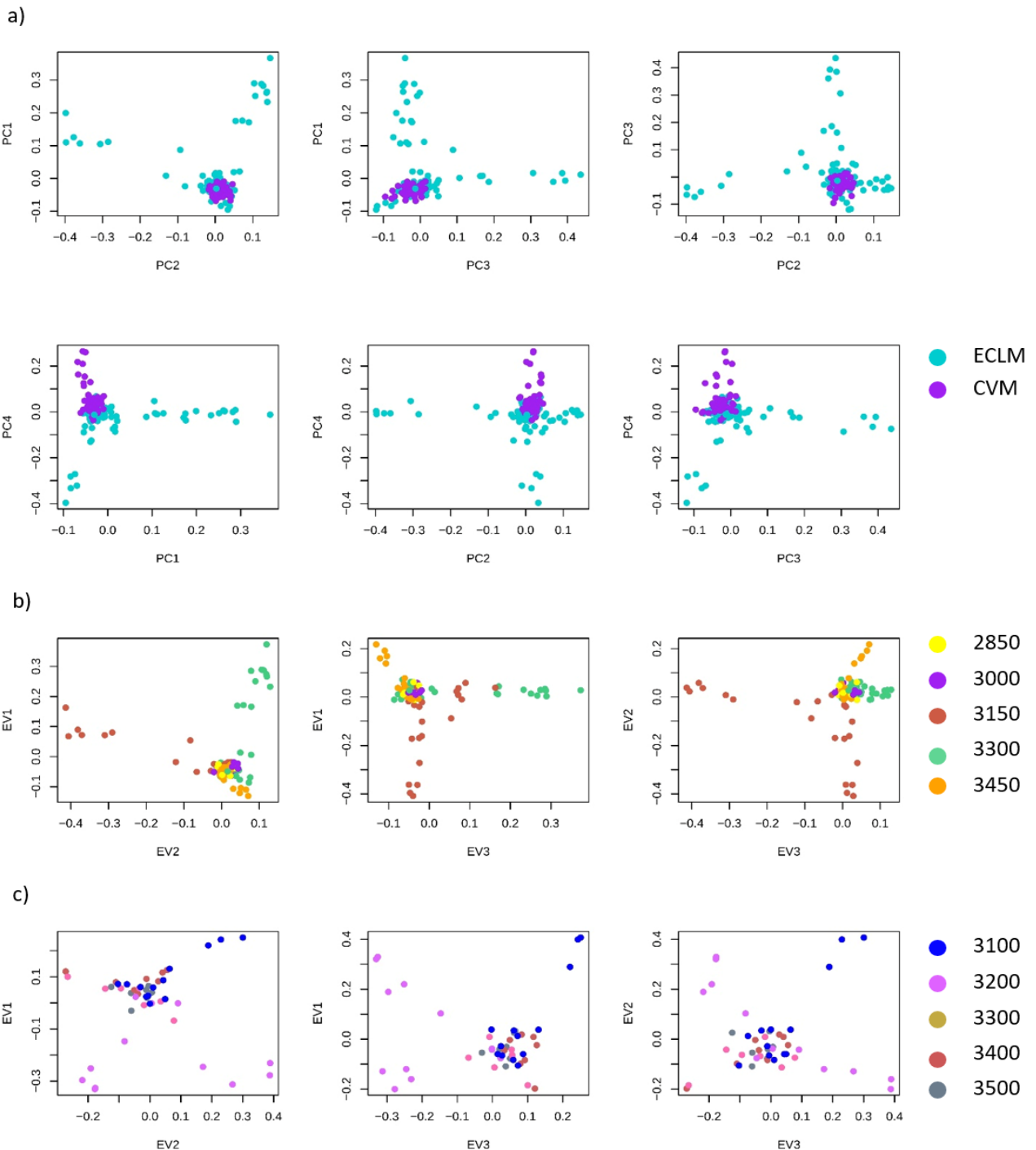
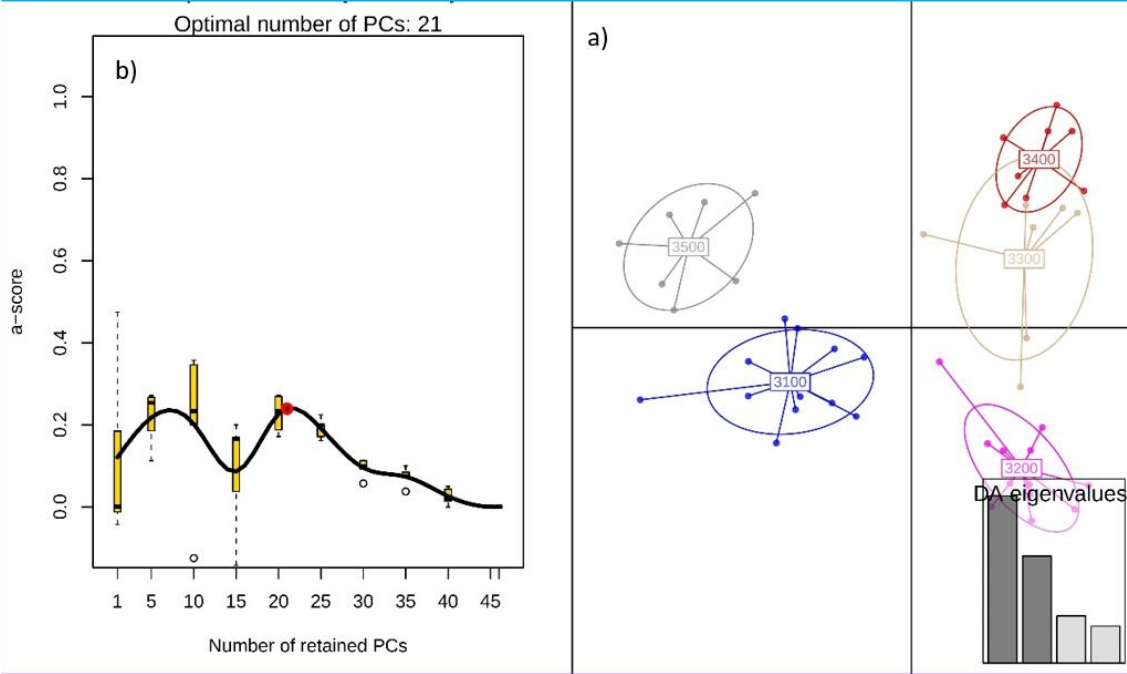


Figure S7. Principal Component Analysis (PCA). **a)** PCA results at the global scale between the CVM and ECLM slopes; only PC4 exhibits moderate differentiation. ECLM shows more within variation. **b)** For the regional scale, results show differentiation in ECLM at the 3150m and 3300m levels. **c)** Results show a mixed pattern for CVM, with differentiation only at the 3200m level.

CVM



ECLM

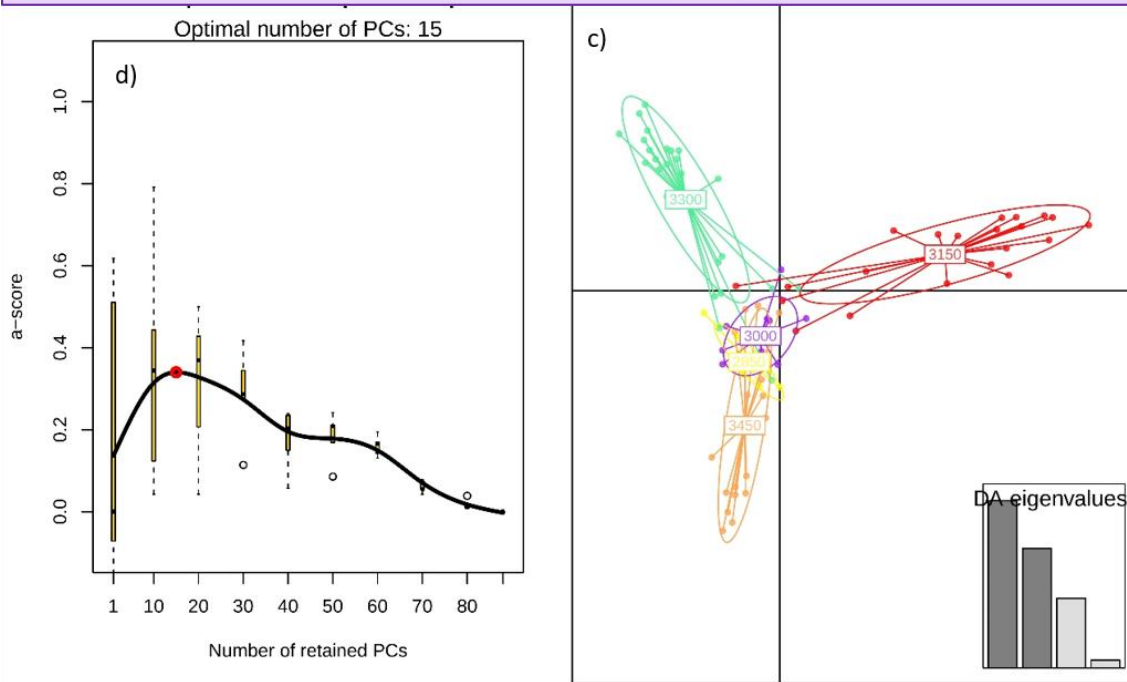


Figure S8. Regional genetic variation based on the elevation levels used as priors for DAPC analysis. **a)** and **c)** show the scatter plot of the five sampled elevation levels within CVM (21 PC) and ECLM (15 PC), respectively. **b)** and **d)** plot the a-score to determine the number of PCs and discriminant functions to retain in DAPC.

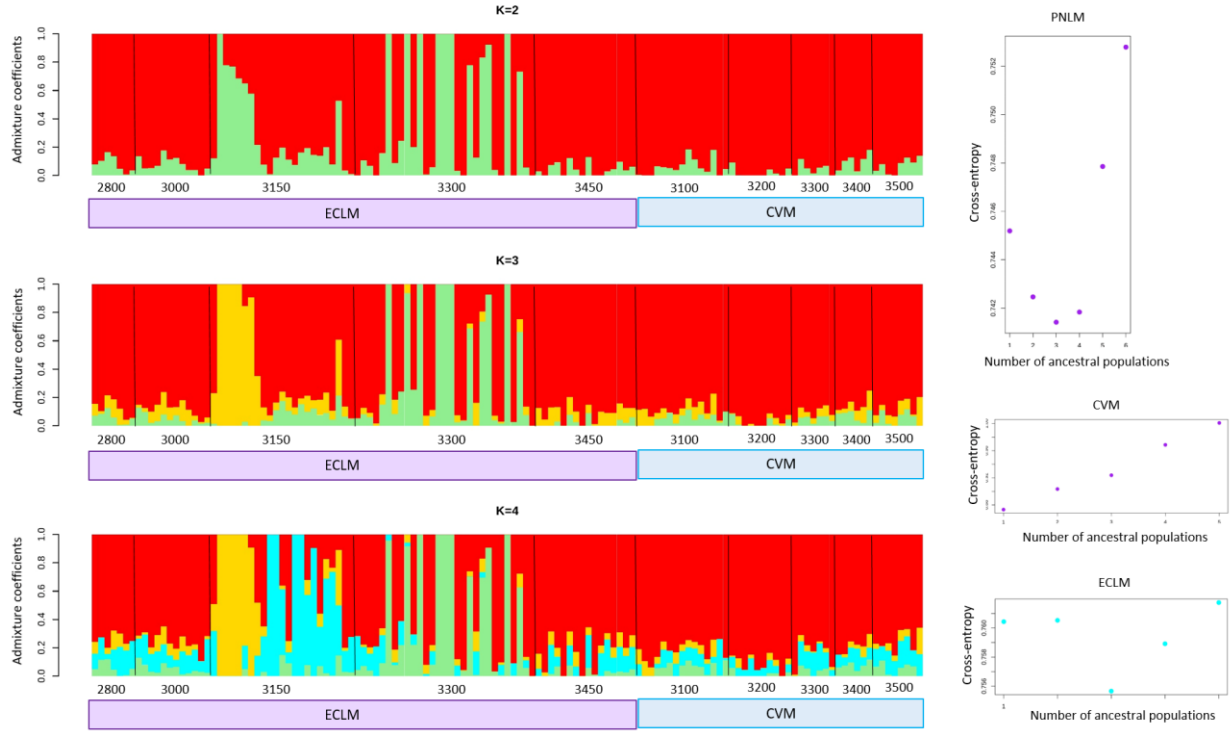


Figure S9. Snmf results for *Peromyscus melanotis* from Parque Nacional La Malinche at the regional scale. Bar plot showing individual membership (each vertical line depicts one individual) for $K=2$ (top graph), $K=3$ (middle) and $K=4$ (bottom) genetic clusters by slope (CVM and ECLM) and elevation level. On the left, cross-entropy plots showing the K with less entropy at global and regional scales.

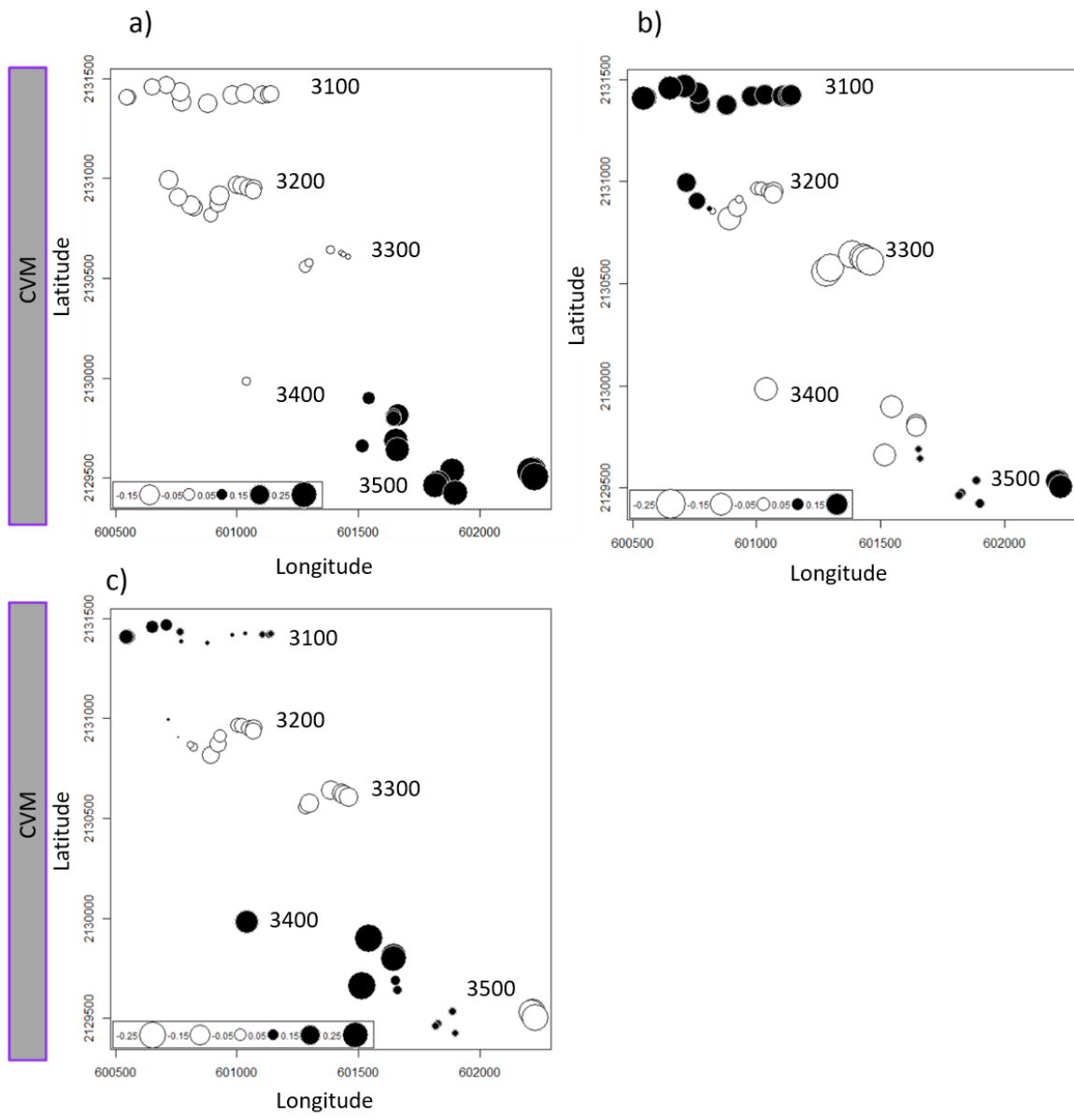


Figure S10. Memgene analysis used to identify genetic neighborhoods in CVM. The three significant Moran's eigenvectors explain **a)** 35.5%, **b)** 34.5% and **c)** 29% of the variation (see the main text). **b)** and **c)** show differences for the intermediate levels (3100m and 3400-3500m, respectively). The graph depicts positive and negative autocorrelation, where circles of similar size and color depict individuals with similar score (i.e. large black and large white circles indicate opposite extremes on the Memgene axes).

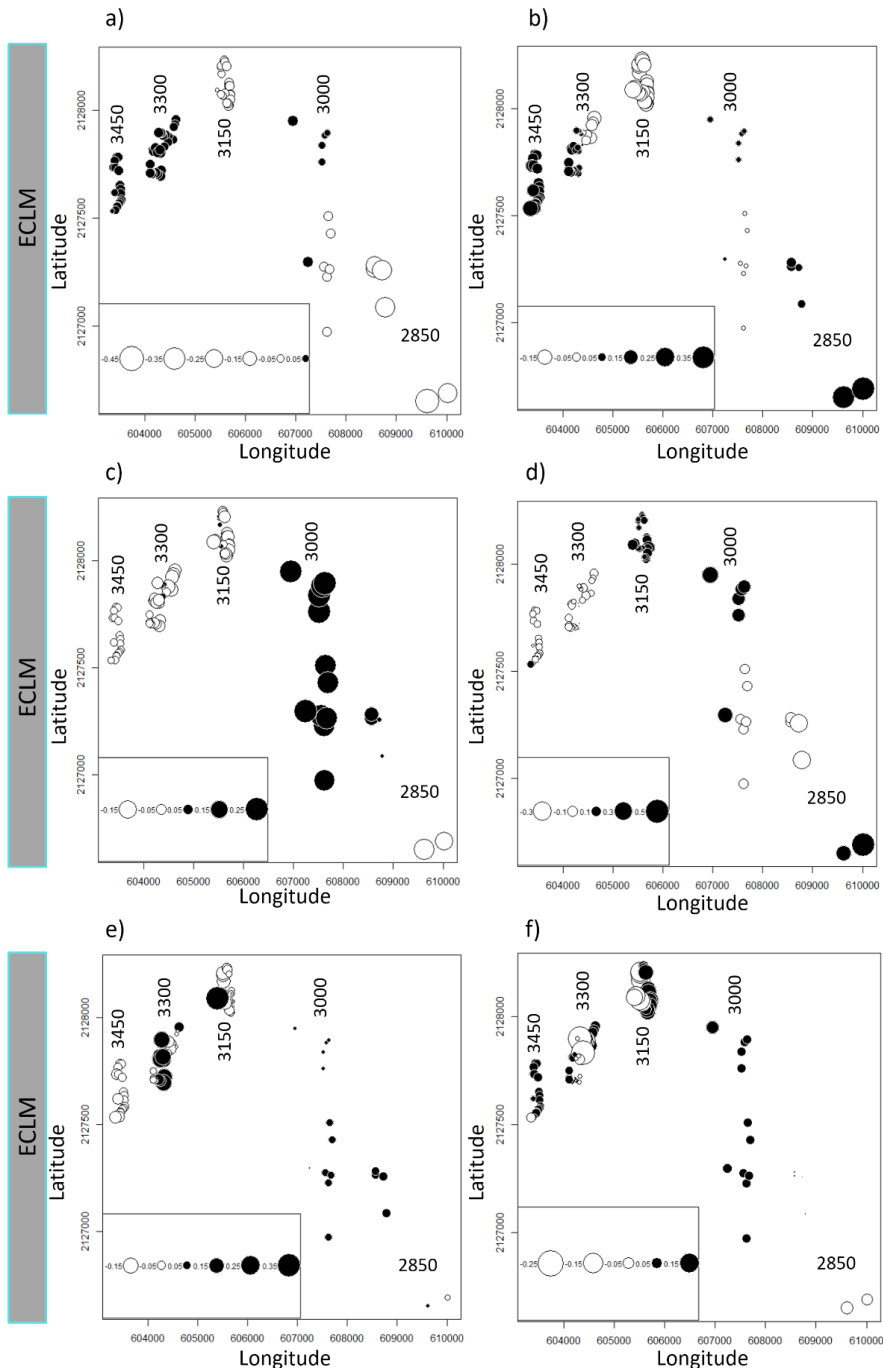


Figure S11. Memgene analysis used to identify genetic neighborhoods in ECLM. The six significant Moran's eigenvectors explain **a)** 18%, **b)** 17.9%, **c)** 17.8%, **d)** 17.5%, **e)** 15% and **f)** 13.6% of the variation (see the main text). **b)** shows a split within the 3300m; **c)** and **d)** a separation of the 3150m level from the rest. The graph depicts positive and negative autocorrelation, where circles of similar size and color depict individuals with similar score (i.e. large black and large white circles indicate opposite extremes on the Memgene axes).

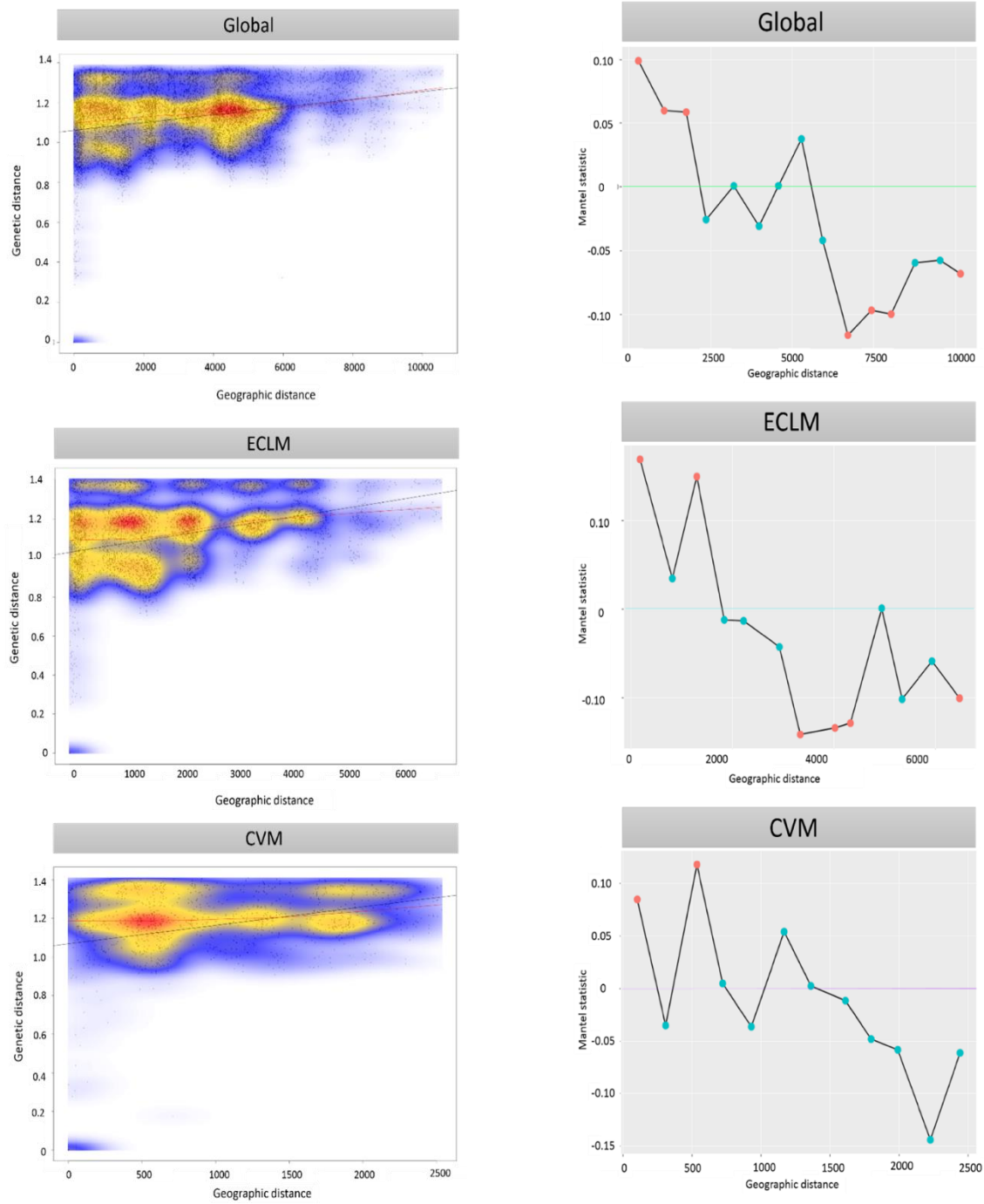


Figure S12. Scatterplot of Mantel tests (on the left) and Mantel correlograms (right) between Euclidean geographic distance (in meters) and genetic distance based on PCA for *Peromyscus melanotis* from Parque Nacional La Malinche. The global (top plots) and regional scales (ECLM and CVM slopes) are shown. The red line in depicts the correlation between both distance matrices; warmer colors indicate higher points densities. Significant values for the correlograms are shown with red circles ($p < 0.05$).

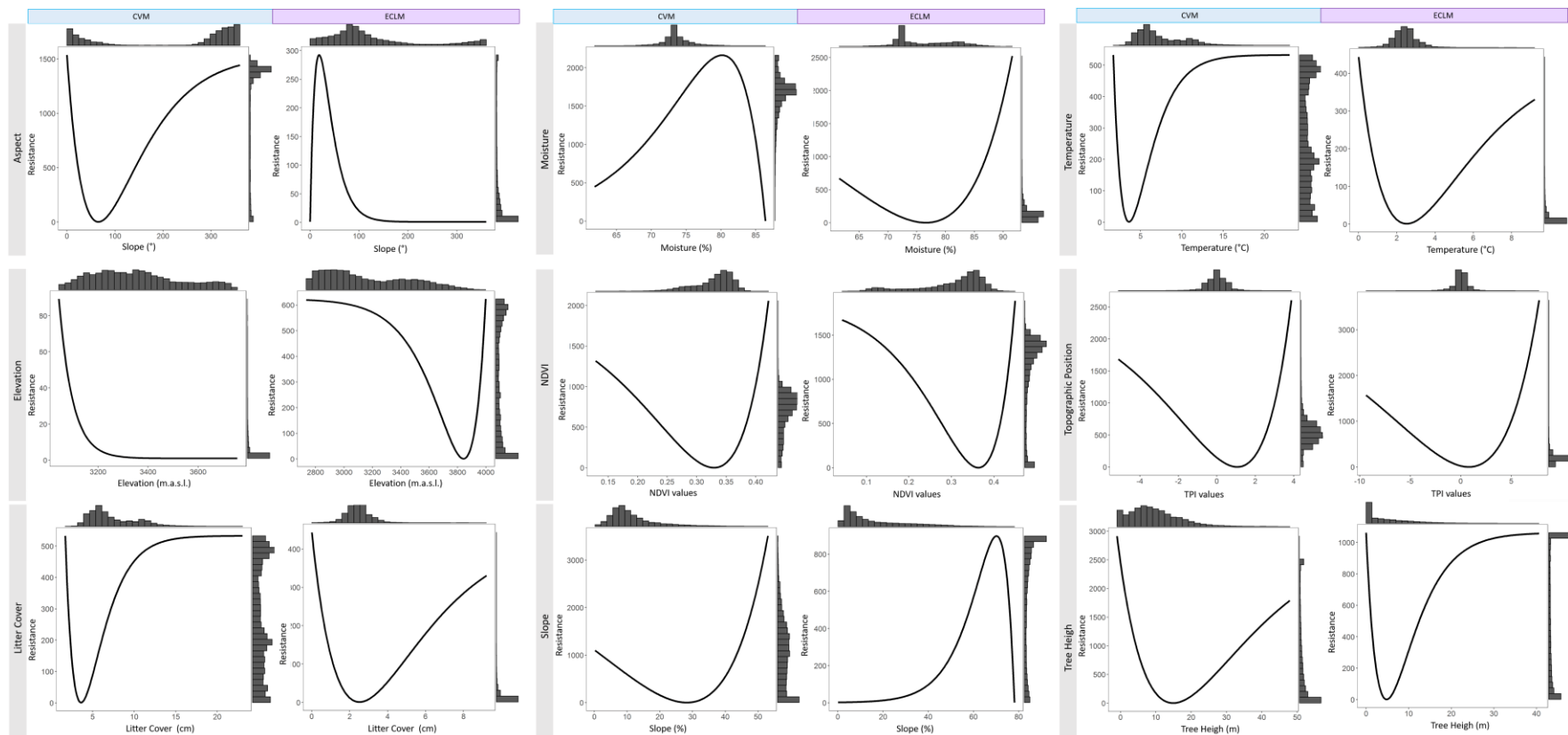


Fig. S13. Single surface optimization response curves for *Peromyscus maniculatus*, at the regional scale (CVM and ECLM slopes at Parque Nacional La Malinche), for the variables aspect, slope, topographic position, NDVI, tree height, moisture, temperature, litter cover, and elevation. Tree height was the best-supported model for CVM, followed by NDVI. Aspect and litter cover were the best-supported models for ECLM

Discusión y conclusión

Discusión

Diversas especies del género *Peromyscus*, en particular *P. maniculatus* y *P. leucopus*, han sido especies modelo en estudios de ecología, evolución, fisiología, genética y más recientemente de genómica. Sin embargo, la mayoría de las especies del género han sido poco estudiadas, sobretodo en México y Centroamérica (Bedford & Hoekstra, 2015). El presente trabajo representa el primer acercamiento a la diversidad, estructura genética y conectividad del ratón de orejas negras, *Peromyscus melanotis*, una especie cuasi-endémica de los bosque templados de tierras altas mexicanas, en dos laderas del Volcán La Malinche (ECLM y CVM), en el Parque Nacional La Malinche (PNLM). Mediante análisis del paisaje en dos y tres dimensiones explicamos cómo la complejidad ambiental del bosque templado, a lo largo de diferentes escalas geográficas, en combinación con gradientes altitudinales, determinan patrones de dispersión, estructura genómica y conectividad en este roedor.

Historia geológica y estructura de la vegetación moldean la estructura genética global de *Peromyscus melanotis*

La Malinche o Matlalcueyatl es un estratovolcán activo en estado de quiescencia, cuya erupción más reciente ocurrió hace 3,100 años. Las fluctuaciones glaciales que caracterizaron el Pleistoceno tardío y el Holoceno, en conjunto con procesos hidrogeomórficos, han moldeado pendientes pronunciadas y la presencia de barrancos profundos (Castillo-Rodríguez et al., 2010; Franco-Ramos et al., 2016). La evidencia geomorfológica sugiere que el material piroclástico de las erupciones más recientes fue arrojado hacia las laderas norte, noreste y noroeste, mientras que los eventos de arrastre más intensos ocurrieron en las laderas noreste y noroeste (Castro-Govea & Siebe, 2007), todo lo cual moldeó una topografía compleja que incide directamente en la estructura y flujo

génico de las poblaciones. Nuestros sitios de muestreo en ECLM están localizados en el Valle de Axltzintle, al interior del cual, de acuerdo con la evidencia dendrocronológica, han ocurrido 17 lahares entre 1970 y 2005, caracterizados por el flujo a gran velocidad de escombros volcánicos, rocas, madera y agua (Franco-Ramos et al., 2016). Los lahares modifican el hábitat afectando la dinámica de las poblaciones, ya sea vía la deriva genética o disminuyendo la diversidad, flujo genético y tamaño efectivo de las poblaciones a lo largo de esta ladera (Mortellini et al, 2010).

Nuestros resultados muestran estructura genética en la escala global de estudio, diferenciando tres grupos genéticos: i) ECLM-3150, ii) ECLM-3300 y iii) el resto de los pisos altitudinales considerando ambas laderas. La composición de las comunidades vegetales al interior de la ladera ECML cambia drásticamente (Fig. 1): bosque de pino-encino (a los 2850 msnm), bosque de pino (3300 m), bosque de pino-oyamel (3150m) y bosque de oyamel (3300-3450 m). Estas comunidades promueven diferentes microambientes y dinámicas ecológicas que pueden restringir el flujo genético y conducir a diferenciación y adaptación local, aún en áreas contiguas (Bradburd, 2013). El nivel de flujo genético depende no sólo de la capacidad de dispersión sino de la preferencia de hábitat de las especies y la adaptación de individuos a ambientes contrastantes (Bertrand et al., 2016). En este sentido, procesos como la selección contra migrantes o la baja adecuación de la descendencia juegan un papel fundamental (Branch et al., 2017; Richardson et al., 2014; Spear et al., 2010). Los resultados genéticos muestran mayor diversidad genética en ECLM-3150 y ECLM-3300, sitios que a pesar de su cercanía geográfica presentan poca o nula migración entre ellos, y además reciben pocos migrantes, pero aportan la mayor cantidad de migrantes al resto de los pisos altitudinales. Adicionalmente, estos dos sitios son ecológicamente divergentes de los demás, no sólo en cuanto a las comunidades arbóreas sino en términos de humedad y estado de conservación. Esta dinámica regional

al interior de ECLM apoya un patrón de divergencia con flujo génico, así como potencial adaptación local (Barrat et al., 2018).

Es interesante que las comunidades vegetales de la ladera CVM son comparativamente más homogéneas (Fig. 1): bosque de pino-encino (3150-3200 m), bosque de pino-alnus (3300-3400 m) característico de bosques perturbados y bosque de pino-oyamel (3500 m). Cabe resaltar que esta pendiente es la más turística, con un hotel estatal localizado montaña abajo. Asimismo, las actividades extractivas de hongos y maderas para uso personal son más comunes. A diferencia de la ladera ECLM, CVM no mostró estructura genética, lo cual podría estar relacionado con el hábitat relativamente más homogéneo que facilita la dispersión de individuos. En hábitats homogéneos es menos frecuente encontrar diferenciación ocasionada por variables ambientales, ya que hay menor presión de selección asociada al ambiente, en particular regiones genómicas sujetas a selección débil (Merondun et al., 2019; Miao et al., 2017). Asimismo, los gradientes altitudinales pueden facilitar la migración y constreñir la divergencia genética en algunas especies (Féijo et. al., 2019). Por ejemplo, la pika *Ochotona roylei* en los Himalaya (Solari, 2018) no presenta estructura genética a lo largo del gradiente altitudinal ni señales de selección, sin embargo sí muestra diferencias transcripcionales.

Se sabe además que la dispersión a larga distancia disminuye la divergencia genética (Van Strien, 2017); la distancia máxima de dispersión calculada en función del ámbito hogareño de *Peromyscus* (Fa et al., 1996) fue de 820.5 m, la cual podría ser mayor dada la falta de estructura observada. Los machos y hembras de *P. melanotis* sobrelapan su distribución a lo largo del año, y durante la época de lluvias los machos se dispersan más y las hembras menos (De la Cruz et al., 2019). Adicionalmente, los bosques secundarios, como los bosques de pino-alnus pueden favorecer la conectividad debido al aumento en la productividad (Carrara et al., 2014).

De esta manera vemos que los diferentes patrones de estructuración entre laderas pueden estar determinados por diferencias demográficas históricas en el tamaño efectivo de las poblaciones y/o flujo génico, resultado de los patrones de actividad geomorfológica contrastantes de cada ladera, tanto antiguos como contemporáneos, por los impactos antropogénicos, y por los cambios ambientales característicos de gradientes altitudinales (House & Hahn, 2018; Polato et al, 2017).

Modelo valle-montaña

Efectivamente, a nivel regional las dos laderas presentan patrones distintos a lo largo del gradiente altitudinal. En concordancia con el modelo de valle-montaña (Funk et al., 2005) encontramos menor diversidad genética en las partes más altas de CVM. De igual manera, los resultados apoyan la hipótesis de este modelo que establece un flujo genético limitado entre la parte baja y alta de la montaña, promoviendo aislamiento espacial de los sitios más elevados (Féijo et. al., 2019; Polato et al., 2017). Efectivamente, identificamos que los niveles de mayor altitud, 3400 y 3500m, funcionan como un vecindario genético, con conectividad limitada, pocos migrantes y aislamiento significativo. El patrón observado en ECLM difiere en cuanto a que las poblaciones más altas presentan mayor diversidad genética, pero donde la menor conectividad y flujo se da en altitudes intermedias (3150 y 3300m). El modelo también postula una mayor conectividad en tierras bajas comparado con tierras altas (Polato et al., 2017), sin embargo, este patrón no se presenta en ninguna de las laderas. Ello puede ser resultado de que las tierras bajas tanto de ECLM como CMV colindan con zonas donde el paisaje está transformado y con alta perturbación. Se sabe que el género *Peromyscus* es sensible a hábitats perturbados (Léon-Tapia et al., 2020). De acuerdo con los resultados de conectividad omnidireccional, la conectividad aumenta en tierras altas, donde el bosque está más conservado, con presencia de árboles que llegan hasta los 35 metros, y por consiguiente el potencial de depredación es menor (Santibañez-

Andrade & Castillo-Argüero, 2009). *Arborimus longicaudus* es un roedor endémico de la costa oeste de Estados Unidos, cuya preferencia de hábitat está determinada por el tamaño de los árboles, particularmente por bosques de coníferas maduros (más de 30 años) y viejos (mas de 80 años) pero bien conservados (Linell et al., 2018).

Variables del paisaje y patrones de conectividad de *Peromyscus melanotis*

Las especies muestran una respuesta unimodal a los recursos limitados en el espacio ecológico n-dimensional, lo que permite definir el máximo y mínimo de tolerancia ante un recurso crítico y sus óptimos fisiológicos (McGarigal & Cushman, 2005). Algunos estudios apuntan que la estructura genética de mamíferos en bosques se explica principalmente por la cobertura de la vegetación, la precipitación, la distancia geográfica y la presencia de barreras naturales y antropogénicas (Barrat et al., 2018; Flores-Manzanero & Vazquez-Dominguez, 2019; Samarasin et al., 2017). Otros señalan que la fragmentación del paisaje, en particular de la vegetación, no es suficiente para explicar la estructura genética, al menos en roedores (Howell et al., 2017). Por lo tanto, esperábamos que diversas variables ambientales y del paisaje influyeran en los patrones de conectividad local de *P. melanotis* en el Parque Nacional La Malinche.

De acuerdo con nuestra predicción, la topografía y la estructura de la vegetación son las características del paisaje que más influyeron en la conectividad de este roedor (Fig. 1). La compleja topografía en la Malinche moldea atributos biofísicos como la distribución de suelos y sus procesos de erosión, la hidrología (Castillo-Rodriguez et al., 2010), patrones de vientos, así como la duración e intensidad de la radiación solar (Meliyo et al., 2014). Todos estos factores repercuten en el clima local y modulan la estructura de las comunidades arbóreas. La topografía, al funcionar como barrera, moldea atributos biológicos al incidir en las rutas de dispersión y la elección de rutas de bajo costo energético. Esto lo observamos en ambas laderas como una migración bidireccional pero preferencial

de lo alto de la montaña a la base, mientras que la tasa de migración diminuyó en sentido inverso, conforme aumenta el costo fisiológico anisotrópico de la dispersión (Murphy et al., 2010; Polato et al., 2017; Rodriguez-Freire & Crecente-Maseda, 2008).

El aspecto y la pendiente fueron las variables identificadas como significativas para el flujo génico en ECLM. En concordancia con la complejidad topográfica de esta ladera, identificamos una alta resistencia sólo en pendientes muy pronunciadas ($\geq 40^\circ$). Por su parte, *P. melanotis* en CVM exhibe una alta resistencia para pendientes suaves ($\leq 20^\circ$), posiblemente como estrategia para evitar la depredación. Este comportamiento se ha observado en pequeños mamíferos como *Heteromys desmarestianus goldmani* en cultivos de café y el corzo *Capreolus caperolus* en bosques, donde muestran preferencia por pendientes pronunciadas y sitios con abundante vegetación para evitar depredación (Norum et al., 2015; Otero-Jiménez et. al., 2020). En concordancia, el movimiento preferencial de algunos depredadores como el puma se asocia a pendientes suaves ($\leq 6^\circ$) (Dickson et al., 2005).

La precipitación y la humedad son mayores en ECLM que CVM como resultado del efecto orográfico, lo que puede explicar que el óptimo de humedad en ECLM esté entre 70 y 80% y en CVM sea 60%. La tolerancia fisiológica de temperatura y humedad imponen límites fisiológicos a la dispersión en diferentes especies, impactando procesos demográficos en pequeños roedores, ya que altera la disponibilidad de alimento, el parasitismo y la tasa de depredación. Por ejemplo, la selección de hábitat en *P. difficilis* depende de valores altos de humedad (Villanueva-Hernandez et al., 2017), mientras que en *P. leucopus* la precipitación de otoño, el frío en invierno y el calor en verano afectan su abundancia (Dhawan et al., 2018). En particular, la abundancia de *P. melanotis* se relaciona con mayores temperaturas que permiten la apertura de conos de *Alnus* y favorecen la presencia de semillas (Flores-Pereido & Vázquez-Domínguez, 2016).

El índice de vegetación normalizado (NDVI) puede ser afectado por los cambios estacionales de la vegetación, la variación climática, el tipo y dominancia de vegetación, y el estrés hídrico; asimismo, en paisajes complejos los píxeles mixtos y la confusión espectral también pueden afectarlo (Kinyanjui et al., 2010; Yang et al., 2019). Por ello, se recomienda el uso de variables tridimensionales para el estudio del paisaje, principalmente la vegetación, para evaluar conectividad funcional en ambientes complejos. Por ejemplo, en el urogallo *Tetrao urogallus* las variables tridimensionales explican mejor la conectividad funcional y preferencia de hábitat que las variables en dos dimensiones (Milanesi, 2017). De acuerdo con lo anterior, el mejor modelo en los análisis univariados para la ladera CVM fue la altura de la vegetación, mientras que en los modelos multivariados fue la interacción entre NDVI y altura de la vegetación. Y para ECLM, el mejor modelo multivariado incluyó la productividad3 (mantillo, altura de la vegetación). En general los roedores prefieren áreas con alta disponibilidad de recursos, donde la mayor acumulación de semillas se encuentra bajo el dosel. En el caso particular de *P. melanotis*, éste prefiere áreas con una cobertura vegetal compleja no solo por la disponibilidad de alimento sino por la protección que brindan, lo mismo que *P. difficilis* que se distribuye preferencialmente en zonas con alta cobertura vegetal (Flores-Peredo & Vázquez-Domínguez, 2016). La preferencia de hábitat de ardilla roja *Sciurus vulgaris*, que se distribuye en bosques, responde a la cantidad y cobertura de vegetación (Mortelliti et al., 2010). La distribución estrechamente asociada con NDVI y cobertura vegetal ha sido también documentada en vertebrados de otros ambientes, por ejemplo la rata canguro *Dipodomys merriami* en desiertos (Flores-Manzanero et al., 2019), *P. leucopus* (Munshi-South, 2012) y la lagartija *Podarcis muralis* (Beninde et al., 2018) en zonas urbanas, y la marta *Martes americana* en el bosque boreal (Aylward et al., 2020).

En cuanto a la altura de la vegetación, los resultados muestran una baja resistencia (alta conectividad) en vegetación de mediana altura (ECLM entre 5 y 15 m; CVM entre 10

y 30m). Los valores por debajo de 5 metros (alta resistencia) incluyen caminos, pastizales y áreas perturbadas, así como zonas de reforestación reciente. Esto contradice la descripción original de la especie (Álvarez-Castañeda 2005), al menos en el PNLM, ya que *P. melanotis* evita los pastizales. Existen diversos ejemplos de que los caminos y veredas afectan la estructura y el flujo génico en vertebrados, por ejemplo los roedores *Lyomis pictus* en selvas bajas mexicanas (Garrido-Garduño et al., 2016), *Calomys venustus* (Chiappero et al., 2016) y *P. leucopus* (Howell et al., 2017) en agrosistemas, la salamandra *Triturus cristatus* (Haugen et al., 2020) en bosques boreales y el marsupial *Sarcophilus harrisii* (Kozakiewicz et al., 2020) en bosques de eucalipto.

En ECLM, la ladera más fría y húmeda, el mantillo fue una de las variables más importantes bajo los modelos univariados y multivariados, explicando el 36% de la variación, resaltando su importancia en la regulación de la temperatura. En *Peromyscus hooperi* también se ha documentado la importancia de la acumulación de mantillo en su distribución (Villanueva-Hernandez et al., 2017). El mantillo se relaciona con la eficiencia de forrajeo al afectar la detección del olor de las semillas, contribuye a reducir la variación de la temperatura y mantener la humedad, y afecta además el riesgo de depredación (Díaz-García et al., 2020; Nicolai, 2020; Pearson & Theimer, 2004).

Es interesante que con los análisis de vecindarios genéticos se pudo identificar que la estructuración de los grupos genéticos ECLM-3150 y ECLM-3300 está también asociada con la presencia de caminos secundarios. Aunque estos caminos son poco accesibles en auto y tienen un tráfico humano limitado, pueden afectar los patrones de dispersión por riesgo de depredación y por cambios del microclima por remoción de la cobertura vegetal original, ya que se crean bordes que producen un incremento de la evaporación y disminuye la humedad (Haugen et al., 2020).

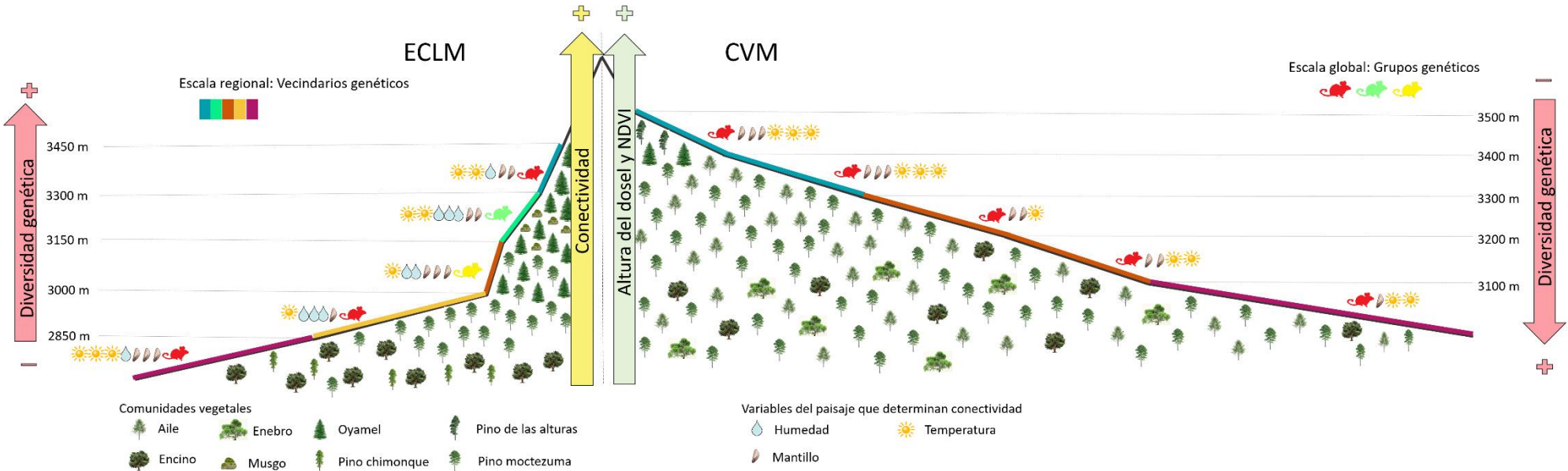


Figura 1. Dinámica de las variables del paisaje que determinan la conectividad y estructura genética de *Peromyscus melanotis* en el Parque Nacional La Malinche a escala global, regional y local. El diagrama muestra las diferencias topográficas (pendiente) entre las laderas ECLM y CVM y la diversidad de comunidades arbóreas en los diferentes pisos altitudinales. Las poblaciones de la ladera ECLM se estructuran en cinco vecindarios genéticos, mientras que en CVM sólo presenta tres vecindarios. La diversidad genética (flecha rosa) tiene una relación positiva con la elevación en ECLM y negativa en CVM. El mayor número de elementos que representan las variables del paisaje (humedad, temperatura, profundidad de mantillo) por piso altitudinal está asociado con una mayor conectividad (flecha amarilla). La altura del dosel y NDVI (flecha verde) en ambas laderas se incrementa a mayor elevación, y son las variables que determinan más significativamente el patrón de conectividad.

Recomendaciones y perspectivas

En función de los resultados obtenidos, enfatizamos la importancia de incluir variables tridimensionales para evaluar conectividad en paisajes complejos, como lo son los bosques templados mexicanos. La topografía a fina escala y la estructura tridimensional de la vegetación controlan otras variables que pueden ser incorporadas a los modelos como el microclima, el pH del suelo y fuerzas hidrodinámicas (D'Urban et al., 2020). Siempre teniendo en mente qué variables son significativas para la especie focal, ya que el poder estadístico disminuye conforme aumenta la complejidad del paisaje; como resultado de ello, la selección del mejor modelo con base en los índices de selección se complica si las capas analizadas provienen de la combinación de superficies multivariadas (Balkenhol & Fortin, 2015; Row et al., 2017). Asimismo, hay que mencionar que a pesar de las ventajas de la fotogrametría aérea para evaluar paisajes tridimensionales, ésta no es adecuada para evaluar la estructura vegetal por abajo del dosel (Ralph et al., 2017). Por ello, es recomendable utilizar enfoques complementarios, como las tecnologías LiDAR o la fotogrametría de corto alcance a nivel de piso.

Los estudios de conectividad buscan elucidar el rol ecológico y evolutivo que juegan la diversidad genética y la adaptación en la persistencia de la vida silvestre, para el rescate de poblaciones naturales y para el mantenimiento de la diversidad genética en un mundo cambiante (Samarasin et al., 2017). Sin embargo, la genética de poblaciones y la genética del paisaje se encuentran subrepresentadas en las prácticas de conservación (Keller et al., 2015). Ello a pesar de que dichas disciplinas proveen información que permite entender los procesos ecológicos y evolutivos que afectan la dinámica de las poblaciones en diversas escalas. Una razón es la incertidumbre de poder generalizar los patrones de conectividad a otras especies o geografías (Mims et al., 2018). En este trabajo mostramos que dentro de una misma montaña los procesos que moldean la estructura, conectividad y diversidad de *P. melanotis* difieren entre pendientes. Por otro lado, también demostramos que la

estructura tridimensional de la vegetación es una de las variables más importantes en ambas laderas, lo cual podría ser extrapolable al Parque Nacional La Malinche y posiblemente a otros bosques templados de tierras altas al interior de la Faja Volcánica Transmexicana.

Con nuestros resultados podemos así recomendar que es imperante controlar las actividades extractivas dentro del PNLM, en particular la tala ilegal, para evitar la pérdida de bosque maduro. Ello es relevante ya que por su categoría de protección como parque nacional, se permiten las actividades extractivas de subsistencia para las comunidades locales. Asimismo, dada la naturaleza turística que tiene, se recomienda controlar la afluencia de visitantes mediante programas de ecoturismo manejados por las comunidades locales. Recomendamos también fortalecer los programas de reforestación existentes e implementar proyectos de restauración ecológica a largo plazo con pinos, oyameles y otras especies nativas para promover la conectividad. Además, de acuerdo con la estructura genética encontrada y la alta diversidad que presentan, se debe priorizar la conservación de las poblaciones ECLM-3150 y ECLM-3300.

Finalmente, es importante mencionar que los cambios microclimáticos a lo largo de gradientes altitudinales pueden determinar diferencias particulares en caracteres morfológicos, fisiológicos o conductuales adaptativos de las especies, asociados con factores como altitud, temperatura o humedad. Por ejemplo, Henry y Rusello (2013) identificaron loci candidatos en un gradiente altitudinal en la pika *Ochotona princeps*; en ranas tibetanas del género *Nanorana* el gradiente altitudinal está asociado con la angiogénesis como respuesta a la hipoxia, el metabolismo de carbohidratos y la reparación de daño celular por radiación UV (Sun et. al., 2018). Se ha visto que en *P. leucopus* el gradiente térmico latitudinal se asocia con loci involucrados con el estrés oxidativo dependiente de hierro, el arresto celular, la inhibición de atrofia muscular y el metabolismo de la glucosa (García-Elfring et al., 2019). Asimismo, en pequeños mamíferos se han

observado diferencias significativas en el tamaño y forma del cráneo, donde el tamaño disminuye conforme la altitud es mayor (Keller et al., 2013) y la forma se relaciona con las interacciones bióticas como la riqueza de depredadores y el tipo y disponibilidad de alimento (Feijó et al., 2019). Para el caso particular de *P. melanotis*, la variación craneal parece estar determinada por una baja productividad primaria y estacionalidad más marcada de las tierras bajas (Gracia-Mendoza et al., 2018). De esta forma, nuestras perspectivas a futuro incluyen evaluar loci candidatos a selección y loci asociados con las variables ambientales identificadas como significativas, así como su asociación a caracteres morfológicos para dilucidar más claramente el rol que juega la adaptación local en la dinámica poblacional de *P. melanotis* en el PNLM.

Literatura citada en introducción y discusión

- Allendorf F. W., Luickart G., Aitken S. N., 2013. Conservation and the genetics of population. Wiley-Blackwell. Oxford.
- Alvarez-Castañeda T., 2005. *Peromyscus melanotis*. Mammalian Species 764:1-4. doi: 10.1644/1545-1410(2005)764[0001:PM]2.0.CO;2
- Amaral K. E., Palace M., O'Brien K. M., Fenderson L. E., Kovach A. I., 2016. Anthropogenic habitats facilitate dispersal of an early successional obligate: implications for restoration of an endangered ecosystem. PLoS ONE 11(3): e0148842. doi: 10.1371/journal.pone.0148842
- Anderson C. S., Meikle D. B., 2010. Genetic estimates of immigration and emigration rates in relation to population density and forest patch area in *Peromyscus leucopus*. Conservation Genetics 11: 1593-1605. doi: 10.1007/s10592-009-0033-8
- Aylward C. M., Murdoch J. D., Kilpatrick C. W., 2020. Multiscale landscape genetics of American marten at their southern range periphery. Heredity 124:550-561. doi: 10.1038/s41437-020-0295-y
- Balkenhol N., Fortin M. J., 2016. Basics of study design: sampling landscape heterogeneity and genetic variation for landscape genetic studies. Landscape genetics: concepts, methods and applications, 1^aedition. Wiley and Sons. doi: 10.1002/9781118525258.ch04
- Barrat C. D., Bwong B. A., Jehle R., Liedtke H.C., Nagel P., Onstein R. E., Portik D. M., Streicher J. W., Loader S. P., 2018. Vanishing refuge? Testing the forest refuge hypothesis in Coastal East Africa using genome-wide sequence data for seven amphibians. Molecular Ecology 27: 4289-4308. doi: 10.1111/mec.14862
- Bayley D. T., Mogg A. O.M., Koldewey H., Purvis A., 2019. Capturing complexity: field testing the use of structure from motion derived virtual models to replicate standard measures of reef physical structure. PeerJ 7: e6540. doi: 10.7717/peerj.6540
- Beaulne D., 2018. The importance of geospatial inputs in assessing fine-scale landscape genetic patterns of a temperate treefrog. Master thesis, Queen's University, Canada.
- Bedford N., Hoekstra H., 2015. *Peromyscus* mice as a model for studying natural variation. eLife 4: e06813. doi: 10.7554/eLife.06813.001
- Beninde J., Feldmeier S., Werner M., Peroverde D., Schulte U., Hochkirch A., Veith M., 2016. Cityscape genetics: structural vs. functional connectivity of an urban lizard population. Molecular Ecology 25(20): 4984-5000. doi: 10.1111/mec.13810
- Bertrand J. A. M., Delahaie B., Bourgeois Y. X. C., Duval T., García-Jiménez R., Cornuault J., Pujol B., Thébaud C., Milá B., 2016. The role of selection and historical factors in driving population differentiation along an elevational gradient in an island bird. Evolutionary Biology 29(4):824-836. doi: 10.1111/jeb.12829
- Bowers J. H., 1973. Evolutionary and genetic studies of selected populations of deer mice (*Peromyscus maniculatus*) and black eared mice (*Peromyscus melanotis*). Doctoral thesis. Texas Tech University.
- Bradbard G., Ralph P., Coop G., 2013. Disentangling the effects of geographic and ecological isolation on genetic differentiation. Evolution 67(11): 3258-3273. doi: 10.1111/evo.12193
- Bradbury I., Hamilton L., Dempson B., Robertson M., Bourret V., Bernatchez L., Verspoor E., 2015. Transatlantic secondary contact in Atlantic salmon, comparing microsatellites, a single nucleotide polymorphism array and restriction-site associated DNA sequencing for the resolution of complex spatial structure. Molecular Ecology 24:5130-5144. doi: 10.1111/mec.13395

- Branch C. L., Jahner J. P., Kozlovsky D. Y., Parchman T. L., Pravosudov W., 2017. Absence of population structure across elevational gradients despite large phenotypic variation in mountain chickadees (*Poecile gambeli*). Royal Society Open Science 4: 170057. Doi: doi:10.1098/rsos.170057
- Carrara E., Arroyo-Rodríguez V., Vega-Rivera J. H., Schondube J. E., M. de Freitas S., Fahrig L., 2015. Impact of landscape composition and configuration on forest specialist and generalist bird species in the fragmented Lacandona rainforest, Mexico. Biological Conservation 184: 117-126. doi: 10.1016/j.biocon.2015.01.014.
- Castillo-Rodríguez M., López-Blanco J., Muñoz-Salinas E.; 2010. A geomorphologic GIS-multivariate analysis approach to delineate environmental units, a case study of La Maliche volcano (Central México). Applied Geography 30: 629-638. doi: 10.1016/j.apgeog.2010.01.003
- Castro-Campillo A., Salame-Méndez A., Vergara-Huerta J., Castillo A., Ramírez-Pulido J., 2008. Fluctuaciones de micromamíferos terrestres en bosques templados aledaños a la Ciudad de México, Distrito Federal, 425-441pp. Lorenzo C., Espinoza E., Ortega J., 2008. Avances en el estudio de los mamíferos de México II, Asociación Mexicana de Mastozoología A.C
- Castro-Campillo A., León-Altamirano L., Herrera-Muñoz J., Salgado-Ugarte I., Mendieta-Márquez E., Contreras-Montiel J. L., Serrano H. F., Ramírez-Pulido J., Salame-Méndez A., 2012. Is there a difference between testosterone contents in two populations of the black eared mouse, living under similar conditions but with differences in population patterns? Acta Zoológica Mexicana 28(3): 525-539. doi: 10.21829/azm.2012.283856
- Castro-Govea R., Siebe C., 2007. Late Pleistocene-Holocene stratigraphy and radiocarbon dating of La Malinche Volcano, Central Mexico. Journal of Volcanology and Geothermal Research 162(1-2): 20-42. doi: 10.1016/j.jvolgeores.2007.01.002
- Chiappero M. B., Sommaro L. V., Priotto J. W., Wiernes M. P., Steinmann A. R., Gardenal C. N., 2016. Spatio temporal genetic structure of the rodent *Calomys venustus* in linear, fragmented habitats. Journal of Mammalogy 97(2): 424-435. doi: 10.1093/jmammal/gyy186
- Chirhart S. E., Honeycutt R. L., Greenbaum I. F., 2005. Microsatellite variation and evolution in the *Peromyscus maniculatus* species group. Molecular Phylogenetics and Evolution 34: 408-415. doi: 10.1016/j.ympev.2004.10.018
- Cleary K. A., Waits L. P., Finegan B., 2016. Comparative landscape genetics of two frugivorous bats in a biological corridor undergoing agricultural intensification. Molecular Ecology 26: 4603-4617. Doi: 10.1111/mec.14230
- D'Urban J., Williams G. J., Walker-Springett G., Davies A. J., 2020. Three-dimensional digital mapping of ecosystems: a new era in spatial ecology. Proceedings Royal Society B 287: 20192383. doi: 10.1098/rspb.2019.2383
- Davey J., Hohenlohe P., Etter P., Boone J., Catchen J., Blaxter M., 2011. Genome-wide genetic marker discovery and genotyping using next-generation sequencing. Nature Reviews Genetics 12(7):499-510. doi: 10.1038/nrg3012
- De la Cruz, I. M., Castro-Campillo A., Zavala-Hurtado A., Salame-Méndez A., Ramírez-Pulido J., 2019. Differentiation pattern in the use of space by males and females of two species of small mammals (*Peromyscus difficilis* and *P. melanotis*) in a temperate forest. Therya 10(1):3-10. doi: 10.12933/therya-19-668
- Dhawan R., Fischhoff I. R., Ostfeld R. S., 2018. Effects of weather variability on population dynamics of white-footed mice (*Peromyscus leucopus*) and eastern chipmunks (*Tamias striatus*) Journal of Mammalogy 99(6): 1436-1443. doi: 10.1093/jmammal/gyy126

- Díaz-García J. M., López-Barrera F., Toledo-Aceves T., Andresen E., Pineda E., 2020. Does forest restoration assist the recovery of threatened species? A study of cloud forest amphibian communities. *Biological Conservation* 242. doi: 10.1016/j.biocon.2019.108400
- Dickinson B. G., Jennes J. S., Beier P., 2005. Influence of vegetation, topography, and roads on cougar movement in Southern California. *The Journal of Wildlife Management* 69(1): 264-276. doi: 10.2193/0022-541X(2005)069<0264:IOVTAR>2.0.CO;2
- Eguiarte, L., Aguirre-Liguori J., Jardón-Barbolla L., Aguirre-Planter E., Souza V.; 2013. Genómica de poblaciones: Nada en evolución va a tener sentido si no es a la luz de la Genómica, y nada en Genómica tendrá sentido si no es a la luz de la Evolución. TIP Revista Especializada en Ciencias Químico-Biológicas, 16: 42-56.
- Fa J. E., Lopez-Paniagua J., Romero J. F., Gomez J. L., Lopez J. C., 1990. Influence of habitat characteristics on small mammals in a Mexican high-altitude grassland. *Journal of the Zoological Society of London* 221: 275-292. doi: 10.1111/j.1469-7998.1990.tb03996.x
- Fa J. E., Sánchez-Cordero V., Méndez A., 1996. Interspecific agonistic behavior in small mammals in a Mexican high-elevational grassland. *Journal of Zoology* 239(2):396-401. doi: 10.1111/j.1469-7998.1996.tb05461.x
- Féijo A., Wen Z., Cheng J., Ge D., Xia L., Yang Q., 2019. Divergent selection gradient along elevational gradients promotes genetic and phenotypic disparities among small mammal populations. *Ecology and Evolution* 9(12): 7080-7095. doi: 10.1002/ece3.5273
- Fernández J. A., García-Campusano F., Hafner M. S.; 2010. *Peromyscus difficilis* (Rodentia: Crictidae). *Mammalian Species* 42(1): 220-229.
- Flores-Manzanero A., Vázquez-Domínguez E., 2019. Landscape genetics of mammals in American ecosystems. *Therya* 10(3): 381-393. doi: 10.12933/therya-19-833.
- Flores-Manzanero, A., M.A. Luna-Bárcenas, R.J. Dyer, E. Vázquez-Domínguez. 2019. Functional connectivity and home range inferred at a microgeographic landscape genetics scale in a desert-dwelling rodent. *Ecology and Evolution*, 9: 437-453. doi: 10.1002/ece3.4762
- Flores-Peredo R., Vázquez-Domínguez G., 2016. Influence of vegetation type and season on rodent assemblage in a Mexican temperate forest mosaic. *Therya* 7(3):357-369. doi: 10.12933/therya-16-390.
- Franco-Ramos O., Stoffel M., Vázquez-Selem L., 2016. Tree-ring based record of intra-eruptive lahar activity: Axaltzintle Valley, Malinche Volcano, Mexico. *Geochronometria* 43(1). doi: 10.1515/geochr-2015-0033
- García-Elfring A., Barret R. D. H., Millien V., 2019. Genomic signatures of selection along a climatic gradient in the northern range margin of the white-footed mouse (*Peromyscus leucopus*). *Journal of Heredity* 110(6): 684-695. Doi: 1 0.1093/jhered/esz045
- García-Mendoza D.F., López-González C, Hortelano-Moncada Y., López-Wilchis R., Ortega J., 2018. Geographic cranial variation in *Peromyscus melanotis* is related to primary productivity. *Journal of Mammalogy* 9(4):898-905. doi: 10.1093/jmammal/gyy062
- Garrido-Garduño T, Vázquez-Domínguez E. 2013. Métodos de análisis genéticos, espaciales y de conectividad en genética del paisaje. *Revista Mexicana de Biodiversidad* 84(3): 1031-1054. doi: 10.7550/rmb.32500
- Garrido-Garduño, T., O. Téllez-Valdés, S. Manel, E. Vázquez-Domínguez. 2016. Role of habitat heterogeneity and landscape connectivity in shaping gene flow and spatial population structure of a dominant rodent species in a tropical dry forest. *Journal of Zoology*, 298: 293-302. doi: 10.1111/jzo.12307

- Glendinning J. I., Mejia A. A., Brower L. P., 1988. Behavioral and ecological interactions of foraging mice (*Peromyscus melanotis*) with overwintering monarch butterflies (*Danaus plexippus*) in Mexico. *Oecologia* 75: 222-227. doi: 10.1007/BF00378602
- Gomez-Ugalde R., 2003. Efectos de la contaminación atmosférica en poblaciones de pequeños roedores silvestres (*Microtus mexicanus*, *Peromyscus melanotis* y *Peromyscus difficilis*) en México D.F. Tesis doctoral. Universitat de Barcelona.
- Guo X., Coops N. C., Gergel S. E., Bater C. W., Nielsen S. E., Stadt J. J., Drever M., 2018. Integrating airborne lidar and satellite imagery to model habitat connectivity dynamics for spatial conservation prioritization. *Landscape Ecology* 33(3): 491-511. Doi: 10.1007/s10980-018-0609-0
- Harris S. E., Xue A., Alvarado-Serrano D., Boehm J., Joseph T., Hickerson M., Munshi-South J., 2016. Urbanization shapes the demographic history of a native rodent (the white-footed mouse, *Peromyscus leucopus*) in New York City. *Biology Letters* 12(4): 20150983. doi: 10.1098/rsbl.2015.0983
- Harris S. E., Munshi-South J., 2017. Signatures of positive selection and local adaptation to urbanization in white-footed mice (*Peromyscus leucopus*). *Molecular Ecology* 26(22): 6336-6350. doi: 10.1111/mec.14369
- Haugen H., Linlokken A., Ostbye K., Heggens J., 2020. Landscape genetics of northern crested newt *Triturus cristatus* populations in a contrastating natural and human-impacted boreal forest. *Conservation Genetics* 21: 515-530. doi: 10.1007/s10592-020-01266-6
- Henry P., Rusello M. A., 2013. Adaptative divergence along environmental gradients in a climate-change-sensitive mammal. *Ecology and Evolution* 3(11): 3906-3917. doi: 10.1002/ece3.776
- Hogan K. M., Davis S. K., Greenbaum I. F., 1997. Mitochondrial-DNA analysis of the systematic relationships within the *Peromyscus maniculatus* species group. *Journal of Mammalogy* 78(3): 733-743. doi: 10.2307/1382932
- Hollenbeck J. P., Olsen M. J., Haig S. M., 2014. Using terrestrial laser scanning to support ecological research in the rocky intertidal zone. *Journal of Coastal Conservation* 18: 701-714. Doi:10.1007/s11852-014-0346-8
- House G., Hahn M., 2018. Evaluating methods to visualize patterns of genetic differentiation on a landscape. *Molecular Ecology Resources* 18(3): 448-460. doi: 10.1111/1755-0998.12747
- Howell P., Delgado L., Scribner K., 2017. Landscape genetic analysis of co-distributed white-footed mice (*Peromyscus leucopus*) and prairie deer mice (*Peromyscus maniculatus bairdi*) in an agroecosystem. *Journal of Mammalogy* 98(3): 793-803. doi: 10.1093/jmammal/gyx042
- Jaime-González C., Aceves P., Mateos A., Mezquida E. T., 2017. Bringing GAPs: On the performance of airbone Lidar to model wood mouse-habitat structure relationship in pine forest. *Plos One* 12 (8):e0182451. doi: 10.1371/journal.pone.0182451
- Keller D., Holderegger R., Van Strien M. J., Bolliger J., 2015. How to make landscape genetics beneficial for conservation management? *Conservation Genetics* 16: 503-512. doi: 10.1007/s10592-014-0684-y
- Keller I., Alexander J. M., Holderegger R., Edwards P. J., 2013. Widespread phenotypic and genetic divergence along altitudinal gradients in animals. *Journal of Evolutionary Biology* 26: 2527-2543. Doi: 10.1002/ece3.5273
- Kinyanjui M., 2010. NDVI based vegetation monitoring in Mau Forest complex, Kenya. *African Journal of Ecology* 49(2):165-174. doi: 10.1111/j.1365-2028.2010.01251.x

- Kozakiewicz C. P., Ricci L., Patton A. H., Stahike A. R., Hendricks S. A., Margres M. J., Ruiz-Aravena M., Hamilton D. G., Hamede R., McCallum H., Jones M. E., Hohenlohe P. A., Storfer A., 2020. Comparative landscape genetics reveal differential effects of environment on host and pathogen genetic structure in Tasmanian devils (*Sarcophilus harrisii*) and their transmissible tumour. *Molecular Ecology* 29(17): 3217-3233. doi: 10.1111/mec.15558
- Languth E. L., Cushman S. A., Schwartz M. K., McKelvey K. S., Murphy M., Luikart G., 2010. Quantifying the lag time to detect barriers in landscape genetics. *Molecular Ecology* 19(19): 4179-4191. doi: 10.1111/j.1365-294X.2010.04808.x
- León-Tapia M. A., Fernández J. A., Rico Y., Cervantes F. A., Espinosa de los Monteros A., 2020. A new mouse of the *Peromyscus maniculatus* group species complex (Cricetidae) from the highlands of central Mexico. *Journal of Mammalogy* 101(4): 1117-11132. doi: 10.1093/jmammal/gyaa027
- Linell M., Davis R., Lesmaister D., Swingle J., 2018. Conservation and relative habitat suitability for an arboreal mammal associated with old forest. *Forest Ecology and Management* 402: 1-11. doi: 10.1016/j.foreco.2017.07.004
- Manel S., Holderegger R.; 2013. Ten years of landscape genetic. *Trends in Ecology and Evolution* 28 (10): 614-621. doi: 10.1016/j.tree.2013.05.012
- Martínez-Coronel M., Ramírez-Pulido J., Alvarez T., 1991. Variación intrapoblacional e interpoblacional de *Peromyscus melanotis* (Rodentia:Muridae) en el Eje Volcánico Transverso, México. *Acta Zoológica Mexicana* 47: 1-51. doi: 10.21829/azm.1991.43471688
- Mastretta-Yanes A., Moreno-Letier A., Piñeiro D., Jorgensen T., Emerson B.; 2015. Biodiversity in mexican highlands and the interaction of geology, geography and climate within the Trans-Mexican Belt. *Journal of Biogeography* 42(9): 1586-1600. doi: 10.1111/jbi.12546
- Matthysen E.; 2012. Multicausality of dispersal: a review. In: Glovert J., Baguette M., Benton T., Bullock J. (eds.), 2012. *Dispersal ecology and evolution*, Oxford University Press, United Kingdom, 462 pp.
- Mateo-Sánchez M. C., Balkenhol N., Cushman S., Pérez T., Domínguez A., Saura S., 2015. Estimating effective landscape distances and movement corridors: comparison of habitat and genetic data. *Ecosphere* 6(4). doi: 10.1890/ES14-00387.1
- McCormack J., Hird S., Zellmer A., Carstens B., Brumfield R., 2013. Applications of next generation sequencing to phylogeography and phylogenetics. *Molecular Phylogenetics and Evolution* 66(22): 526-538. doi: 10.1016/j.ympev.2011.12.007
- McGarigal K. U., Cushman S., 2005. The Gradient Concept of Landscape Structure. In: Wiens, John A.; Moss, Michael R., eds. *Issues and Perspectives in Landscape Ecology*. Cambridge University Press. p. 112-119.
- Meliyo J. L., Massawe B. H. J., Msanya B. M., Kimaro D. N., Hieronimo P., Mulungu L. S., Kihupi N. I., Deckers J. A., Gulink H., Leirs H., 2014. Landform and surface attributes for prediction of rodent burrows in the Western Usambara Mountains, Tanzania *Journal Health Research* 16(3):182-93. doi: 10.4314/thrb.v16i3.5
- Milanesi P., Holderegger R., Bollmann K., Gugerli F., Zellweger F., 2017. Three-dimensional habitat structure and landscape genetics: a step forward in estimating functional connectivity. *Ecology* 98(2):393-402. doi: 10.1002/ecy.1645
- Mims M. C., Hartfield Kirk E. E., Lytle D. A. Olden J. D., 2018. Traits-based approaches support the conservation relevance of landscape genetics. *Conservation Genetics* 19: 17-26. Doi: 10.1007/s10592-017-1028-5
- Mortellini A., Amori G., Capizzi D., Cervone C., Fagiani S., Pollini B., Boitani L., 2010. Independent effects of habitat loss, fragmentation and structural connectivity on the

- distribution of two boreal rodents. *Journal of Applied Ecology* 48(1):153-162. doi: 10.1111/j.1365-2664.2010.01918.x
- Munshi-South J., 2012. Urban landscape genetics: canopy predicts gene flow between white-footed mouse (*Peromyscus leucopus*) populations in New York City. *Molecular Ecology* 21(6):1360-1378. Doi: 10.1111/j.1365-294X.2012.05476.x
- Munshi-South J., Zolnik C., Harris S., 2016. Population genomics of the Anthropocene: urbanization is negatively associated with genome-wide variation in white-footed mouse populations. *Evolutionary Applications* 9(4): 546-564. doi: 10.1111/eva.12357
- Murphy M. A., Dezzani R., Pilliod D. S., Storfer A., 2010. Landscape genetics of high mountain frog metapopulations. *Molecular Ecology* 19(17): 3634-3649. doi: 10.1111/j.1365-294X.2010.04723.x
- Nicolai N., 2020. Rodents' responses to manipulated plant litter and seed densities: implications for restoration. *PeerJ* 8: e9465. doi: 10.7717/peerj.9465
- Nielsen R., Paul J., Albrechtsen A., Song Y., 2011. Genotype and SNP calling from next-generation sequencing data. *Nature Reviews Genetics* 12(6): 443-451. Doi: 10.1038/nrg2986
- Norum J. K., Lone K., Linell J. D. C., Odden J., Loe L. E., Mysterud A., 2015. Landscape of risk to roe deer imposed by lynx and different human hunting tactics. *European Jouernal of Wildlife Research* 61: 831-840. doi: 10.1007/s10344-015-0959-8
- Otero-Jiménez B., Li K., Tucker P. K., 2020. Landscape drivers of connectivity for a forest rodent in a coffee agroecosystem. *Landscape Ecology* 35: 1249-1261. doi: 10.1007/s10980-020-00999-6
- Pearson K. M., Theimer T. C., 2004. Seed-caching responses to substrate and rock cover by two *Peromyscus* species: implications for pinyon pine establishment. *Oecologia* 141(1): 76-83. Doi: 10.1007/s00442-004-1638-8
- Pelletier D., Clark M., Anderson M. G., Rayfield B., Wulder M. A., Cardille J. A., 2014. Applying Circuit Theory for Corridor Expansion and Management at Regional Scales: Tiling, Pinch Points, and Omnidirectional connectivity. *PLoS ONE* 9(1): e84135. Doi: 10.1371/journal.pone.0084135
- Peterman W. E., 2018. Resistance GA: An R package for the optimization of resistance surfaces using genetic algorithms. *Methods in Ecology and Evolution* 9:1630-1647. doi: 10.1111/2041-210X.12984
- Peterson B. K., Weber J. N., Kay E. H., Fisher H. S., Hoekstra H. E., 2012. Double Digest RADseq: An inexpensive method for De novo SNP discovery and genotyping in model and non-model species. *Plos One* 7(5): e37135.
- Pettorelli N., Laurance W. F., O'Brien T. G., Wegmann M., Nagendra H., Turner W., 2014. Satellite remote sensing for applied ecologists: opportunities and challenges. *Journal of Applied Ecology* 51: 839-848. doi: 10.1111/1365-2664.12261
- Polato N. R., Gray M. M., Gill B. A., Becker C. G., Casner K. L., Flecker A. S., Kondratieff B. C., Encalada A. C., Poff N. L., Funk W. C., Zamudio K. R., 2017. Genetic diversity and gene flow decline with elevation in mayflies. *Heredity* 119(2):107-116. doi:10.1038/hdy.2017.23
- Rahlf J., Breidenbach J., Solberg S., Naesset E., Astrup R., 2017. Digital aerial photogrammetry can efficiently support large-area forest inventories in Norway. *Forestry* 90(5):710-718. doi: 10.1093/forestry/cpx027
- Richardson J. L., Urban M. C., Bolnick D. I., Skelly D. K., 2014. Microgeographic adaptation and the spatial scale of evolution. *Trends in Ecology and Evolution* 29(3): 165-176. Doi: 10.1016/j.tree.2014.01.002
- Richardson J. L., Michaelides S., Combs M., Djan M., Bisch L., Barret K., Silveira G., Butler J., Aye T. T., Munshi-South J., DiMatteo M., Brown C., McGreevy T. J., 2021. Dispersal

- ability predicts spatial genetic structure in native mammals persisting across an urbanization gradient. *Evolutionary Applications* 14(1): 163-177. doi: 10.1111/eva.13133
- Rodríguez-Freire M., Crecente-Maseda R., 2008. Directional connectivity of wolf (*Canis lupus*) populations in northwest Spain and anthropogenic effects on dispersal patterns. *Environmental Modeling and Assessment* 13(1):35-51. doi: 10.1007/s10666-006-9078-y
- Row J.R., Knick S.T., Oyler-McCance S. J., Lougheed S. C., Fedy B. C., 2017. Developing approaches for linear mixed modeling in landscape genetics through landscape direct dispersal simulations. *Ecology and Evolution* 7(11):3751-3761. doi: 10.1002/ece3.2825
- Rzedowski, 2006. Capítulo 17 Bosque de Coníferas. *Vegetación de México*. Comisión Nacional para el Conocimiento y Uso de la Biodiversidad, CONABIO. 1° edición.
- Samarasin P., Shuter B., Wright S., Rodd H., 2017. The problem of estimating recent genetic connectivity in a changing world. *Conservation Biology* 31(1): 126-135. doi: 10.1111/cobi.12765
- Sánchez-Cordero V., Illoldi-Rangel P., Linaje M., Sarkar S., Peterson T. A, 2005. Deforestation and extant distributions of Mexican endemic mammals. *Biological Conservation* 126: 465-473. doi: 10.1016/j.biocon.2005.06.022
- Santibañez-Andrade G., Castillo-Arguero S., 2009. Composición y estructura del bosque de *Abies religiosa* en función de la heterogeneidad ambiental y determinación de su grado de conservación en la Cuenca del Río Magdalena, México D.F. Posgrado en Ciencias Biológicas, UNAM.
- Shafer A. B., Peart C. R., Tusso S., Maayan I., Brelsford A., Wheat C. W., Wolf J. B. W., 2017. Bioinformatic processing of RAD-seq data dramatically impacts downstream population genetic inference. *Methods in Ecology and Evolution* 8(8): 907-917. doi: 10.1111/2041-210X.12700
- Soha M., Bastien M., Iquira E., Tardivel A., Légaré G., Boyle B., Normandeau É., Laroche J., Larose S., Jean M., Belzile F., 2013. An improved Genotyping by Sequencing (GBS) approach offering increased versatility and efficiency of SNP discovery and genotyping. *PLoS ONE* 8(1): e54603. doi: 10.1371/journal.pone.0054603
- Spear S. F., Storfer A., 2008. Landscape genetic structure of coastal tailed frog (*Ascaphus truei*) in protected vs. Managed forest. *Molecular Ecology* 17: 4642-4659. Doi: 10.1111/j.1365-294X.2008.03952.x
- Spear S. F., Cushman S. y McRae B., 2016. Resistance surface modelling in landscape genetics. *Landscape genetics: concepts, methods and applications*, 1st edition. Wiley and Sons.
- Starrfelt J., Kokko H.; 2012. The theory of dispersal under multiple influences. In: Globert J. Baguette M., Benton T. G., Bullock J. M. (eds.). *Dispersal ecology and evolution*, Oxford University Press, Oxford, United Kingdom, 462 pp.
- Sun Y., Fu T., Jin J., Murphy R. W., Hillis D. M., Zhang Y., Che J., 2018. Species groups distributed across elevational gradients reveal convergent and continuous genetic adaptation to high elevations. *PNAS* 115(45): E10634-E10641. doi: 10.1073/pnas.1813593115
- Vanhala T., Watts K., A'Hara S., Cottrell J., 2014. Population genetics of *Formica aquilonia* Wood ants in Scotland: the effects of long-term forest fragmentation and recent reforestation. *Conservation Genetics* 15: 853-868. Doi: 10.1007/s10592-014-0584-1

- Van Strien M., 2017. Consequences of population topology for studying gene flow using link-based landscape genetic methods. *Ecology and Evolution* 7(114): 5070-5081. doi: 10.1002/ece3.3075
- Vega R., Vázquez-Domínguez E., White T.A., Valenzuela-Galván D., Searle J.; 2017. Population genomics applications for conservation: the case of the tropical dry forest dweller *Peromyscus melanophris*. *Conservation Genetics* 18: 313-326. Doi: 10.1007/s10592-016-0907-5
- Velázquez A., Toledo V., Luna-Vega I., 2000. Mexican temperate vegetation. Barbour M.G., Billings W. D. (eds.), 2000. North American Terrestrial Vegetation. 2nd edition. 573-592.
- Villanueva-Hernández A., Delgado-Zamora D., Heynes-Silerio S., Ruacho-González L., López-González C., 2017. Habitat selection by rodents at the transition between the Sierra Madre Occidental and the Mexican Plateau, México. *Journal of Mammalogy* 98(1):293-301. doi: 10.1093/jmammal/gyw173
- Waits L., Storfer A., 2015. Basics of population Genetics: Quantifying Neutral and Adaptive Genetic Variation for Landscape Genetic Studies. In: *Landscape genetics: Concepts, Methods, and Applications*. Pp 35-57. doi: 10.1002/9781118525258.ch03
- Wang K., Franklin S. E., Guo X., Cattet M., 2010. Remote sensing of ecology, biodiversity and conservation: a review from the perspective of remote sensing specialists. *Sensors* 10(11): 9647-9667. doi: 10.3390/s101109647
- Wang Y., Cao X., Zhao Y., Fei J., Hu X., Li N., 2017. Optimized double-digest genotyping by sequencing (ddGBS) method with high-density SNP markers and high genotyping accuracy for chickens. *PLoS ONE* 12(6): e0179073. doi: 10.1371/journal.pone.0179073
- Wiens J. A., 1995. Landscape mosaics and ecological theory. Hansson L., Fahring L., Merriam G., 1995. *Mosaic Landscapes and ecological processes*. Chapman and Hall.
- Wilson Ian, 2019. Using unnamed aerial systems to classify land cover and assess productivity in forested wetlands in Nova Scotia. Thesis from Saint Mary's University, Halifax, Nova Scotia, Canada.
- Zhu F., Cui Q., Hou Z., 2016. SNP discovery and genotyping using genotyping by sequencing in Pekin ducks. *Scientific Reports* 6(36223). doi: 10.1038/srep36223